NCSX

Design Basis Analysis

VV Structural Analysis

NCSX-CALC-12-007-001

July 5, 2005

Prepared by:

Signature Not Verified Fred Dahlgren

Digitally signed by Fred Dahlgren
DN: cn=Fred Dahlgren, c=US
Date: 2005.07.05 14:31:08 -04'00'

Fred Dahlgren, PPPL

Contributers:

Art Brooks, PPPL & Peter Titus, MIT, Keven Freudenberg, ORNL

I have reviewed this calculation and, to my professional satisfaction, it is properly performed and correct. I concur with analysis methodology and inputs and with the reasonableness of the results and their interpretation.

Reviewed by:

Signature Not Verified Paul Goranson

Digitally signed by Paul Goranson
DN: cn=Paul Goranson, c=US
Date: 2005.07.06 08:34:24 -04'00'

P. Goranson, ORNL Engineer

I. Executive Summary

The purpose of this analysis was to determine the stresses, displacements, and structural stability of the vacuum vessel shell, ports, and structural support attachments in response to various loading conditions and to verify the adequacy of the current design. Several anticipated loading conditions were investigated including external atmospheric pressure, gravity, thermal loads due to bakeout and normal operations, disruption eddy current loads, and seismic loading conditions. The following are the main findings of this analysis:

-Stresses from the normal operating load runs (Atmospheric, Gravity, Thermal, + 250 lb cantilevered load) in the shell and ports are generally well below the code allowable stress with the exception of the Port-18 & 15 cantilevered loading condition. (Note, the actual port load limits are specified in the NCSX project document IDC-121-300-0001)

Recommend either:
a) thickening the turret wall and port nozzle to reduce stress at the nozzle/port intersection and to reduce vertical deflections of the port,
b) Implement a radially compliant vertical nozzle support off the cryostat, or
c) Limit the cantilevered loading on Port-15 and the RF ports.

-Shell displacements for normal operations are generally low with the exception of the area between Port-2 and port-9 which indicate a displacement of 0.125" total. This results in a .25" deflection of these ports at the 1st flange. These displacements may be reduced by thickening or reinforcing the shell locally to reduce these deflections if necessary.

-Dynamic loading from VDE (10cm vertically displaced) plasma disruptions are the most severe but the peak (Main flange) stress intensities are below allowables for the full 1.0x DLF (Dynamic Load Factor). Where we assume the interior welds in the peak stress (flange) regions experience the same stresses, and using a weld efficiency of 0.7, we have a margin of 20% on code allowables.

-Critical Buckling loads were calculated by using Nastrans' eigenvalue extraction of the lowest buckling mode for each loading condition specified. For the worst VDE disruption load (using DLF=1.0) and including atmospheric and gravity loading, the critical load factor was 12. Due to the irregular shape of this vessel local buckling modes predominate, generally localized in the shell near ports 2 and 9. Peter Titus has provided a validation of the vessel stability using an independent non-linear, large deflection ANSYS analysis of a 360 degree model which indicated no bifurcation up to 3X the atmospheric pressure.

-Modal analysis indicates the undamped primary structural mode of 0.8 Hz with the vessel rocking on the vertical supports. Numerous low frequency modes are present in ports 15, 2, 9, rf-1 & rf-2. Several are in the frequency range of earthquake spectrum and are anticipated to participate in the horizontal and vertical accelerations of any seismic event. Since their mass is relatively low, and deflections of these ports are limited by the Cryostat penetrations, no significant permanent damage to the vessel or structure from a seismic event is anticipated although some dampening, perhaps from the cryostat boots and feed-thrus might be implemented with good effect here.

-Areas where local bending + membrane stress may exceed yield, and areas of discontinuity or stress concentration were evaluated for fatigue. The primary cyclic loading (apart from the low number of pump-down/bakeout cycles) will be disruption loads. Assuming a conservative estimate of 5 disruption loads per day, over 10 years of operation, the cumulative number of cycles will be ~12,500. The stress range will vary based on location and residual stress. Specialty Metals/Huntington Alloys data indicates a fatigue life well in excess of 100 million cycles at the maximum anticipated cyclic stress for the base metal. For weld filler material, the literature indicates high margins for the cycle life and stress range anticipated. After accounting for shakedown, all stress excursions will fall well within the elastic range for all loading conditions considered.

-The creep-rupture properties at the maximum bakeout temperature of 400 C are extremely good for this material (Inconel 625) with rupture life in excess of 100,000 hrs (11.4 years) for the peak stress levels calculated. The accumulated vessel exposure to bakeout temperatures is not expected to exceed 10% of the rupture life (10,000 hrs).

--The seismic analysis per P. Titus (see Appendix I), indicated moderate stresses on the vessel due to horizontal accelerations. The lowest flexible (rocking) mode found was ~2 Hz which is higher than the Nastran modal analysis. This discrepancy appears to be due to the use of both the inner and outer vertical support rods in the seismic analysis. When the detailed vessel support design is finalized this issue should be revisited. The thermal stress due to unequal length support rods also needs further review.

-Appendix B2 is a summary of the stresses developed in a port nozzle at the Inconel-Stainless interface under bakeout conditions. This assumes a 302 deg.F to 655 deg.F linear thermal gradient from the port nozzle root to the flange in a neutral beam port. The max shear resulting from the differences in thermal expansion is seen to be 10.8 ksi and appears to be independent of where the SS-Inconel transition weld is located.

II. Assumptions

-Vessel & port configuration as of 2 April '04 Pro-E models (based on Se121-011 ver.94 –Half Period Ass'y).

-Material of shell & port nozzles and cover plates fabricated from 0.375 thick Inconel 625
Annealed – Grade 1 sheet per ASTM B 443 (plate).

-Material properties (Linear elastic, isotropic material properties) taken from the Huntington Alloys International Inconel 625 product bulletin.

-Preliminary runs assumed rigid vertical structural support to eliminate rigid body modes. (Subsequent runs were also made with elastic support rods with the rod-end bushing compliance included).

-Cyclically symmetric boundary conditions at the main closure weld flanges for the 1-period model.

-Preliminary static model runs assumed isothermal, 1-g gravity, 1 Atmosphere external pressure @14.7psi.

-Subsequent runs include a calculated thermal distribution in the port nozzles during bakeout conditions by holding the shell at 350 deg.C and the 1st flange at 150 deg.C.

-Disruption loads are derived from Spark ver.20b inductive solutions for a stationary center plasma and a plasma displaced 10 cm vertically up from its central equilibrium position. (scenario from Tech Data Sheet TDS_C07R00_I).

III. Analysis Methodology and Inputs

Software and data files

The FEA codes used in these analysis was MSC/Nastran – 2001-rev3 – Windows edition, and ANSYS 8.1 –Windows edition. The disruption loading was calculated using the PPPL code Spark ver.20b. Seismic and verification runs were made using Ansys Release 7.0.

The Pro-E files listed below were the current files as of 17 March thru 7 April 2004 with the part/asm version numbers indicated by the file suffix. The Pro-E port, shell, spool, and flanges were exported via Iges files which were then read by MSC/Patran (the modeling front-end and post processor for MSC/Nastran). The FEA model itself was generated and meshed in Patran from these surface geometries, and is comprised of triangular and quadrilateral shell elements (CQUAD4 & CTRIA3) which include both bending and membrane stiffness.

Analysis of seismic loading and weld stresses appearing in the appendices utilized both the solid and plate elements of the ANSYS 8.1 FEA code where noted.

Drawings and models

Pro-E files used:

Se-121-011.prt.15	shell
Se-121-013.prt.13	spool-outer flg.
Se-121-015.prt.18	spool piece
Se-121-016.prt.19	spool-inner flg
Se-122-017.prt.22	vertical port-12
Se-122-021.prt.41	6” port-9
Se-122-023.prt.43	4” port-2
Se-122-029.prt.45	6” port-5
Se-122-031.prt.47	10” port-6
Se-122-034.prt.	2” port-3
Se-122-037.prt.34	8” port-7
Se-122-039.prt.36	4” port-8
Se-122-043.prt.38	10” port-10
Se-122-047.prt.42	horizontal (angled) port-4
Se-122-055.prt.47	4” port-14
Se-122-059.prt.49	4” port-15
Se-122-071.prt.54	nbl port

Nastran FEA Input files:

ANALYSIS	MODEL FILE INPUT (model-)
Thermal Steady State	120bbe2a-Thermal4.bdf
Atm. Only	120bbe3.bdf
Atm. + Gravity	120bbe3g.bdf
Atm. + Gravity + Cant. Load	120bbe3gf.bdf
Atm. + Gravity + Thermal	120bb3a-tstress4.bdf
Atm. + Gravity + Ohmic Disrpt.	120bbe2a-OHMIC.bdf
Atm. + Gravity + VDE Disrpt.	120bbe2a-VDE.bdf
Atm. + Gravity + HiBeta Disrpt.	120bbe2a-HIGHBETA.bdf
Atm. Only –Buckling	120bbe2a-bucklePonly.bdf
Atm. + Gravity -Buckling	120bbe2a-bucklePG.bdf
Atm. + Gravity + VDE –Buckling	120bbe2a-VDE-dyne.bdf
Atm. + Gravity + OHMIC –Buckling	120bbe2a-OHMIC-buckling.bdf
Atm. + Gravity + HIGHBETA –Buckling	120bbe2a-HIGHBETA-bucklin.bdf
Atm. + Gravity + VDEx2 –Buckling	120bbe2a-VDE-buckle2X.bdf
Atm. + Gravity + HIGHBETAx2 –Buckling	120bbe2a-HIBETA-2X-bucklin.bdf

Material Properties

- Material Properties(@ 200 deg.C - 392 deg.F):
  -Youngs Modulus 28.7e6 psi
  -Shear Modulus 11.1e6 psi
  -Poissons' Ratio 0.286
  -Density 0.305 lbs/cu. in.
  -Coeff. of Thermal Exp. 7.3e-6 in./in.-deg.F

- Material Properties (@ 400 deg.C – 750 deg.F):
  -Youngs Modulus 27.1e6 psi
  -Shear Modulus 10.5e6 psi
  -Poissons' Ratio 0.294
  -Density 0.305 lbs/cu. In.
  -Coeff. of Thermal Exp. 7.6e-6 in./in.-deg.F

(From Huntington Alloys/Specialty Metals publication for Inconel 625)

Material Thicknesses & port diameters for VV model (inches):

Part	**Thickness**	**Diameter**
Shell	0.375	
N.B. duct	0.500	27.5 x 37.0~
Port 2	0.125	4.0
Port 3	0.125	4.0
Port 4	0.500	25.0 x 36.0~
Port 5	0.125	6.0
Port 6	0.250	10.0
Port 7	0.125	8.0
Port 8	0.125	4.0
Port 9	0.125	6.0
Port 10	0.125	10.0
Port 11	0.125	4.0
Port 12	0.500	6.38 – 11.75 x 15.5
Port 15	0.125	4.0
RF-Turret	0.188*	16.0
Port 17	0.125	4.0
Port 18	0.125	4.0

Main Flange Dimensions: 0.65 wide x 0.85 deep, 0.375 weld

- Analysis was also re-run with 0.375" thick Inconel Turret.

Project Reference Documents:

NCSX-ASPEC-GRD-02 – "General Requirements Document for NCSX"
NCSX-BSPEC-12-00 - "Systems Requirement Document for the Vacuum Vessel System (WBS-12)"
NCSX-CRIT-CRYO-00 - "NCSX Structural Design Criteria"
NCSX-CRIT-SEIS-00 - "Seismic Requirements of NCSX"
NCSX-CALC-12-004-00 - "Vacuum Vessel Support Rod Analysis"
NCSX-CALC-12-005-00 - "Diagnostic Port Flange Weld Stress Resulting From Loss of Power Fault Condition in NCSX Vacuum Vessel"
IDC-121-300-0001 - "Vacuum Vessel Diagnostic Port Allocation and Orientation"

IV. Results and Discussion:

Introduction:

Figure 1. below shows the basic 120 degree single period FEA Nastran model of the vessel with cyclic-symmetric boundary conditions. To the left are the model details and loading conditions investigated. (This model was also used as input for the Spark disruption modeling).

Model Details:
38,906 DOF's
7782 GRID POINTS
7,228 CQUAD4
1,018 CTRIA3
40 MPC's
4 SPC's

Boundary Conditions:
Cylic-Symmetry @ welded edge via MPC's, vertically fixed @ top clevis, circumferentially top & bot. of NB port

Normal Operating Loads:
Uniform external 14.7 psi
Gravity – 1g
Temperature 200 deg.C (max.)
Bakeout: 400 deg.C (max)

Off-Normal (EM Disruption) Loads:
320kA Plasma @ 1.7T
210kA Plasma @ 2.0T (High Beta)
320kA Plasma @ 1.7T @dZ=10cm
(Inductively coupled solutions)

NCSX VACUUM VESSEL NASTRAN 120 DEG. FEA MODEL

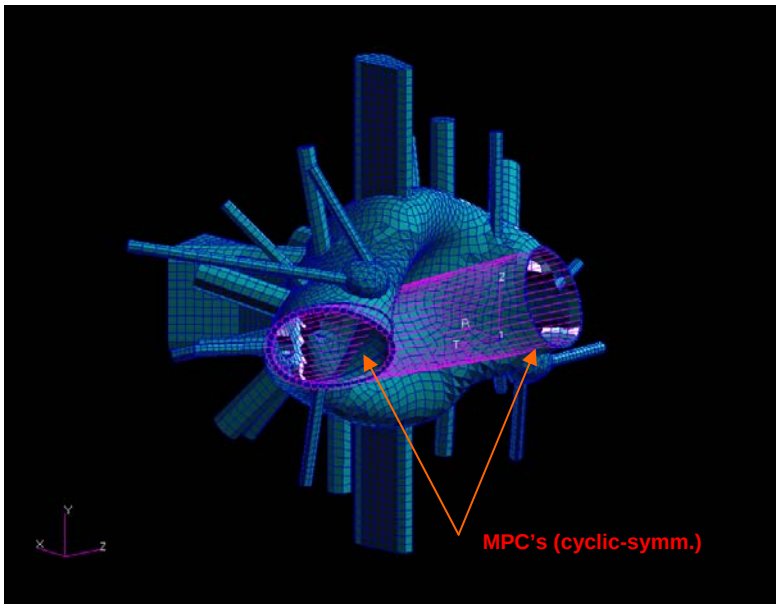

Figure 1. NCSX Vacuum Vessel Nastran FEA Model

The model contains all diagnostic and Neutral Beam ports as of 2 April '04 including the two new RF turret ports. The closure weld flanges and spool section are also modeled (see section III for a detailed list of the ports). The cyclic-symmetric boundary conditions are modeled using multipoint constraints (MPC's – the magenta lines shown in Fig. 1) which constrain identical displacements to occur at the corresponding grid points on both weld flange boundaries (simulating the stiffness of the full 360 degree structure).

Atmospheric loads:

Figure 2. is a contour plot of displacements due to atmospheric pressure showing a peak displacement of 0.25" at the upper and lower ends of port-2 (at the 1st port flange). The deflection of ports 2 (and 9) are the result of a local inward displacement of the vessel shell in the flat area of the shell in the vicinity of these two ports as shown in Figure 3 (note the upper range of the contour levels in this plot has been limited to 0.125" to accentuate the local displacement contours).
Figure 4. shows the Tresca stress contours on the outer shell surface for atmospheric loading with the peak stress of 15.2 ksi occurring in the areas of high curvature near the top (and bottom) of the shell.

To reduce the shell and port deflections in the vicinity of ports 2 and 9, some internal reinforcing ribs may be employed. Figure 5. illustrates the effect of adding some 0.375 thick, 1" high tee section reinforcing ribs on the shell interior. The peak shell displacement between ports 2 and 9 is reduced by about a third with the addition of these ribs. The displacement at the end of port 2 has also been reduced from 0.25" to 0.15". The peak Tresca stress in the high curvature region of the shell however, remains about the same (15 ksi)

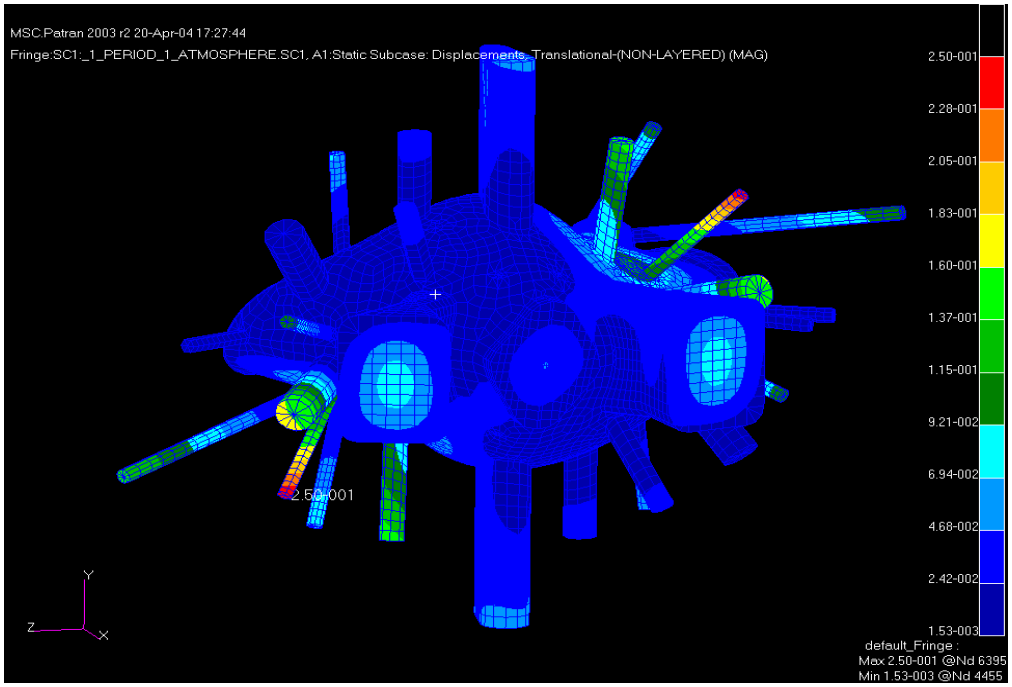

Figure 2. Run 120bbe3: 1 Atmosphere External Pressure Only

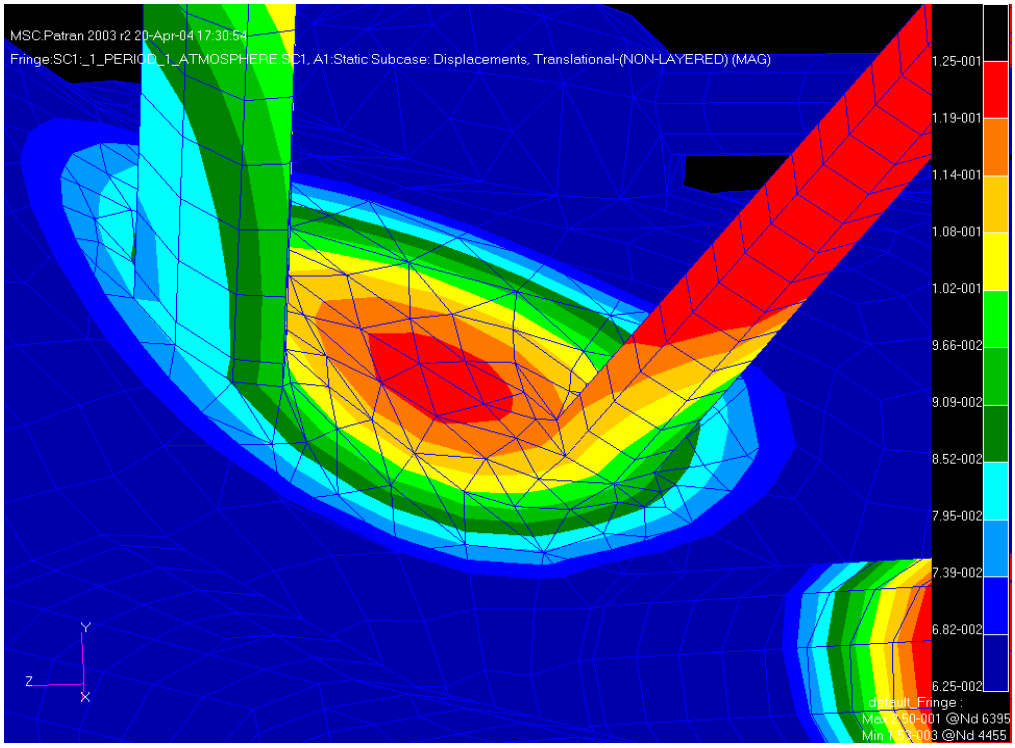

Figure 3. Run 120bbe3: 1 Atmosphere External Pressure Only – showing a peak shell displacement of 0.125” between ports 2 & 9

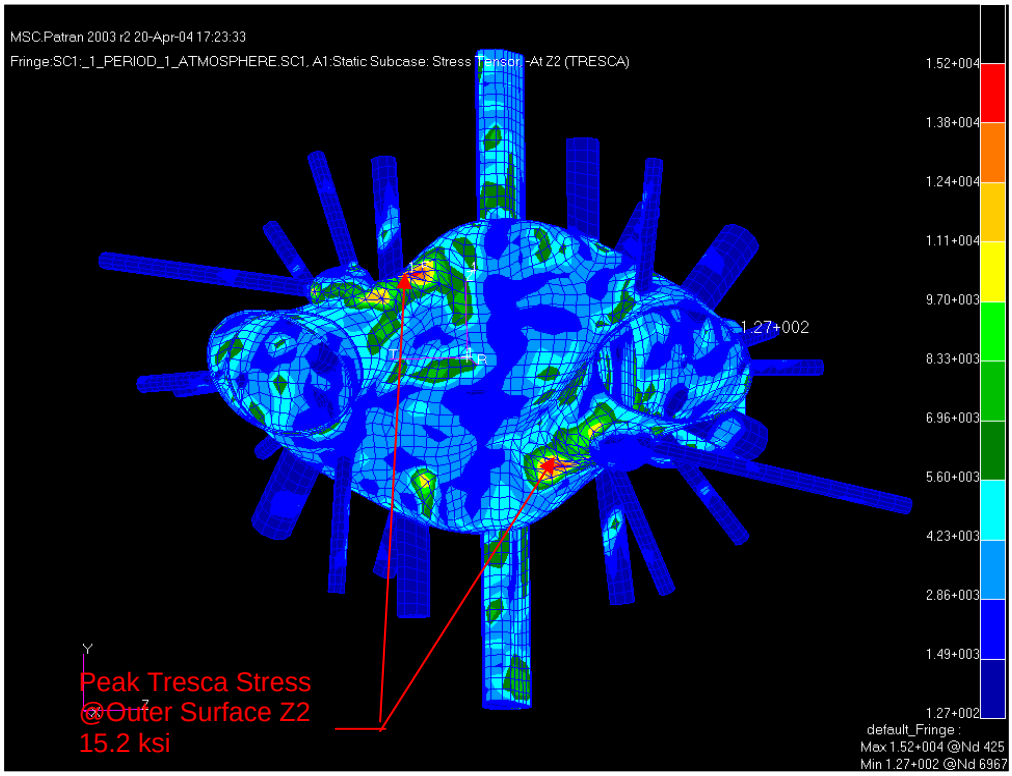

Figure 4. Run 120bbe3: 1 Atmosphere External Pressure Only –Tresca Stress - Z2

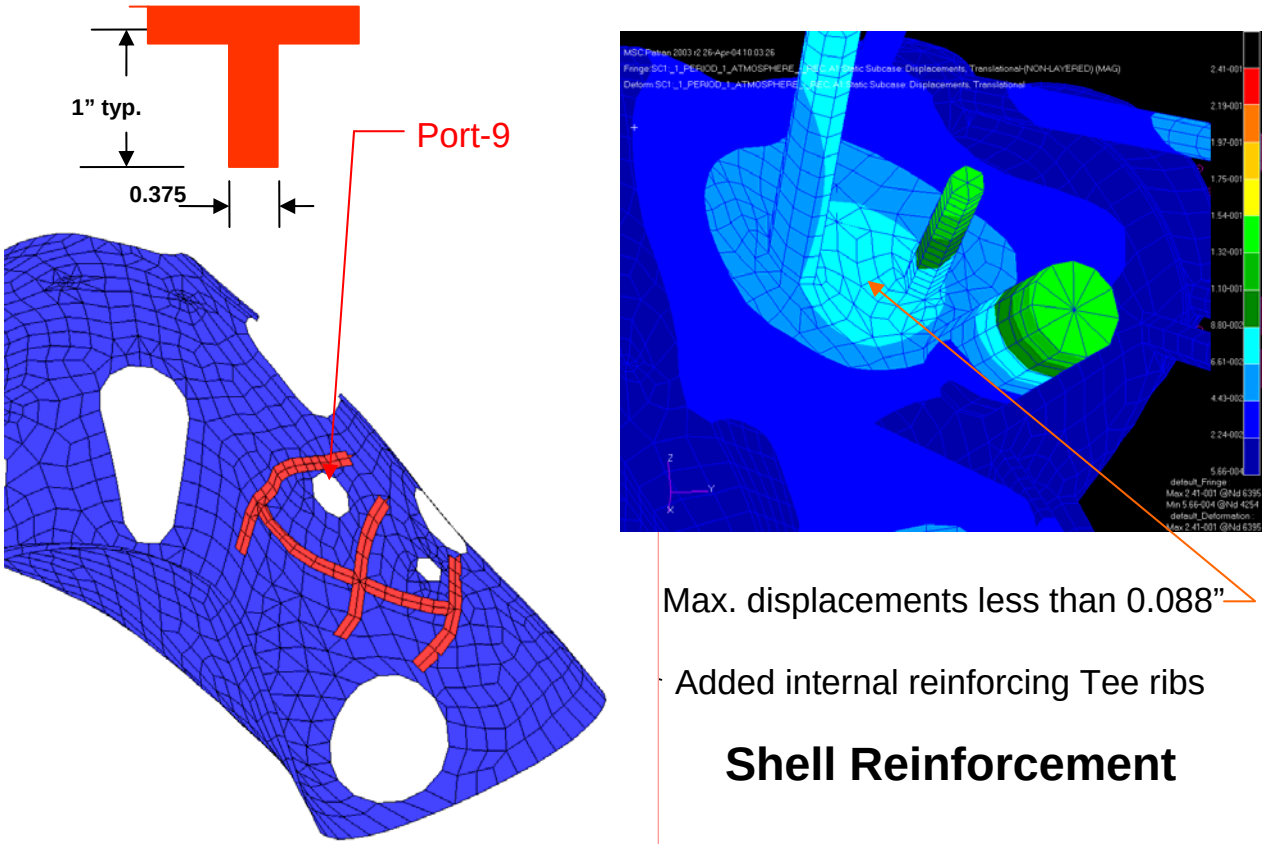

Figure 5. Run 120bbe2a-tribsf with internal shell reinforcement (disp. Reduced by 30%)

Atmospheric + Gravity loads:

Figure 6. is a plot of displacement contours for the atmospheric + gravity loading condition indicating a peak displacement of 0.255" at port 2. In general, the results for this loading condition are similar to the pressure only condition, the main difference being the Tresca stress contours shown in figure 7. which indicate a peak of 20.9 ksi at the base of the RF port turret intersecting the shell. The stress distribution in the other portions of the shell are similar to the pressure only loading condition.

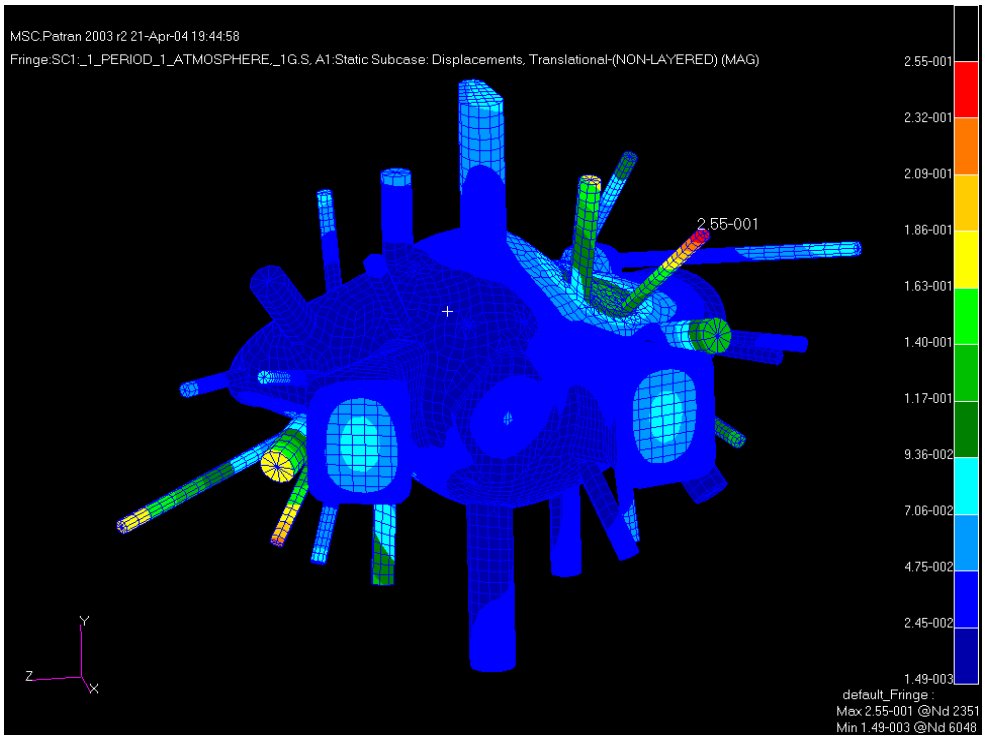

Figure 6. Run 120bbe3g – 1 Atmosphere External Pressure + 1g Gravity Loading

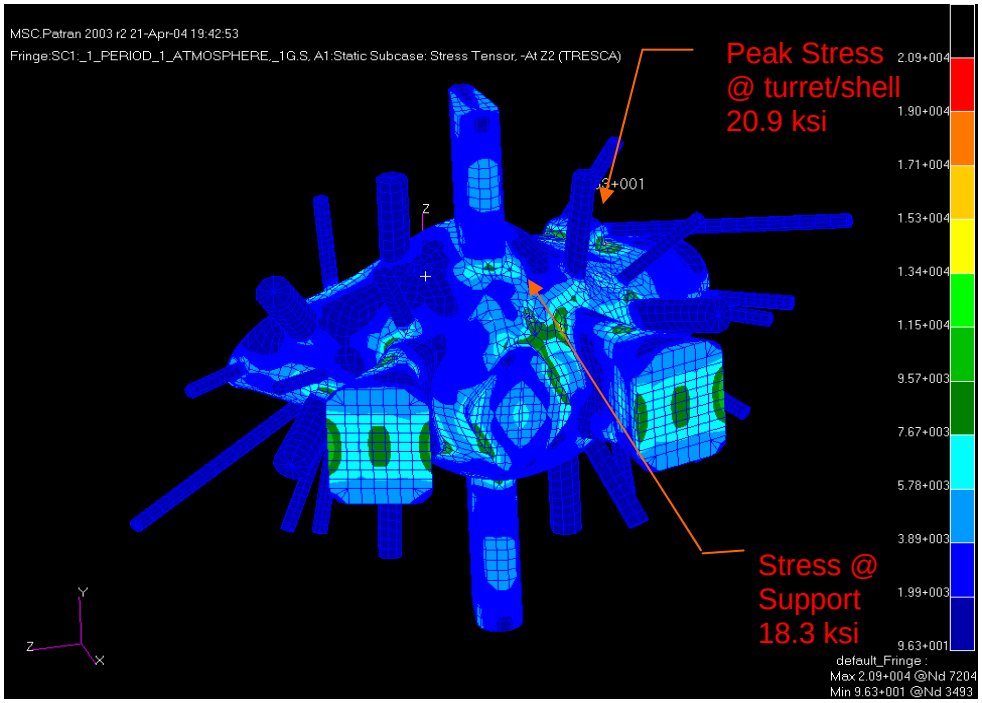

Figure 7. Run 120bbe3g – 1 Atmosphere External Pressure + 1g Gravity Loading

To simulate a typical diagnostic load or step loading condition on the ports, a cantilevered mass, at various port ends, was applied via a concentrated weight of 500lbs. This simulates a 250lb load at the end of the full port extension (2x length =2x bending load). Figure 8. shows the worst case result at the RF ports and indicates a maximum displacement of 1.26" at the 1st flange end. The peak Tresca stress at the root of the RF port exterior (Z2) surface is 34.2 ksi as shown in Figure 9.

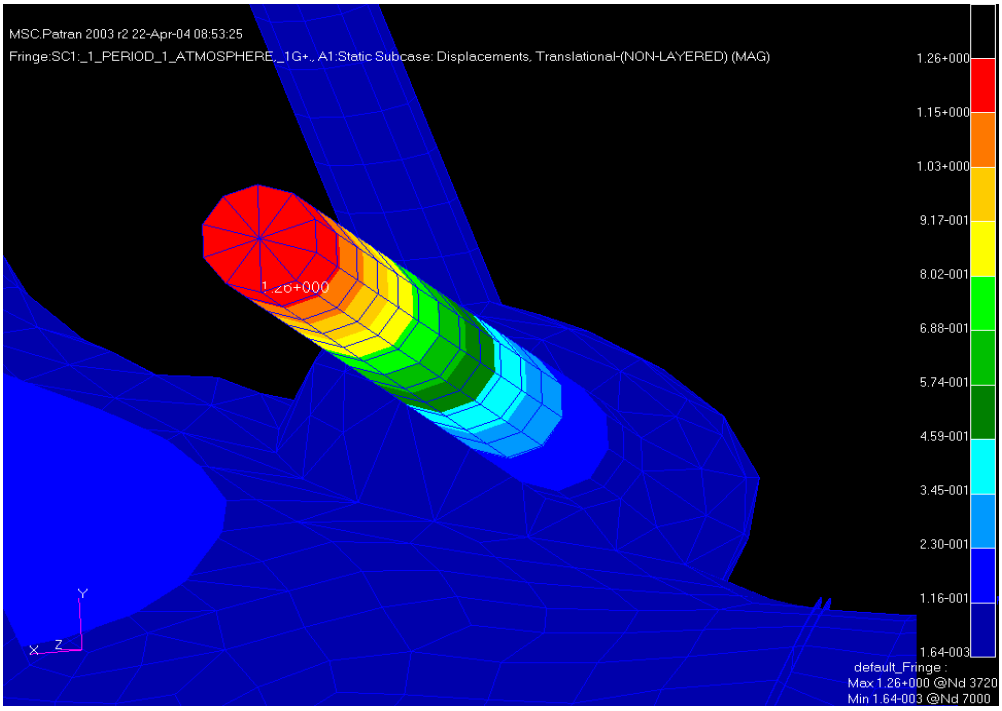

Figure 8. Displacements - Run 120bbe3gf Cantilevered Loading Of Ports

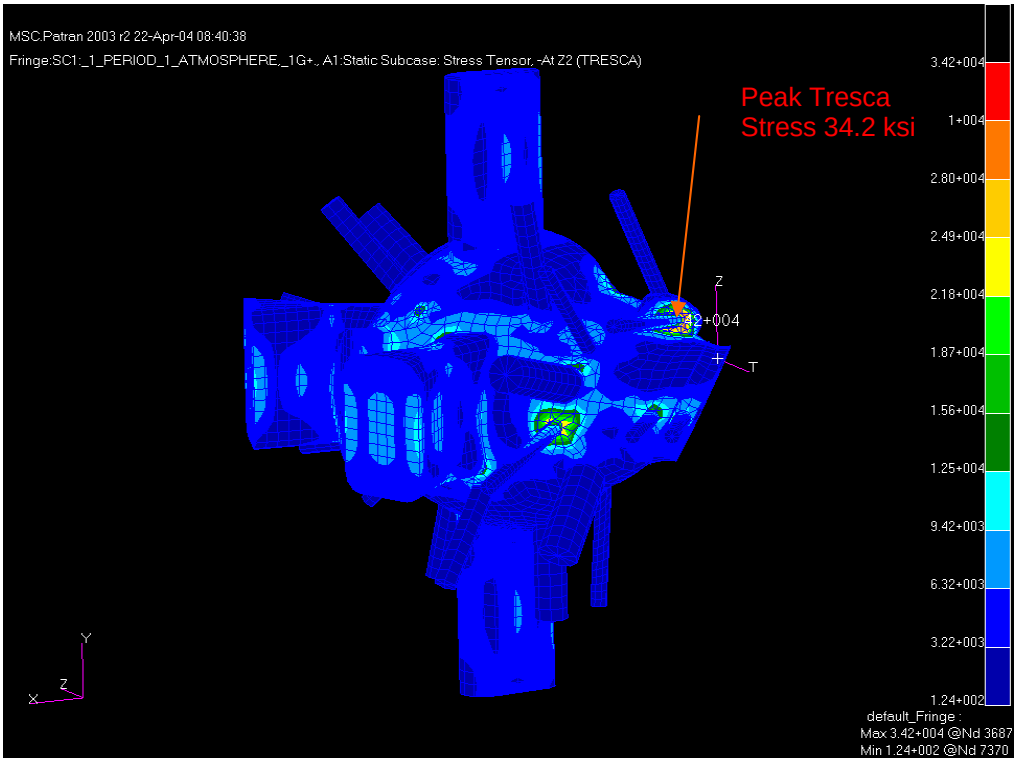

Figure 9. Run 120bbe3gf – 1 Atmosphere External Pressure + 1g Gravity Loading + 500lbs cantilevered –Tresca stress Z2 surface

Figure 10 below shows the Tresca stress contours on the Z1 inner surface peaking at 48.2 ksi at the turret base. Figure 11. shows the reduced inner surface stress of 30 ksi, when the turret thickness is increased to .375".

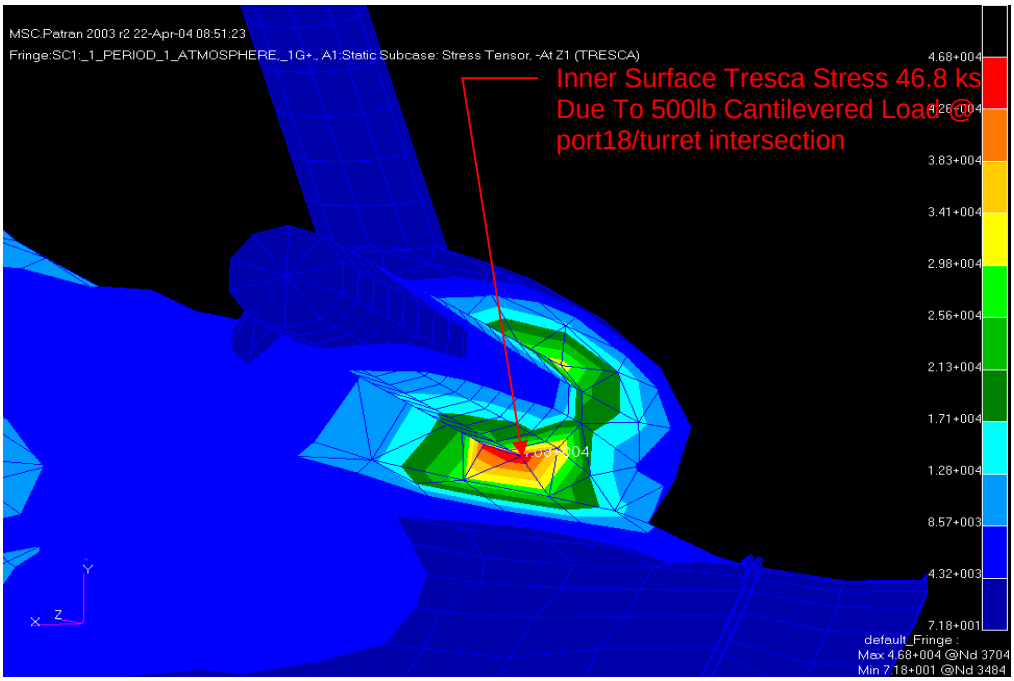

Figure 10. Run 120bbe3gf – 1 Atmosphere External Pressure + 1g Gravity Loading + 500lbs cantilevered – Tresca Stress Z1 surface.

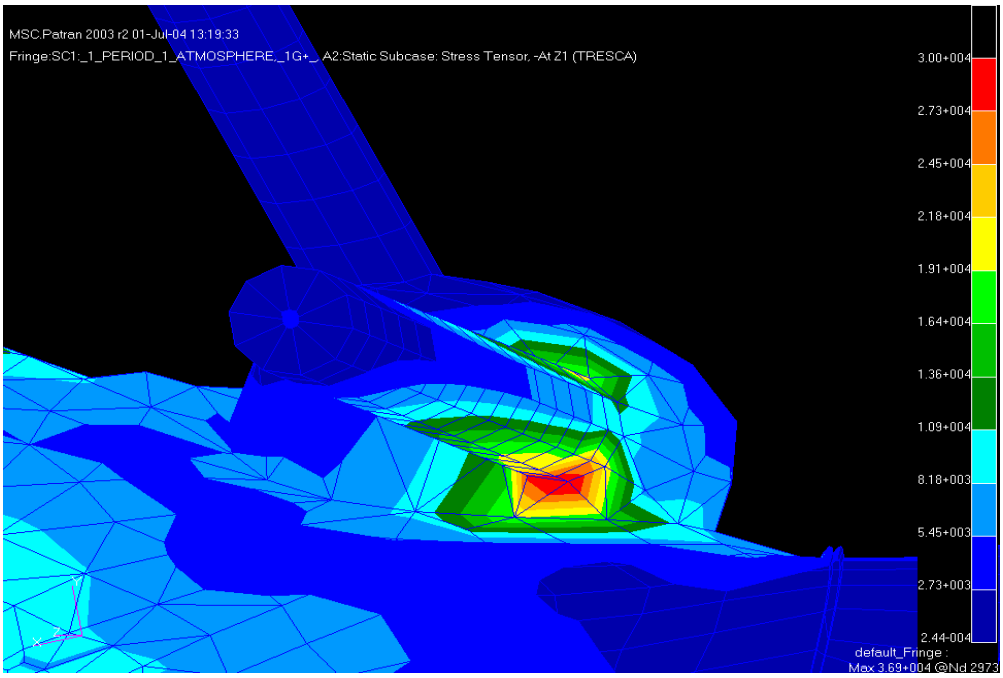

Figure 11. Run 120bbe3gf-2 – 1 Atmosphere External Pressure + 1g Gravity Loading + 500lbs cantilevered, 0.375" thk turret – Tresca Stress Z1 surface.

Thermal loads:

A steady state thermal analysis was run to determine the temperature distribution during a bakeout condition. The model assumes a fixed shell temperature of 400 ^{o}C and a fixed temperature of 150 ^{o}C at the port flanges. Figure 12 shows the resulting iso-thermal contours. Figure 13. indicates a maximum displacement of 0.54" for port 4 & 18.

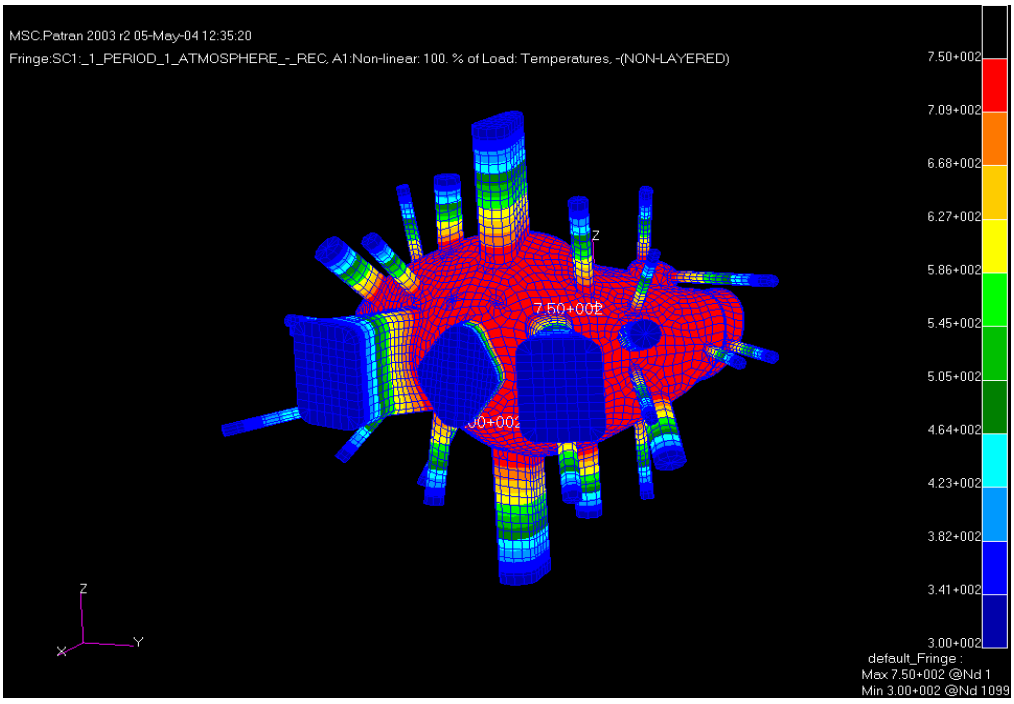

Figure 12. Nominal 400 deg.C uniform shell, 150 deg.C @ Port Flanges. Run 120bbe2a-Thermal4 – Steady State Bakeout

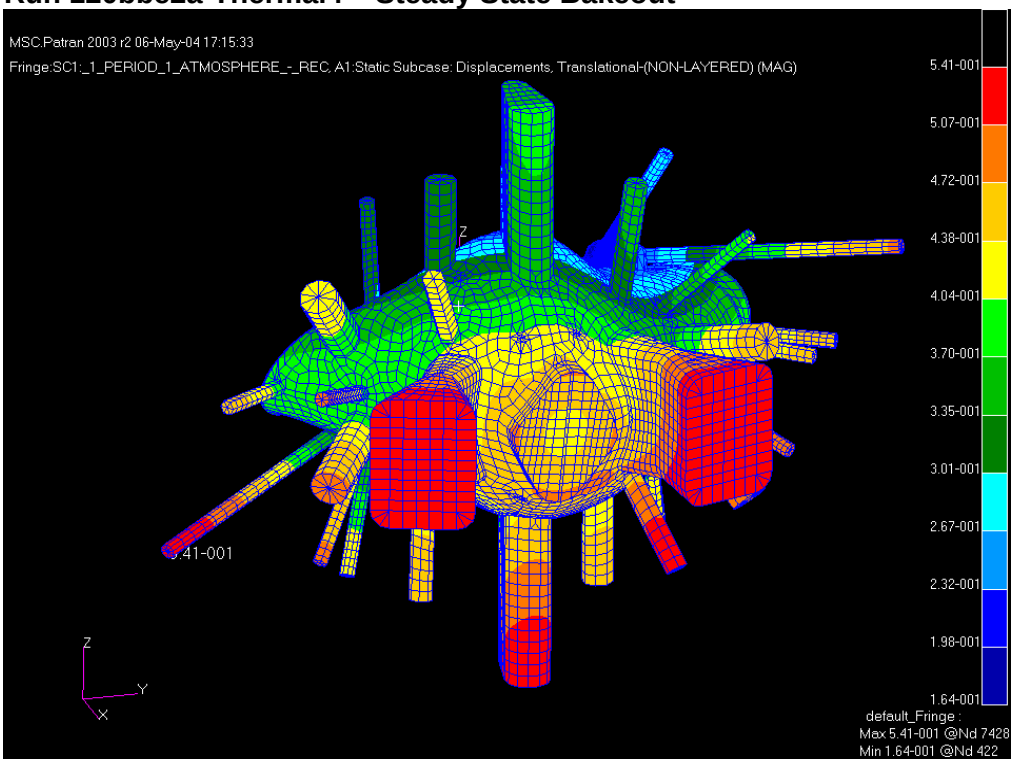

Figure 13. Total Displacements 400 deg.C shell 150 deg.C at port flanges. Run 120bbe2a-tstress4 – Thermal Displacements

Figure 14. is contour plot of the Tresca stress on the outer (Z2) surface due to the combined effects of the 400 deg.C bakeout plus gravity and 1 atmosphere external pressure. The peak stress at the corners of the shell/NB Port intersection is 37 ksi. This is primarily due to the large (artificial) thermal gradient imposed by fixing the end temperature of the short neutral beam port stub at 150 deg.C while maintaining the shell bakeout temperature of 400 deg.C. The actual thermal gradient in the neutral beam ports will be much less severe than this condition indicates and the stresses here are not anticipated to exceed 20 ksi under this combined loading condition. The stresses in the remainder of the vessel do not exceed 13.5 ksi on the outer surface and 12 ksi on the inner surface.

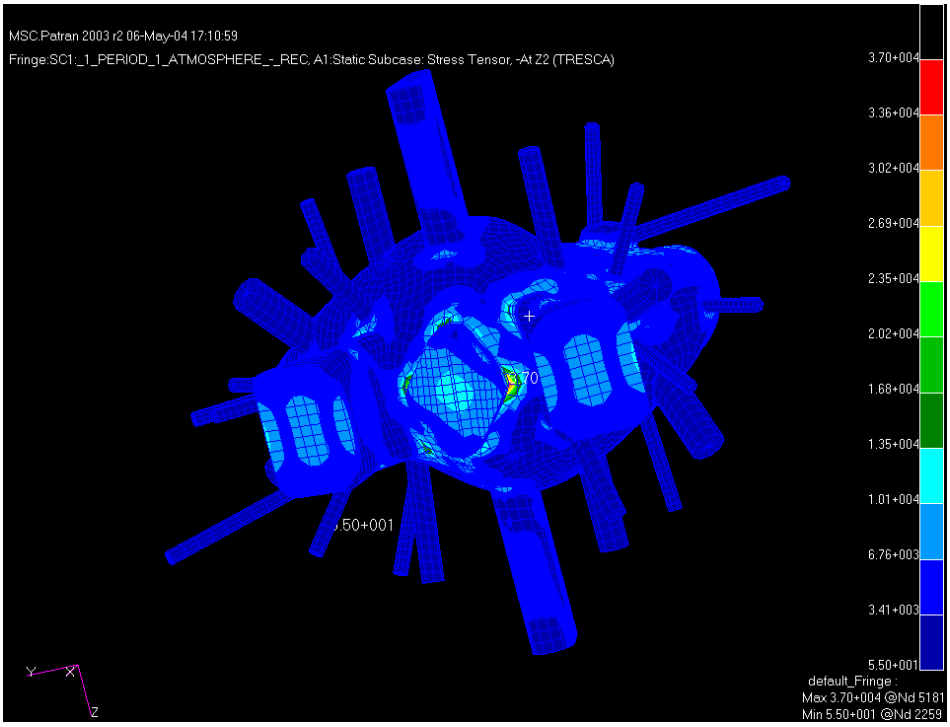

Figure 14. Contour Plot of Tresca Stress on the Outer (Z2) Surface. Run 120bbe2a-tstress4 – Thermal Stresses

Buckling Analysis:

External Pressure only:

To determine the structural stability of the vessel due to the external pressure and disruption loads, a buckling analysis was performed. In Nastran the common method of determining structural stability is to apply the loading conditions anticipated in normal service as a static loading condition and from that result calculate the differential stiffness matrix and then solve the resulting eigenvalue problem below:

$$[K + \lambda_i K_d] \{u\} = 0$$

The resulting (primary) eigenvalue is then the factor by which the applied load must be multiplied to produce buckling. If the static load applied is one atmosphere the resulting eigenvalue is then the critical buckling load factor or safety factor. For a single external atmospheric load (14.7 psi), the critical buckling load factor was found to be 12.99 indicating it would theoretically require approximately 191 psi external pressure to collapse the vessel. The resulting eigenvector seen in figure 15 shows the primary buckled mode shape which is a locally buckled region in the vicinity of ports 2 and 9.

Buckling Analysis Disscussion:

While 12.99 appears to be quite a large margin such results are typically viewed with some caution. The ASME-BPV code generally requires minimum safety factors of 5x or greater on critical buckling of externally loaded vessels due to the uncertainties in geometry, loading conditions, and material properties. Regularly shaped structures commonly used in autoclaves, like spheres, torrispherical heads and cylindrical shells, tend to be more sensitive to variations in thickness and deviations from their theoretical geometry and tend to buckle at loads significantly lower than normal stability theory might predict (hence the large safety factors of 5x or greater), however, due to the highly irregular shape of the NCSX vessel, it is less likely to be susceptible to premature buckling due to minor variations in thickness or geometry. That said, there are still other considerations that tend to produce lower margins than this

eigenvalue analysis predicts, and suggests these margins should only be used as an upper bound indicator of global structural stability. There are several assumptions inherent in the current method of buckling analysis, the principle one being that the entire structure at temperature and under load remains linearly elastic and therefore small deflection theory still applies (ie. the applied loads from which the differential stiffness is derived, maintain the same magnitude, direction, and point of application as the structure deflects).

As an illustration, a full 12.99x (191psi) external load was applied to the vessel model as a static load to evaluate the structural response of the model. Figure 16a is a narrowed range (> 60 ksi)contour plot of Tresca stresses (peak 185ksi) that exceed the yield stress of Inconel-625 at 400 deg.C (~60 ksi) when the full 191 psi (12.99 x 14.7 psi) uniform external pressure load is applied. The non-white contours represent areas above the 60 ksi yield stress of the Inconel. Clearly, these localized areas of high stress would have yielded, producing much larger shell displacements, long before a 191 psi pressure was reached, so the safety factor quoted above of 12.99 is not necessarily a true indicator of the margin for structural failure (in this context structural failure is considered displacements significantly greater than the shell thickness of 0.375"). Figure 16b is a full range Tresca stress contour plot for a external 5x atmospheric (73.5 psi) loading condition with a greatly reduced stress range(peak 68 ksi). It can be seen that only a very small region of the shell at the corner intersection with the rectangular ports exceeds yield and it therefore can be concluded that only localized yielding and small displacements would occur under these loading conditions. The basic conclusion that can be drawn from these results is that the buckling margin, at a minimum, exceeds 5x for atmospheric loading at the maximum bakeout temperature.

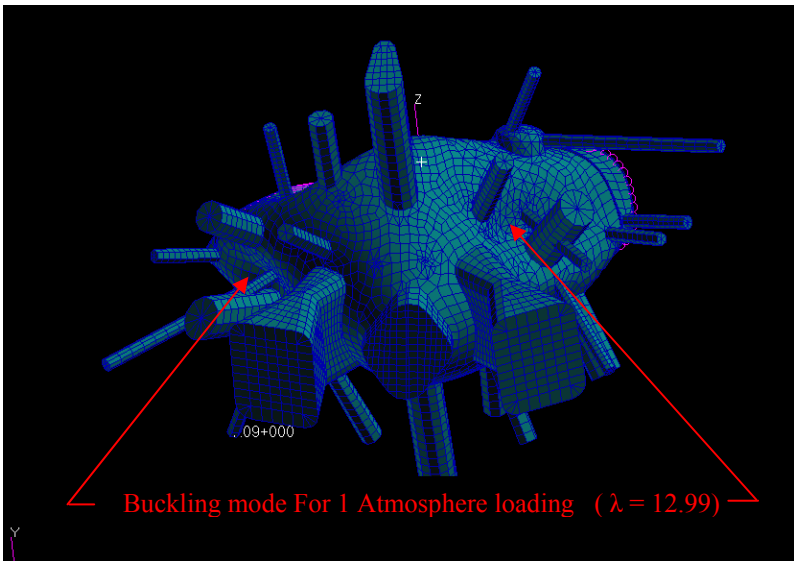

Figure 15. Run 120bbe3-buckle – Pre-load: 1 Atmosphere, Eigenvalue extraction method: Lanczos

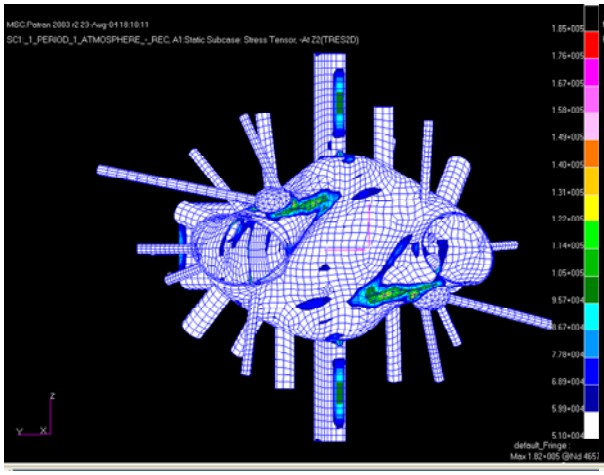

Figure 16a. Tresca Peak Stress 185 ksi (12.99x) (Stress range > 60 ksi)

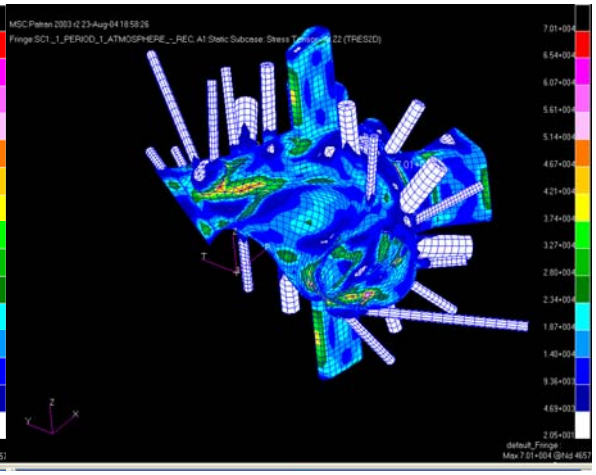

Figure 16b Tresca Peak Stress 68 ksi (5x) (Full stress range contours)

Disruption Loads:

Three disruption loading conditions were considered:

- VDE – 320kA plasma @ 1.7 Tesla (Stationary – but plasma displaced 10 cm upward)
- Ohmic – 320kA plasma @ 1.7 Tesla (Stationary)
- High Beta – 210kA plasma @ 2 Tesla (Stationary)

These disruptions are assumed to occur instantaneously and are modeled with the fully inductive SPARK solution (from Spark ver.20b). Plasma Driver Modeled (single filament on axis) for three scenarios from Tech Data Sheet TDS_C07R00_I

Summary of Disruption Forces

	Current, kA		Loads from:	Forces, Newtons			Moments, Newton-meters		
Scenario	Toroidal	Poloidal		Fx	Fy	Fz	Mx	My	Mz
		(per period)			1st Period (-60 to 60 deg)			1st Period (-60 to 60 deg)	
2T_HighBeta	-210	-26.8	Self	17678	-390	0	-2193	-96	-403
			Coils	-43995	991	902	18609	714	-1957
			Total	-26317	601	902	16417	618	-2361
320kA_ohmic	-320	-44.3	Self	42081	-821	-33	-5797	-183	-985
			Coils	-86871	1843	1719	8790	1009	-3060
			Total	-44790	1022	1685	2994	826	-4045
320kA_VDE	-320	-45.2	Self	42242	341	281	-4840	4909	-1615
(Plasma Current displaced 10 cm vertically)			Coils	-90785	45722	24836	14999	-12415	16921
			Total	-48543	46062	25117	10160	-7507	15307

VDE Disruption:

Figure 17 is a vector plot of the resulting Lorentz EM self forces applied to the model grid points as a result of the VDE 10 cm upward plasma displacement and disruption. These are forces resulting from the induced eddy currents reacting with their self fields (ie. With no external PF or TF superimposed). The highest radial and vertical forces are seen to be concentrated in a relatively narrow band on the inner midplane portion of the shell.

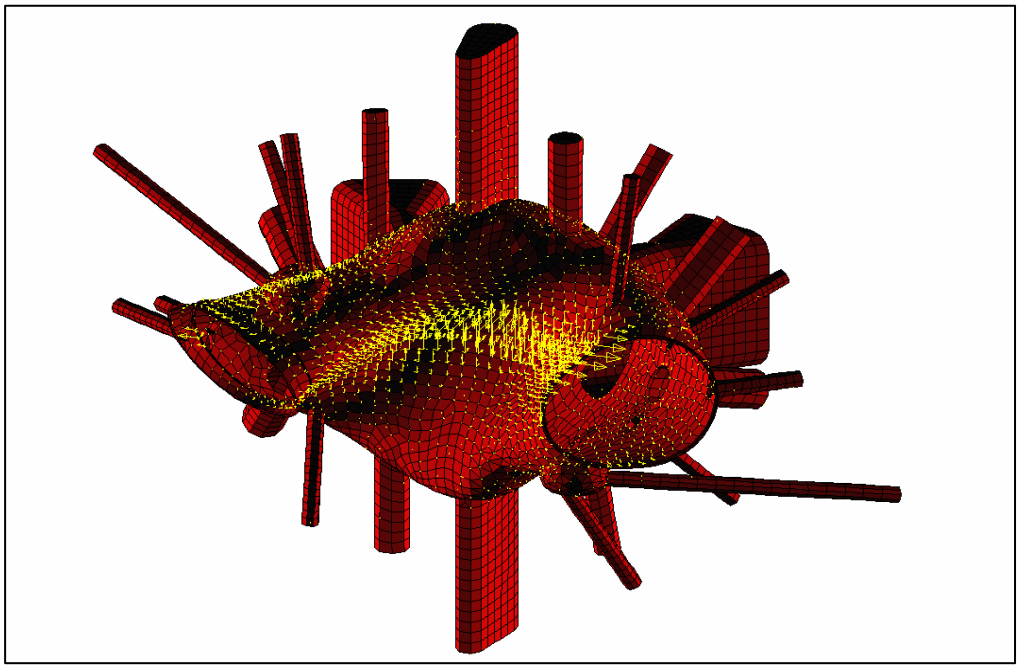

Figure 17. Force Distribution From VDE-UP(Self Forces) – 1.7 Tesla, 320kA Plasma Current Stationary

Figure 18. below is a vector plot of the Lorentz forces due to the external field interaction with the induced eddy currents in the vessel. These forces while also concentrated around the inner shell, tend to be more diffuse and extend further above and below the mid-plane of the vessel.

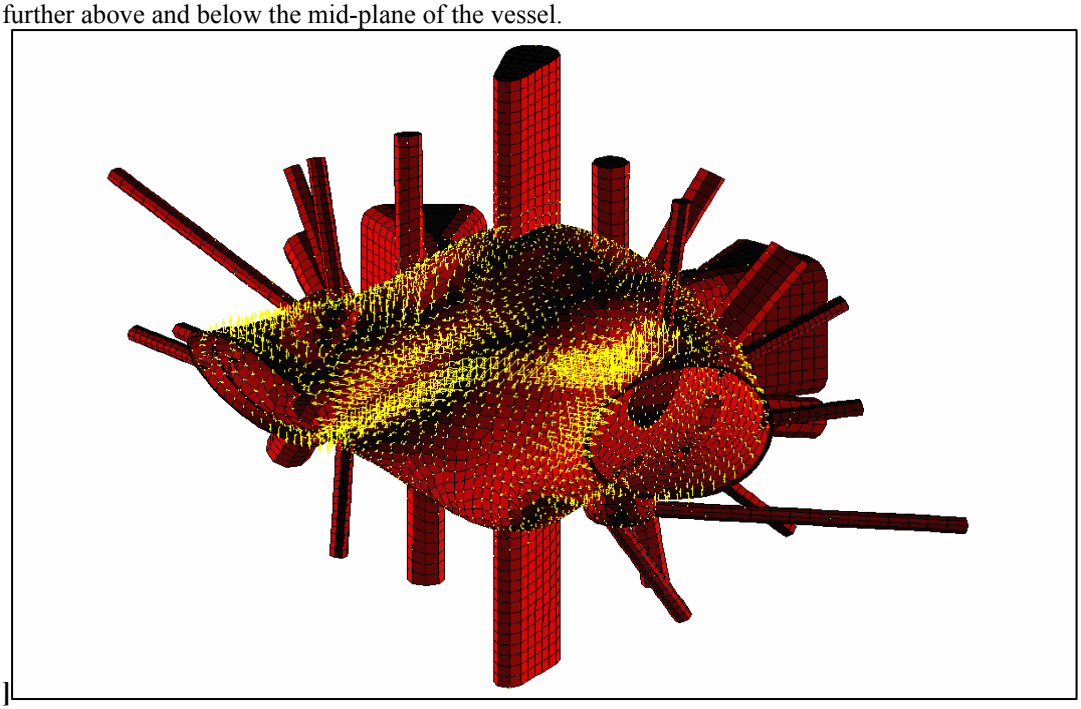

Figure 18. Force Distribution From VDE-UP(External Field Forces) – 1.7 Tesla, 320kA Plasma Current Stationary @ 10cm

Figure 19. shows the contours of Tresca stress on the outer surface (Z1 surface) for the VDE disruption, including 1 atmosphere of external pressure and gravity, with the peak stress intensity (Tresca stress) of 22 ksi occurring at the nozzle-shell intersection of port-10. The peak primary (bending) stress intensity of 17.6 ksi in the shell is also indicated at the upper and lower regions of high curvature in the shell.

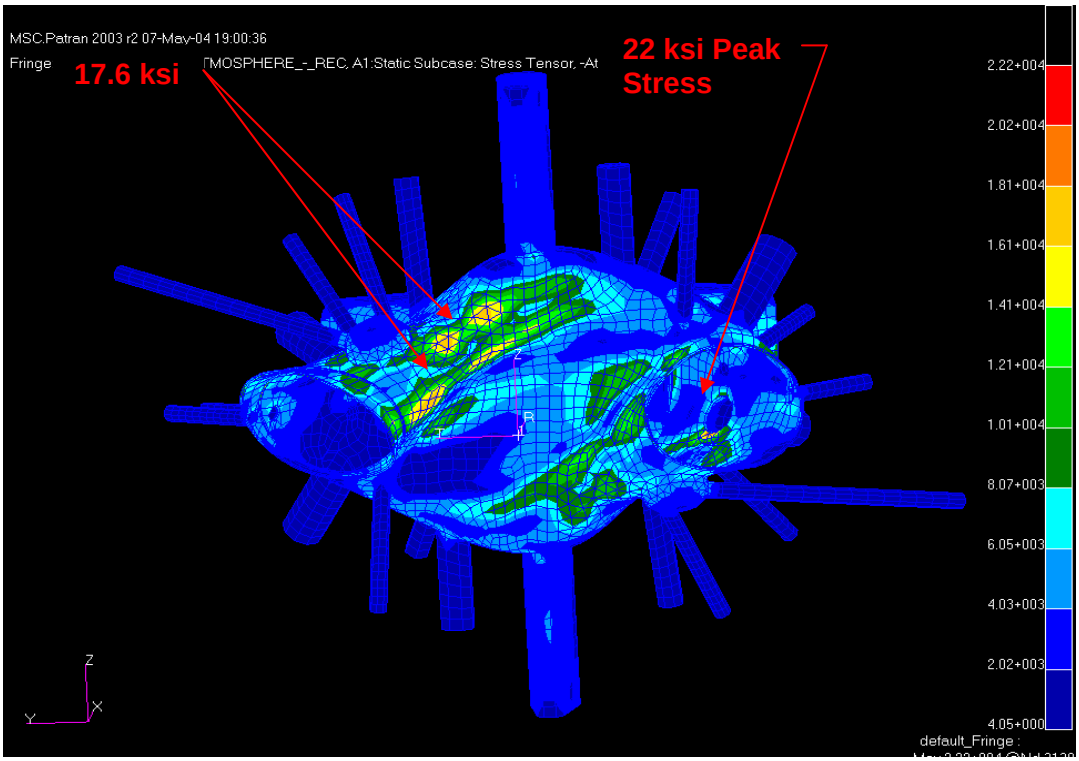

Figure 19. Tresca Stresses-Z1 (outer) Shell Surface For VDE-UP Eddy Currents + Atmospheric Pressure + Gravity (Run: 120bbe2a-VDE)

Figure 20. shows the peak Tresca stress contours for this loading condition on the inner shell wall with the peak stress of 17.2 ksi at the intersection of the RF port turret with the shell. In addition to these localized stresses the highest Tresca stresses (in the range of 15 – 17 ksi) in the high curvature regions (top & bottom) are also due primarily to bending in these regions.

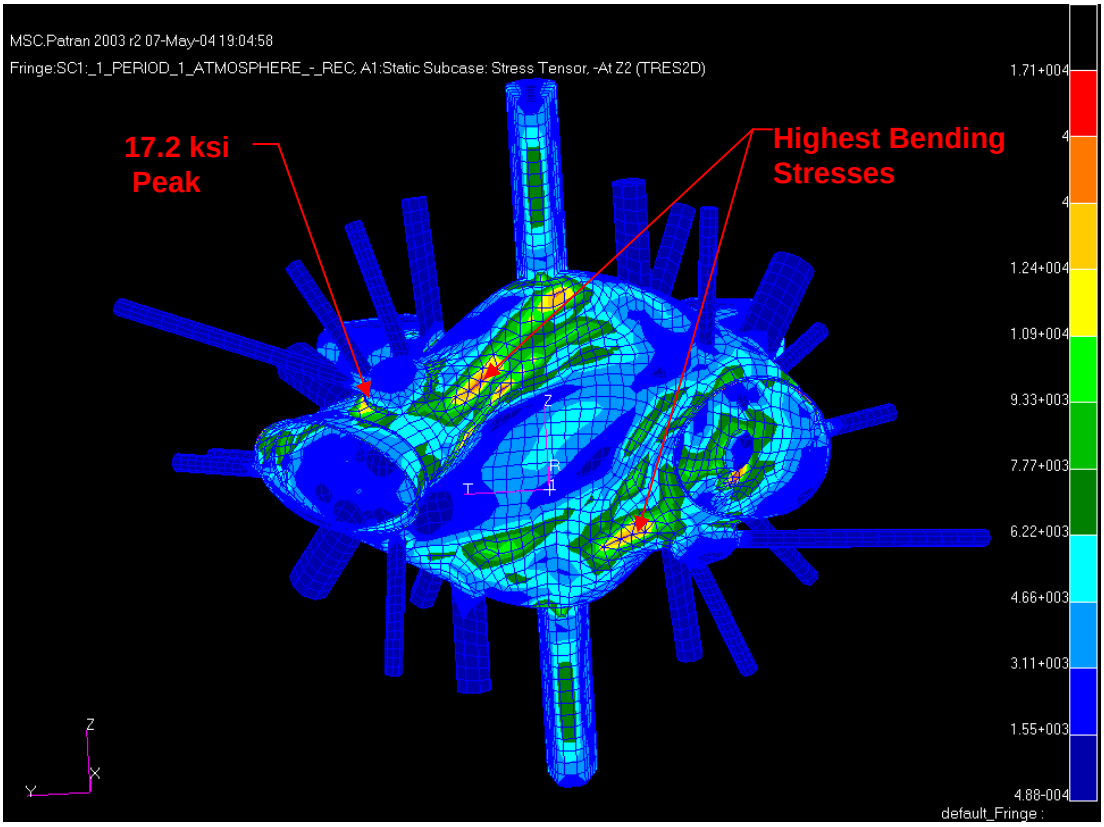

Figure 20. Tresca Stresses-Z2 (inner) Shell Surface For VDE-UP Eddy Currents + Atmospheric Pressure + Gravity (Run: 120bbe2a-VDE)

High Beta Disruption:

Figure 21a. is a vector plot of grid point forces (self forces) for a high beta, 2 Tesla disruption and 21b. for the external field forces.

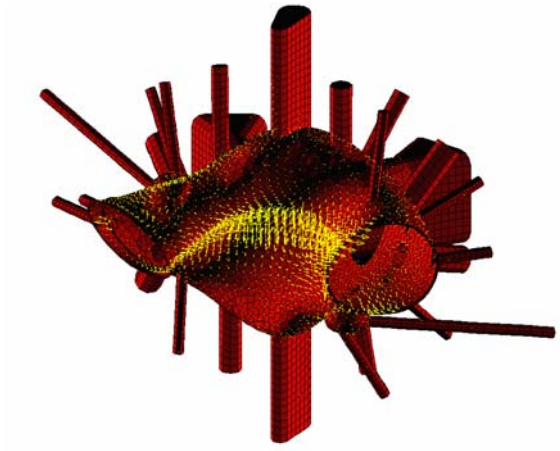

Figure 21a. High Beta self forces

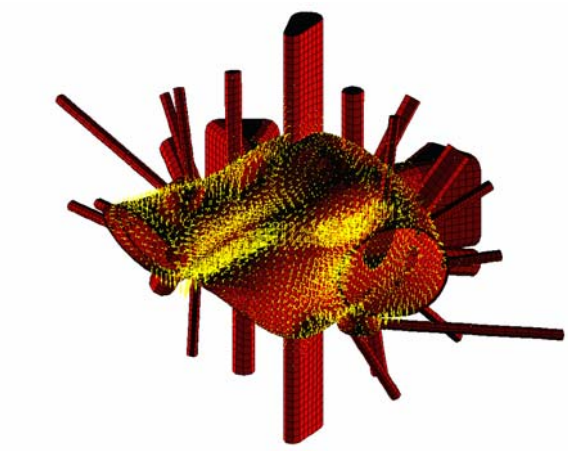

Figure 21b. High Beta forces from external fields

Results or the high beta disruption load case are summarized in in Figures 22a & 22b for the displacements and the Tresca stress contours in Figure 23 below. The peak Tresca stress is 17.1 ksi on the outer surface, and is seen to be in the region of maximum curvature.

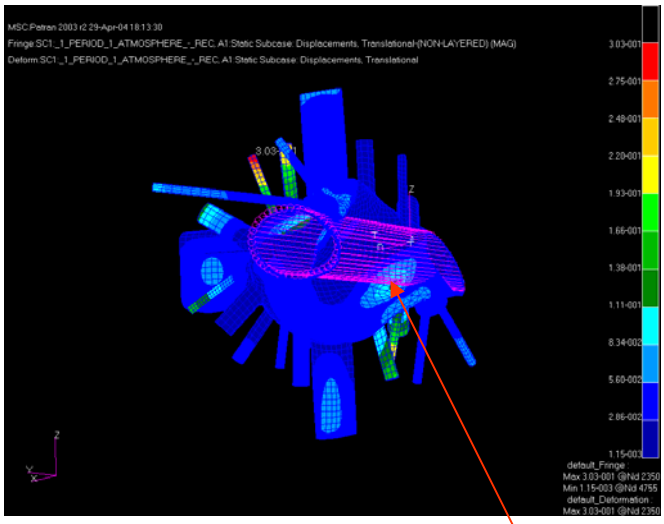

Figure 22a Inner shell wall displacements

Peak Displacements Inner Wall: 0.138”

Peak Displacements Outer Wall: 0.166”

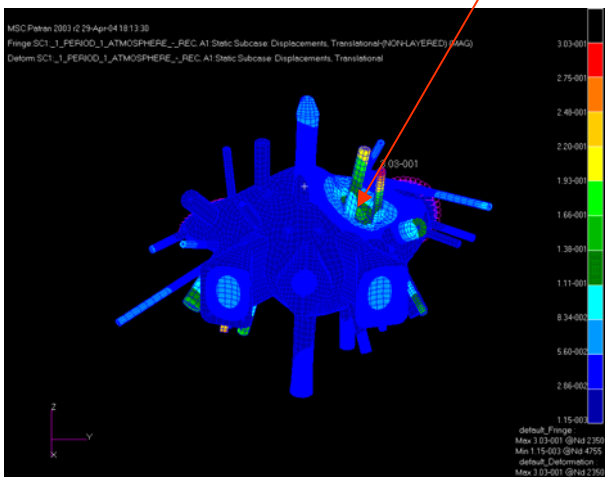

Displacements Due to High Beta Disruption
Run: 120bbe2a-HighBeta

Figure 22b Outer shell wall displacements

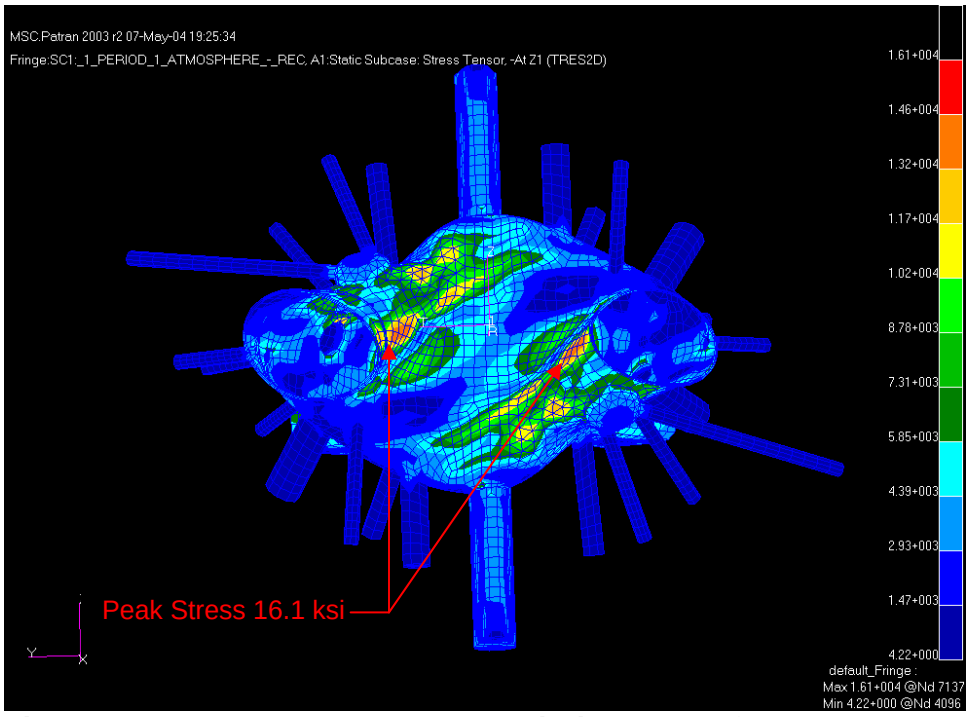

Figure 23. Tresca Stress Contours on (Z1) Outer Surface.

Ohmic Disruption:

Figures 24a & 24b are the self forces and external field forces for an Ohmic disruption condition.

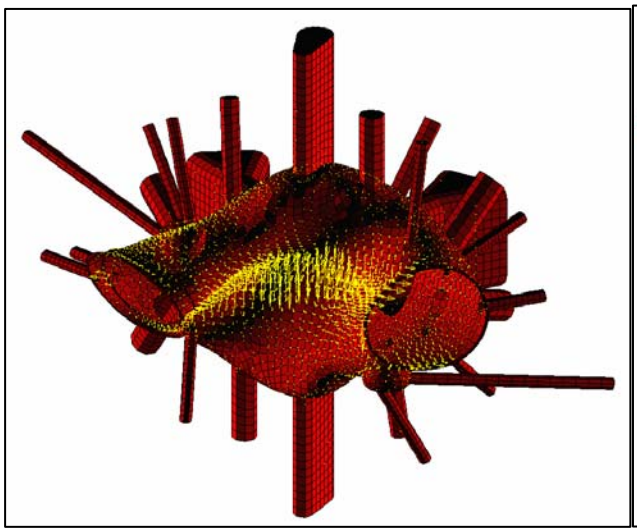

Figure 24a. Ohmic Disruption Self Forces

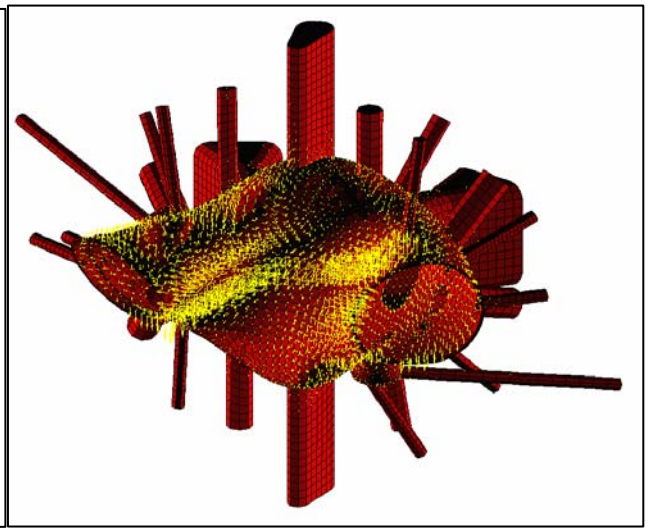

Figure 24b. Ohmic Forces From External Fields

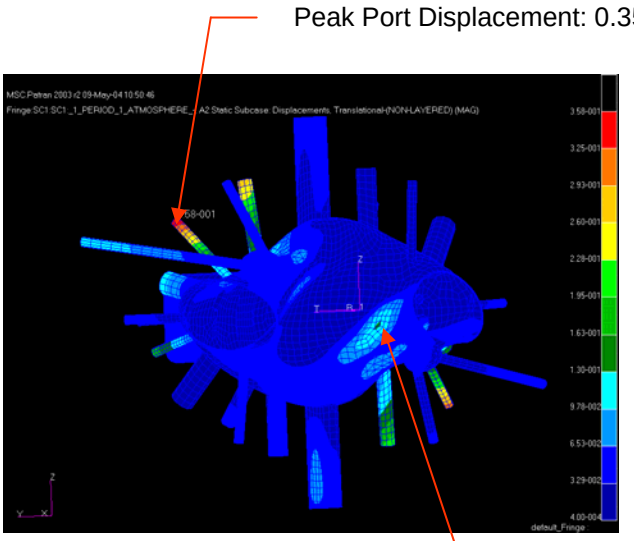

Figure 25a Displacements due to ohmic Disruption (+Atmospheric + Gravity)

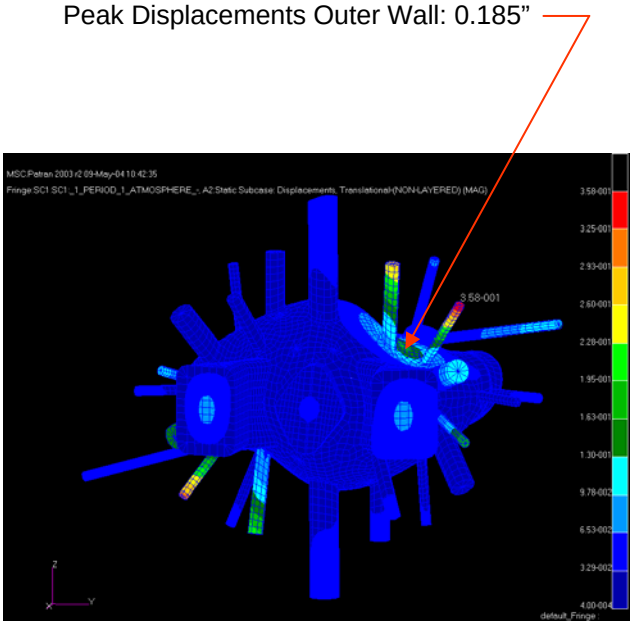

Figure 25b Displacements due to ohmic Disruption (+Atmospheric + Gravity)

The maximum displacements are seen in Figure 25b to be 0.185” for the unreinforced region between ports 2 and 9. The majority of this displacement is due to the atmospheric loading.

The Tresca Stress contours for the Ohmic disruption are shown in Figure 26 below and indicate a peak stress of 16.1 ksi on the Z2 (Inner) surface, again in the area of highest curvature in the upper and lower regions of the shell.

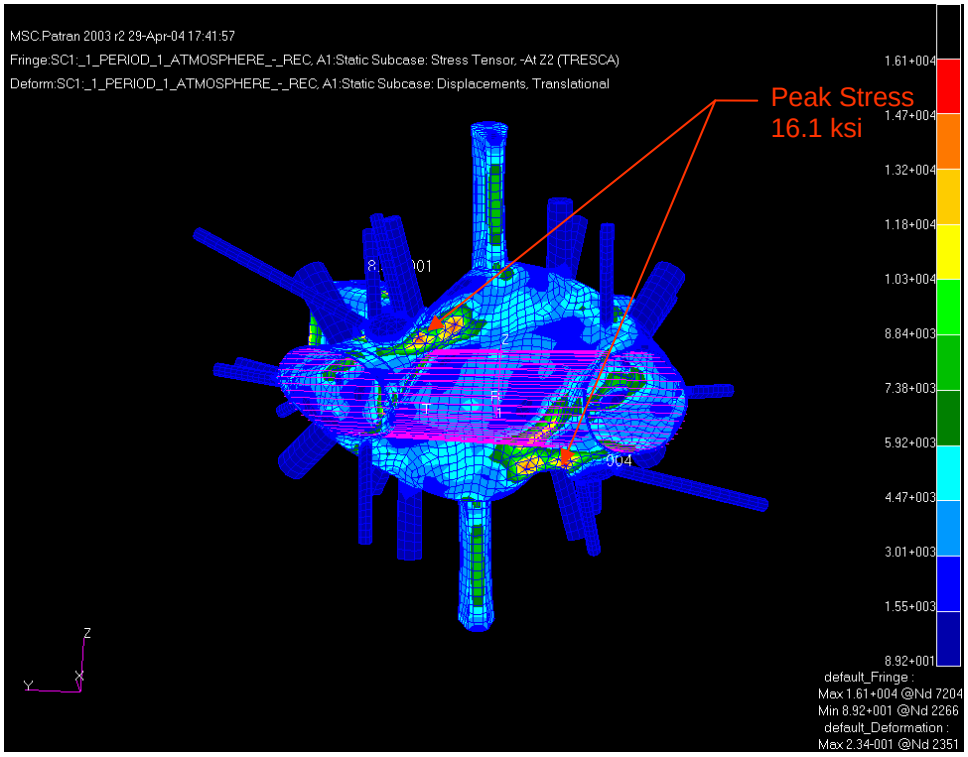

Figure 26. Tresca Stresses-Z2 (inner) Surface For Ohmic Eddy Currents + Atmospheric Pressure + Gravity. (Run: 120bbe2a-OHMIC)

Dynamic Effects:

Assuming a worst case amplification of the most severe disruption loading, 2 x VDE statically applied represents an upper bound on the vessel structural response (structural damping and off-resonance attenuation will produce a much less severe response). Figures 27a & 27b below are the Tresca stress contours on the inner and outer shell surfaces for this upper bound loading condition.

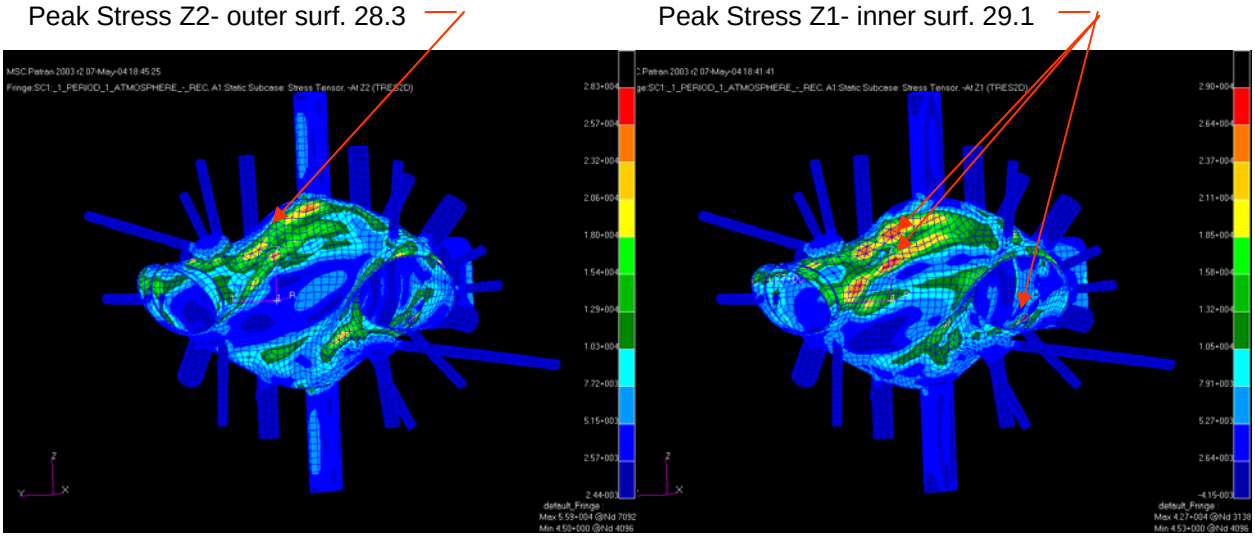

Figure 27a. Tresca Stress on Z2 (outer)surf. Figure 27b Tresca Stress on Z1 (inner) surf.

Even with this extreme loading condition the peak stress intensity is below the design allowables for Inconel625.

Modal Analysis:

Figure 28 is the primary mode shape extracted from a modal analysis of the vessel structure. The period T is seen to be approximately 1.25 seconds and is a rocking mode around the two vertical suspension rod supports which straddle the top of the Neutral Beam (N.B.) port (with circumferential restraints at the top and bottom of the N.B. port).

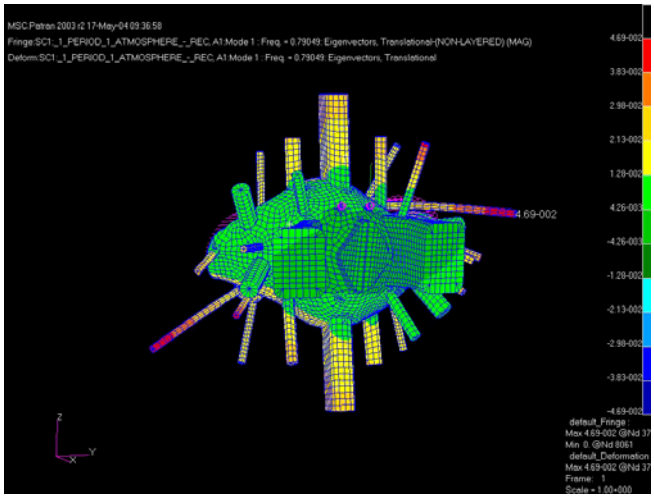

Figure 28a. Primary flexible mode for two upper suspension rod supports

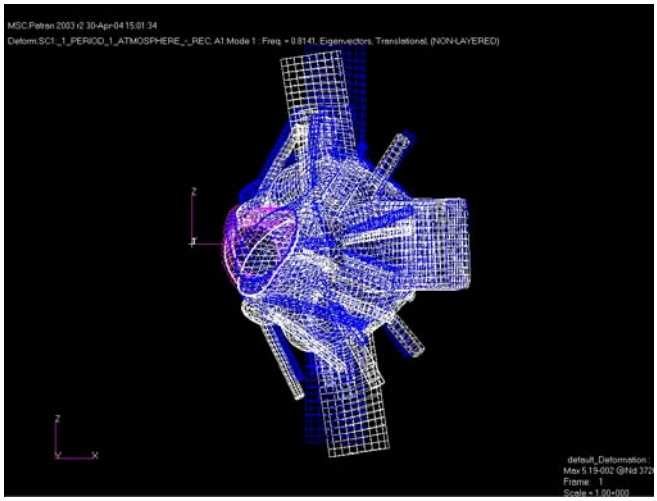

Figure 28b. Side view of the rocking mode

Figure 29 is a plot of a typical DLF (Dynamic Load Factor) plotted against the ratio of the loading period to natural period of a structural system. The two curves represent the response amplification (>1.0) or attenuation (<1.0) to a step (Rectangular - instantaneous) loading and a ramped loading cycle (Triangular - similar to a postulated plasma disruption loading). For a T_d/T ratio of 0.04 (assuming a 1MA/msec. postulated plasma disruption), the DLF will be ~0.14 indicating a weakly coupled structural response to loads applied in this frequency range.

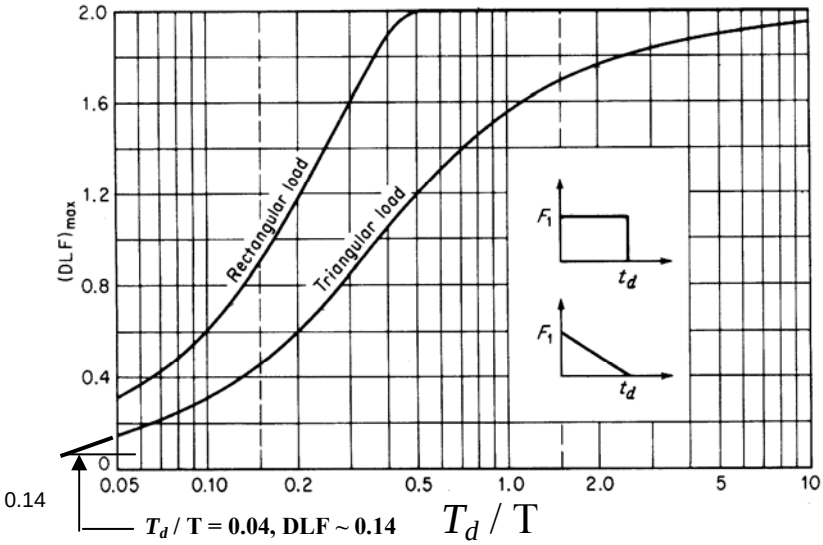

Figure 29. Maximum Dynamic Load Factors

The actual plasma disruption frequencies cannot be determined at this juncture but the 1MA/msec. disruption postulated should represent the upper bound frequency for disruptions. The frequency would have to be more 10 times lower to produce loads in excess of the static loads considered in this analysis (ie. DLF > 1.0).
In reviewing the results of the modal analysis, several low frequency 2-10 Hz (in addition to the rocking mode) were also present in the structure mostly involving vertical and lateral displacements of the thinner walled cantelevered ports. These low frequency modes are typically in the peak range of seismic accelerations and are addressed in P. Titus memo included in Appendix A of this report.

Fatigue & Creep:

Areas where local bending + membrane stress may exceed yield, and areas of discontinuity or stress concentration were evaluated for fatigue. The primary cyclic loading (apart from the low number of pump-down/bakeout cycles) will be disruption loads. Assuming a conservative estimate of 5 disruption loads per day, over 10 years of operation, the cumulative number of cycles will be ~12,500. The stress range will vary based on location and residual stress. Specialty Metals/Huntington Alloys data shown in Fig. 30, indicates a fatigue life well in excess of 100 million cycles at the maximum anticipated cyclic stress for the base metal.

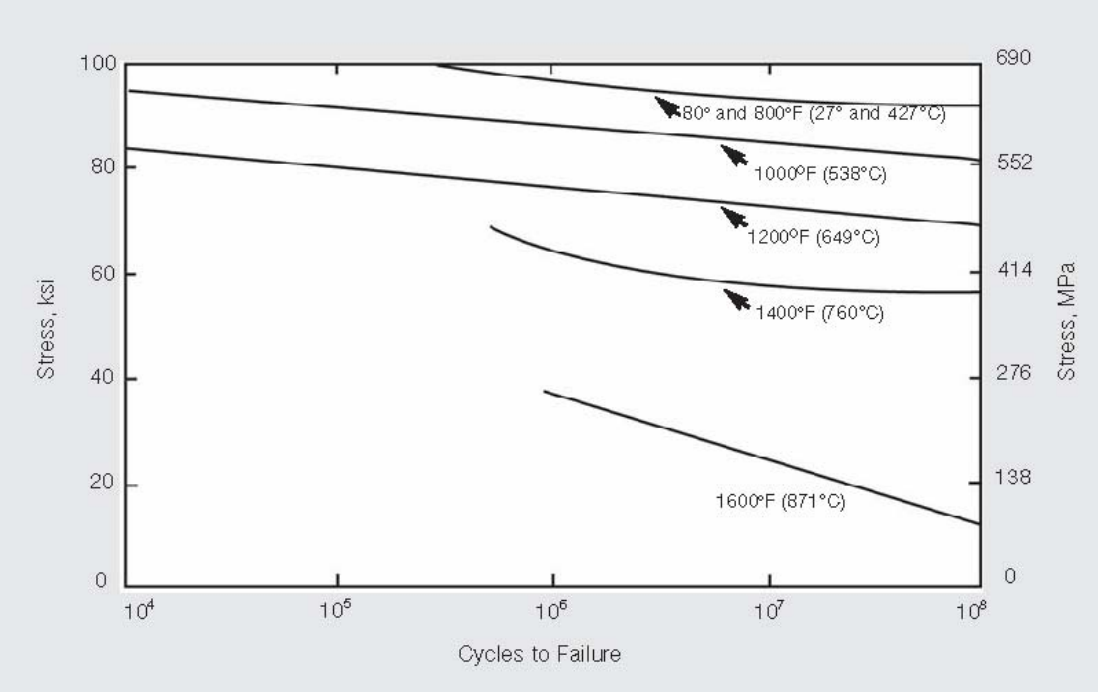

Figure 30. Fatigue of Hot rolled and annealed 625 Inconel (rotating beam data)

For weld filler material, the literature indicates high margins for the cycle life and stress range anticipated. After accounting for shakedown, all stress excursions will fall well within the elastic range for all loading conditions considered. Figures 31 and 32 indicate the as welded properties (625 filler) and creep-rupture properties (for a similar 112 filler material).

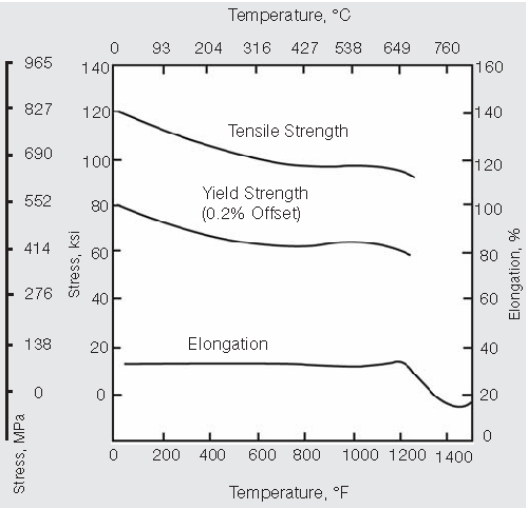

Figure 31. GTAW weld properties 625

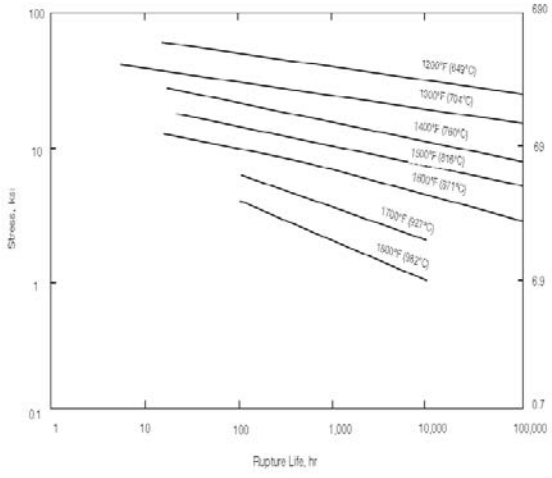

Figure 32. Creep-Rupture Properties 112 filler

The creep-rupture properties at the maximum bakeout temperature of 400 C are extremely good for this material (Inconel 625) with rupture life in excess of 100,000 hrs (11.4 years) for the peak stress levels calculated. Figure 33 shows the typical rupture life of the material. The accumulated vessel exposure to bakeout temperatures is not expected to exceed 10% of the rupture life (10,000 hrs).

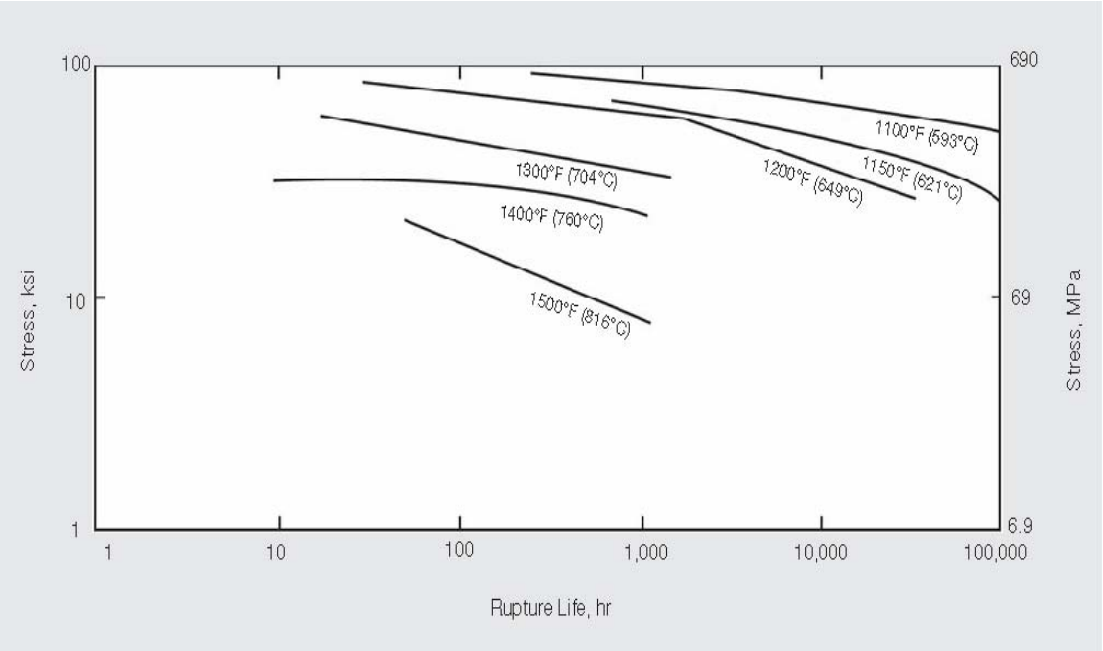

Figure 33. Creep-Rupture Properties of 625 Inconel at High Temperature

Analysis of Allowable Stress Results:

The main results of the analysis are summarized in Table 2 below

Table 2. Comparison of Stress Intensity results with Code Allowables

Loading	Peak Stress Intensity (ksi)	Stress Category (per ASME BPVC)	Weld Efficiency (c) No Rad. Insp.	Allowable Stress (ksi) (for category)	Safety Margin (above Allow.)	Notes
Press.	16.1	PL + Pb	0.7 -> 23.0 ksi	1.5 x Sm 50.1	2.1	@Turret
Press. + Grav.	15.7	PL + Pb	0.7 -> 22.4 ksi	1.5 x Sm 50.1	2.1	@Turret
Press. + Grav. + 500lb Cant.	34.3	PL +Pb + Q	0.5 -> 68.6 ksi	3.0 x Sm 100.2	1.4	@Turret RF-1 Administratively controlled
Ohmic Disrupt. 320kA-1.7T(+P+G)	17.7	PL + Pb	0.7 -> 25.3 ksi	1.5 x Sm 50.1	2.0	@Turret DLF = 1.0 (s/b less ~ 0.12)
Hi-Beta Disrupt. 210kA-2.0T(+P+G)	16.1	PL + Pb	0.7 -> 23.0 ksi	1.5 x Sm 50.1	2.1	@weld flange DLF = 1.0 (s/b less ~ 0.12)
VDE Disrupt. (+P+G) 320kA-1.7T-10cm	27.6	PL + Pb	0.7 -> 39.4 ksi	1.5 x Sm 50.1	1.2	@weld flange DLF = 1.0 (s/b less ~ 0.12)
Press. + Grav. +Thermal 400 C	31.0	PL + Pb + Q	0.5 -> 62.0	3.0 x Sm 100.2	1.6	@NB-Port Excessive gradient assumed

The ASME Pressure Vessel Code Criteria is summarized below:

Table 2B – Section II of the ASME BPVC indicates a design stress intensity (S**m**) of 30.4 ksi at the maximum operating temperature of 750 deg.F (~400 deg.C). For normal operations the maximum operating temperature will be 400 deg.F (~200 deg.C), for which S**m** is 33.4 ksi. Appendix 4, Section VIII – Division 2 the general stress criteria and categories for vessel design based on stress analysis:

Category	Description	Not to exceed
P**m**	Primary membrane Stress (Average across solid section, produced only by body forces and mechanical loads).	1.0k x S**m**
P**L**	Local Primary membrane Stress (Average stress across solid section, includes discontinuities but not Stress concentrations).	1.5k x S**m***
P**b**	Primary bending stress (Stresses proportional to the distance from the centroid of a solid section – excludes discontinuities & str.conc.).	1.5k x S**m***
Q	Secondary Membrane + bending stresses, self equilibrating, due to thermal or mechanical loads, or discontinuities (excludes local stress concentrations.	3.0k x S**m****
F	Incremental stress added by stress concentrations (notch), thermal stresses producing thermal fatigue.	na

* Pl or Pl + Pb < 1.5k x Sm, (k typically = 1.0), ** PL + Pb + Q < 3.0k x Sm (stress intensity range)

VI. Summary and Recommendations

A review of the vessel stress analysis indicates the following:

- For normal operating conditions at 200 deg.C the worst case disruption loading (including 2X dynamic load factor) will produce a stress intensity of 49.1ksi in the flange at the interior flange surface. Since this may be considered a primary bending stress **Pb** the allowable (not to exceed) stress will be:
  SPeak Tresca = 49.1 < 1.5k**Sm** = 50.1 ksi

- For Bakeout at 400 deg.C (max temp) under gravity and atmospheric pressures:

  SPeak Tresca = 31.0 < 1.5k**Sm** = 45.6 ksi (lower due to higher operating temp.)

- For 200 deg.C worst case Tresca stress at welded sections:
  The peak VDE-2X Stress @ the lower port-10/shell intersection is 33.4 ksi.
  With a weld efficiency of 0.50:
  SPeak Tresca = 33.4/.50 = 66.8 ksi < 3k**Sm** = 100.2 ksi

Since this stress intensity includes primary + secondary stresses the code permits a value of 3k**Sm** for the total range of stress intensity. The rational for this is the assumption that some localized plastic deformation in ductile materials is permissible during shakedown as long as the subsequent stress range in the locally yielded regions will remain in the elastic range.

Conclusions & Recommendations:

Stresses from the normal operating load runs in the shell and ports are generally well below the code allowable stress with the exception of the Port-18 & 15 cantilevered loading condition.
Recommend either:
a) thickening the turret wall and port nozzle to reduce stress at the nozzle/port intersection and to reduce vertical deflections of the port,
b) implement a radially compliant vertical nozzle support off the cryostat, or
c) limit the cantilevered loading on Port-15 and the RF ports.

Shell displacements for normal operations are generally low with the exception of the area between port-2 and port-9 which indicate a displacement of 0.125" total. This may be reduced by thickening or reinforcing the shell locally to reduce these deflections if necessary.
Dynamic loading from VDE plasma disruptions are the most severe but the peak (Main flange) stress intensities are below allowables for the full 1.0x DLF (Dynamic Load Factor). Where we assume the interior welds in the peak stress (flange) regions experience the same stresses, and using a weld efficiency of 0.7, we have a margin of 20% on code allowables.

Critical Buckling loads were calculated by using Nastrans' eigenvalue extraction of the lowest buckling mode for each loading condition specified. For the worst VDE disruption load (using DLF=1.0) the critical load factor was 12. Due to the irregular shape of this vessel local buckling modes predominate.

Modal analysis indicates the undamped primary structural mode of 0.8 Hz with the vessel rocking on the vertical supports. Numerous low frequency modes are present in ports 15, 2, 9, rf-1 & rf-2. Several are in the frequency range of earthquake spectrum and are anticipated to participate in the horizontal and vertical accelerations of any seismic event. Since their mass is relatively low, and deflections of these ports are limited by the Cryostat penetrations, no significant permanent damage to the vessel or structure from a seismic event is anticipated although some dampening, perhaps from the cryostat boots and feed-thrus might be implemented with good effect here.

Areas where local bending + membrane stress may exceed yield, and areas of discontinuity or stress concentration must be evaluated for fatigue. The primary cyclic loading (apart from the low number of pump-down/bakeout cycles) will be disruption loads. Assuming a conservative estimate of 5 disruption loads per day, over 10 years operations, the cumulative number of cycles will be ~12,500. The stress range will vary based on location and residual stress. Manufacturers data indicates a fatigue life well in excess of 100 million cycles at the maximum anticipated cyclic stress for the base metal. For weld filler material, the literature indicates high margins for the cycle life and stress range anticipated. Accounting for shakedown, all stress excursions will fall well within the elastic range for all loading conditions considered.

The creep-rupture properties at the maximum bakeout temperature of 400 C are extremely good for this material with rupture life in excess of 100,000 hrs (11.4 years) for the peak stress levels calculated.

NCSX VACUUM VESSEL STRUCTURAL ANALYSIS

APPENDICES – A & B

PSFC/JA-03-

DRAFT

SEISMIC ANALYSIS OF THE NATIONAL COMPACT STELLERATOR (NCSX)

Peter H. Titus

May 17 2004 Revision

MIT Plasma Science and Fusion Center
185 Albany Street, Cambridge Ma 02139

1 2

Table of Contents

1.0 Introduction

Seismic analysis and qualification of NCSX is presented. DOE requirements as outlined in DOE-STD-1020-2002 are followed for determination of the necessity for seismic qualification of the stellarator and its related systems. IBC-2000 is followed for the qualification requirements. The stellarator presents minimal occupational hazards and hazards to the public. The qualification effort is intended to preserve the viability of continuing the experiment after an earthquake, and to explore the sensitivity of the design to dynamic loading from sources other than normal operation. A response spectra modal analysis has been employed. The model is an assemblage of the simpler models of the vessel, and modular coil shells; being employed to qualify these components for normal operational loading. Outer TF and PF coil models and models of the cold mass supports have been generated and added to form a complete model of the stellarator system. The scale of the model is limited by the computational capacity of the windows/Intel system used for the analysis, and the efforts to control runtimes and file sizes are described. Much of the stellarator is robust to resist normal Lorentz forces. Areas sensitive to lateral loads and dynamic application of non-Lorentz loading, include the nested cylinder cold mass support columns, cantilevered vessel ducts, and the radial guides connecting the vessel ducts and modular coil shell. Loads on these structures are quantified, and design adequacy is assessed.

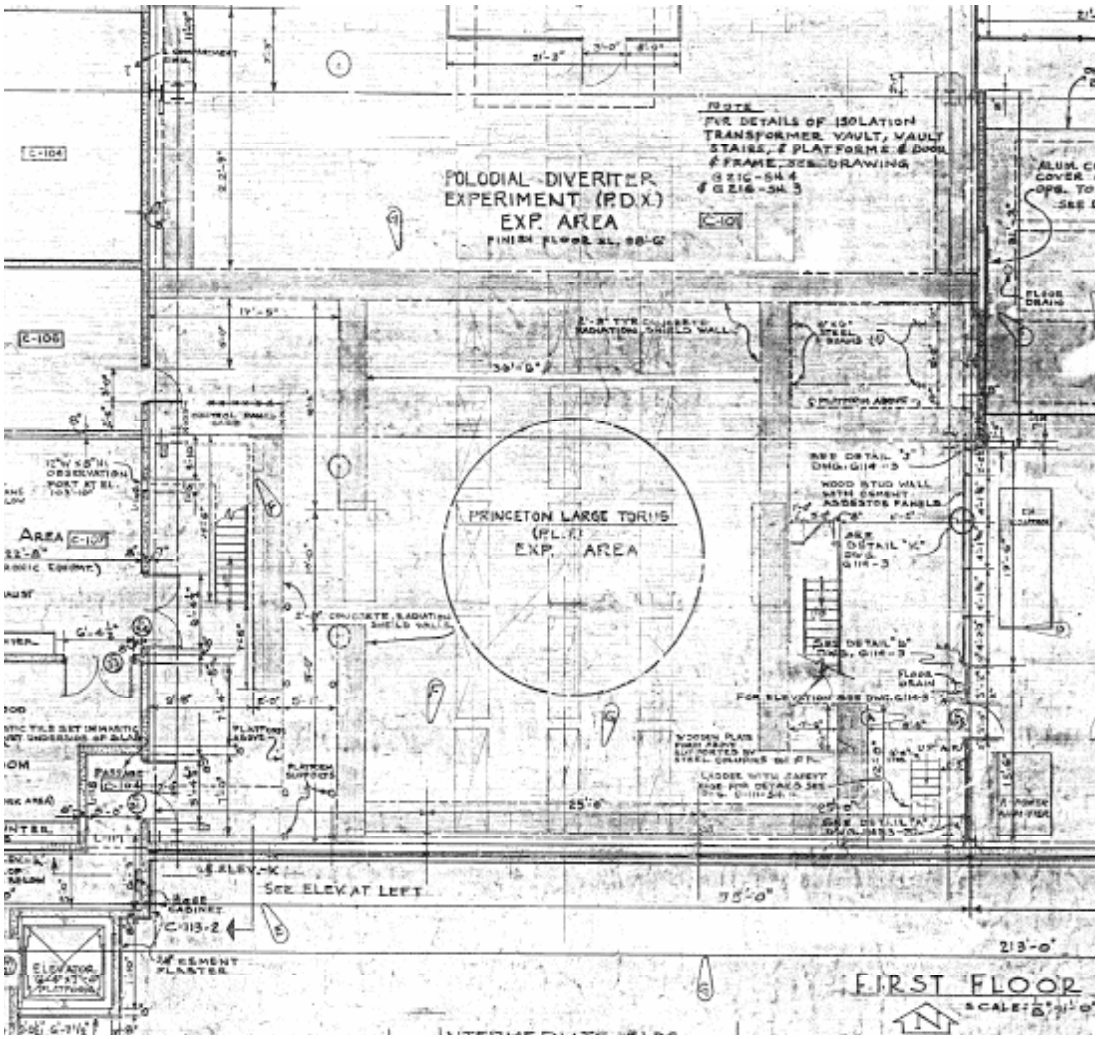

Figure 1.0-1 NCSX will be located in the PLT test cell.

2.0 Summary of Results

The main elements of the Stellarator are robust to take their normal electromagnetic, thermal and "disruption" loads. The gravity support was not analyzed in detail statically prior to this seismic analysis effort, and to form a baseline for stress evaluation, the gravity support was analyzed for cooldown and deadweight. The complex model used for this analysis was probably not necessary. The fundamental mode was a lateral translation with the support columns cantilevered and displacing with clamped –guided end fixity. There was some rocking behavior along with the shear translation, but the first mode behavior could have been obtained with a simple lumped mass-beam model. This lowest frequency mode was 2.1 cps. Entering the ARS this would yield a global acceleration of .72 g in each of the horizontal directions. The next series of mode shapes involved the ports as rigid "sticks" rotating about their connection with the vessel shell with the local shell flexibility providing the rotational spring rate. These make for "wild" looking mode shape animations. Some of these are posted at http://www.psfc.mit.edu/people/titus/ under NCSX memos. Vertical response is ignored in this analysis. At .15 g in the TFTR cell data, combined using SRSS, it would contribute little to the response of the stellarator.Within the stellarator the seismic stresses are modest. Interesting stresses occur at the port/vessel connections and in the support columns. Because of the size of the model, the number of modes extracted must be limited. In run#7 only 10 modes were extracted. Stress results were checked with a second analysis (run#10) with 14 modes extracted and the peak column support stress went from 165 MPa to 167 Mpa.

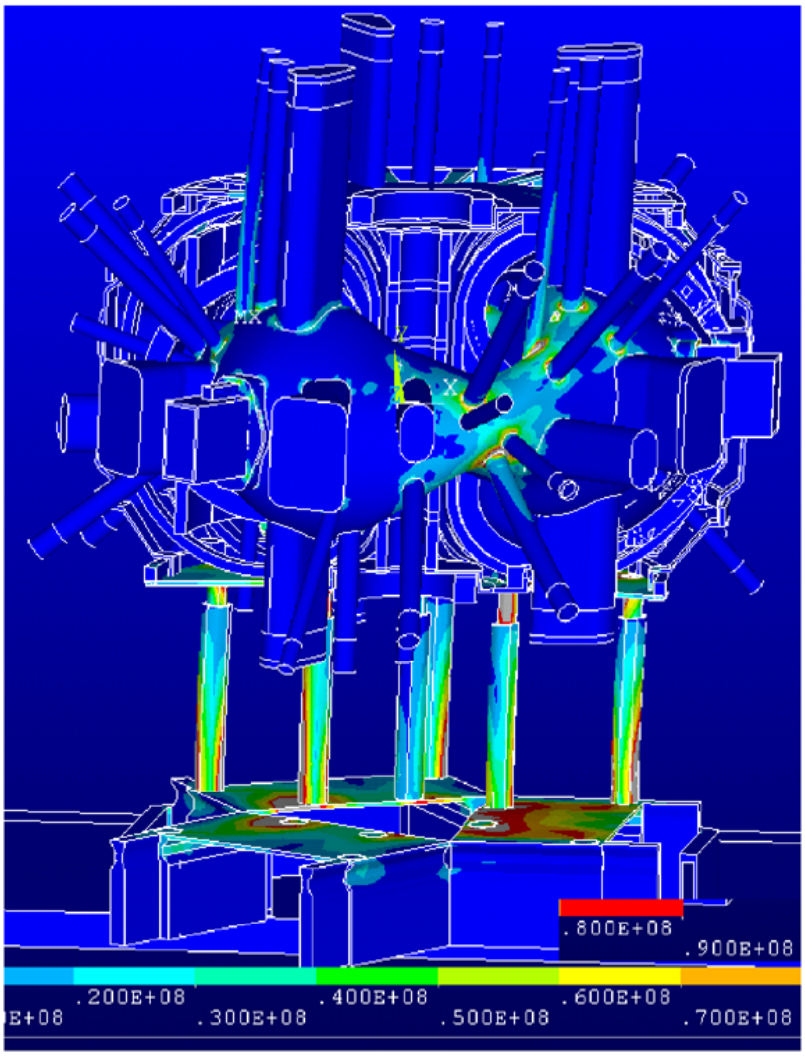

Figure 2.0-1 Seismic Stresses are significant in the support columns, and in the vessel due to port and port extension motions

Figure 10.2-2 shows the restraint link axial stress of 25.1 Mpa. These are modeled as having a 1 square inch cross section, and as taking tension and compression, but the design appears to allow only compression. The load at each restraint is :25.1e6/6895*2* 1.0in^2= 7251.6 lbs

Table 2.0-1Stress in MPa

Component	D	P	TO	FDBE (1)	IR	Total Stress	Allow*K	
Outer Support Columns	15		90	233		338	330 (289 weld) (3)	.97
Vessel to Port Intersection	90	30		254		374	370.33(4)	.99

(1) Multiplied be SQRT(2) – This accounts for having only modeled one ARS direction.
(2) K=1.2 for Unlikely Events
(3) 316 SST at RT
(4) Inconel 625 from Table 5, ref [10] multiplied by a K value of 1.2

Interface reaction loads are included in the modeling, in that an attempt is made to model the full stellarator system. Preloads are not included.

Stresses in the modular coil shell are significant in the thermal analysis. This was because the lateral struts or jacks were modeled as tight against the vessel lugs. Some gap should be provided to allow these struts to be warm with respect to the shell, or a single radius rod type restraint should be considered. The only appreciable seismic stress is in the vessel lateral support brackets. This does not appear to be a problem. The major loading of this shell are the modular coil Lorentz forces. The areas of the shell which support these stresses are essentially un-effected by the seismic loading.

2.1 Conclusions/Recommendations

The stellarator core and its proposed gravity/cold mass support system meet conservative seismic requirements. There remains a significant amount of work to assess the effects of peripheral systems on the stellarator.

Differential lengths of the vessel hanger rods appear to stress the vessel shell due to differential temperatures between the modular coil castings, and vessel. This should be investigated further.
If lateral restraints are hard up against the port lug prior to cooldown, the bracket stress due to cooldown is large. A one-sided radius rod type restraint might be wiser.

3.0 Criteria

From Ref [2]:

I-1.8 Seismic Loads (FDBE)

The NCSX facility will be classified as a Low Hazard (LC)/Hazard Category 3 (HC3) facility. All Structures, Systems, and Components (SSC) of NCSX shall be categorized in accordance with DOE-STD-1021-93 ("Natural Phenomena Hazards Performance Categorization Criteria for Structures, Systems, and Components," 7/93) to determine the appropriate Performance Category. For those SSCs that require seismic design, the applicable Design Basis Earthquake (DBE) acceleration values and evaluation techniques specified in DOE-STD-1020-94 ("Natural Phenomena Hazards Design and Evaluation Criteria for Department of Energy Facilities," 4/94) and DOE-STD-1024-92 ("Guidelines for Use of Probabilistic Seismic Hazard Curves at Department of Energy Sites," 12/92) shall be used.

I-2.3 Unlikely Events 10-2 > P ≥ 10-4

D + P + TO + FDBE + IR + L
D + P + TO + (EM-F per FMECA)+ IR + L

D=Deadweight, P-Design Pressure, FDBE = Seismic, Design Basis Earthquake, TO=Normal operation thermal effects, IR= Interaction Loads , L=preloads

Unlikely	**In addition to the challenged component, inspection may reveal localized large damage, which may call for repair of the affected components.**	**Material plasticity, local insulation failure or local melting which may necessitate the removal of the component from service for inspection or repair of damage to the component orsupport.**	**The facility may require major replacement of faulty component or repair work.**

• Primary membrane plus bending stresses shall not exceed 1.5 KSm
• For unlikely conditions, K = 1.2; evaluation of secondary stress not required
Input ARS
This comes from ref __ via ref. 7. It is the recommended ground motion, exclusive of any amplification of a building. No seismic analysis of the PLT cell is available. To estimate the effects of building amplification, the TFTR cell results will be used. These were used by Scott Perfect in the TPX gravity support qualification The ground motion ARS peaks out at .36g and the TFTR/TPX ARS peak at around twice this.

	G, Spectral Acceleration	
Period, Sec	MCE	5% Damped MCE
0.00	0.144	0.096
0.05	0.360	0.240
0.20	0.360	0.240
0.24	0.360	0.240
0.30	0.284	0.189
0.40	0.213	0.142
0.50	0.170	0.113
0.60	0.142	0.095
0.70	0.122	0.081
0.80	0.106	0.071
0.90	0.095	0.063
1.00	0.085	0.057
1.10	0.077	0.051
1.20	0.071	0.047
1.30	0.065	0.043
1.40	0.061	0.041
1.50	0.057	0.038
1.60	0.053	0.035
1.70	0.050	0.033
1.80	0.047	0.031
1.90	0.045	0.030
2.00	0.043	0.029

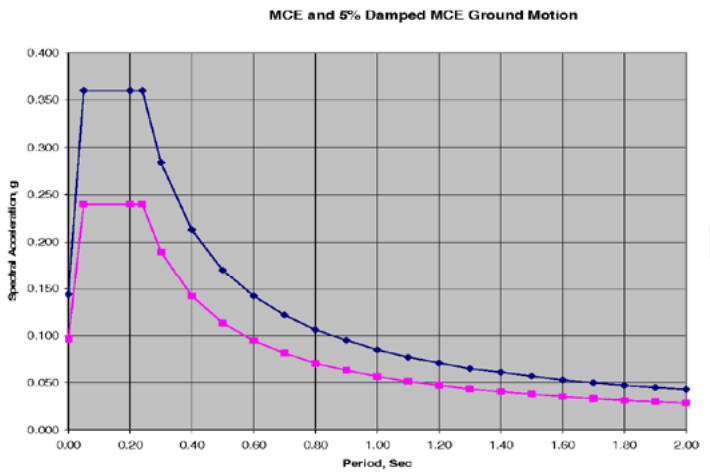

Figure 3.0-1 Required ground motion amplified response spectrum. Dark Blue is MCE and Magenta is 5% Damped MCE

```
!ANSYS SPECTRU INPUT
spopt,sprs,10,yes
svtyp,2,2.0*9.8
sed,1,0,0
FREQ,.55555556,.58823529,.625,.66666667,.71428571,.769
23077,.83333333,.90909091,1
FREQ,1.1111111,1.25,1.4285714,1.6666667,2,2.5,3.333333
3,4.1666667,5
FREQ,20,100
sv,0.0,.047,.05,.053,.057,.061,.065,.071,.077,.085
sv,0.0,.095,.106,.122,.142,.17,.213,.284,.36,.36
sv,0.0,.36,.144
sv,0.05,.031,.033,.035,.039,.041,.043,.047,.051,.057
sv,0.05,.063,.071,.081,.095,.113,.142,.189,.24,.24
sv,0.05,.24,.096
```

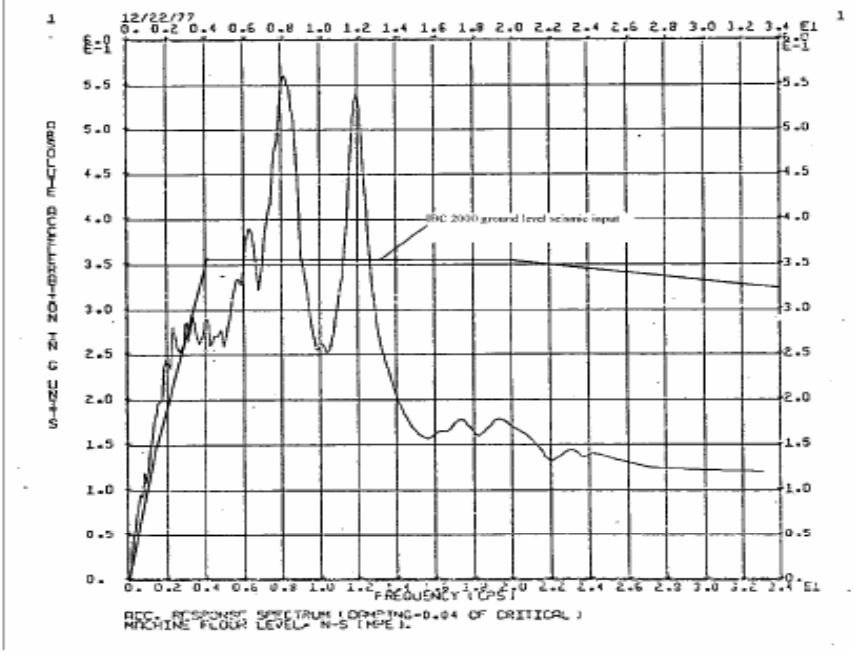

Figire 3.0-2North-South Response Spectrum Curve, TFTR/TPX Test Cell, ref [5]

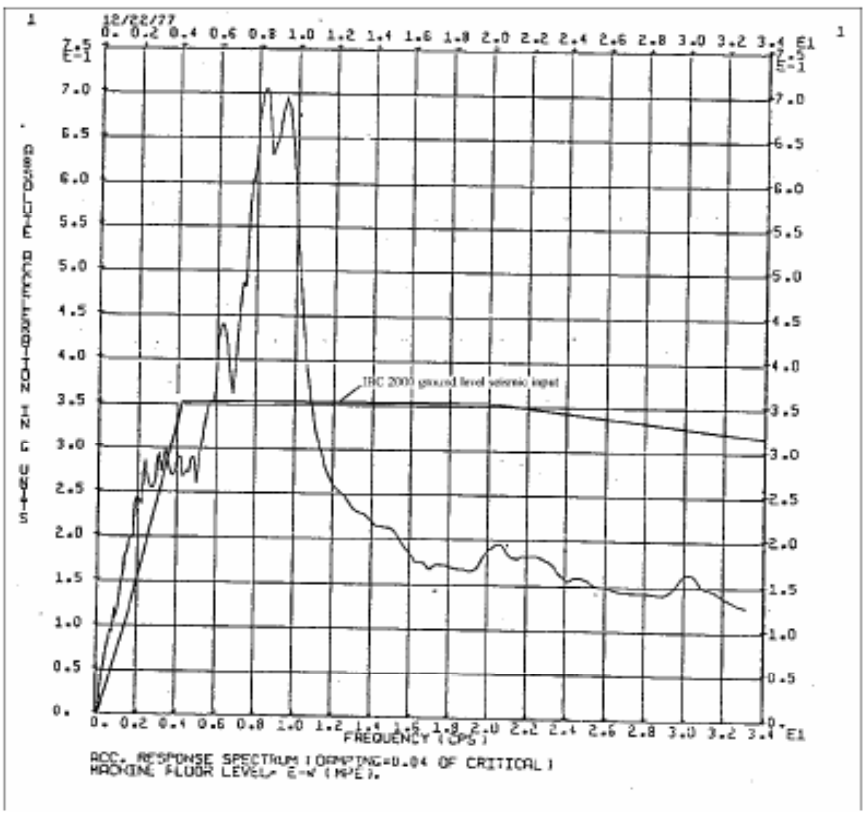

Figure 3.0-3East-West Response Spectrum Curve, TFTR/TPX Test Cell, ref [5]

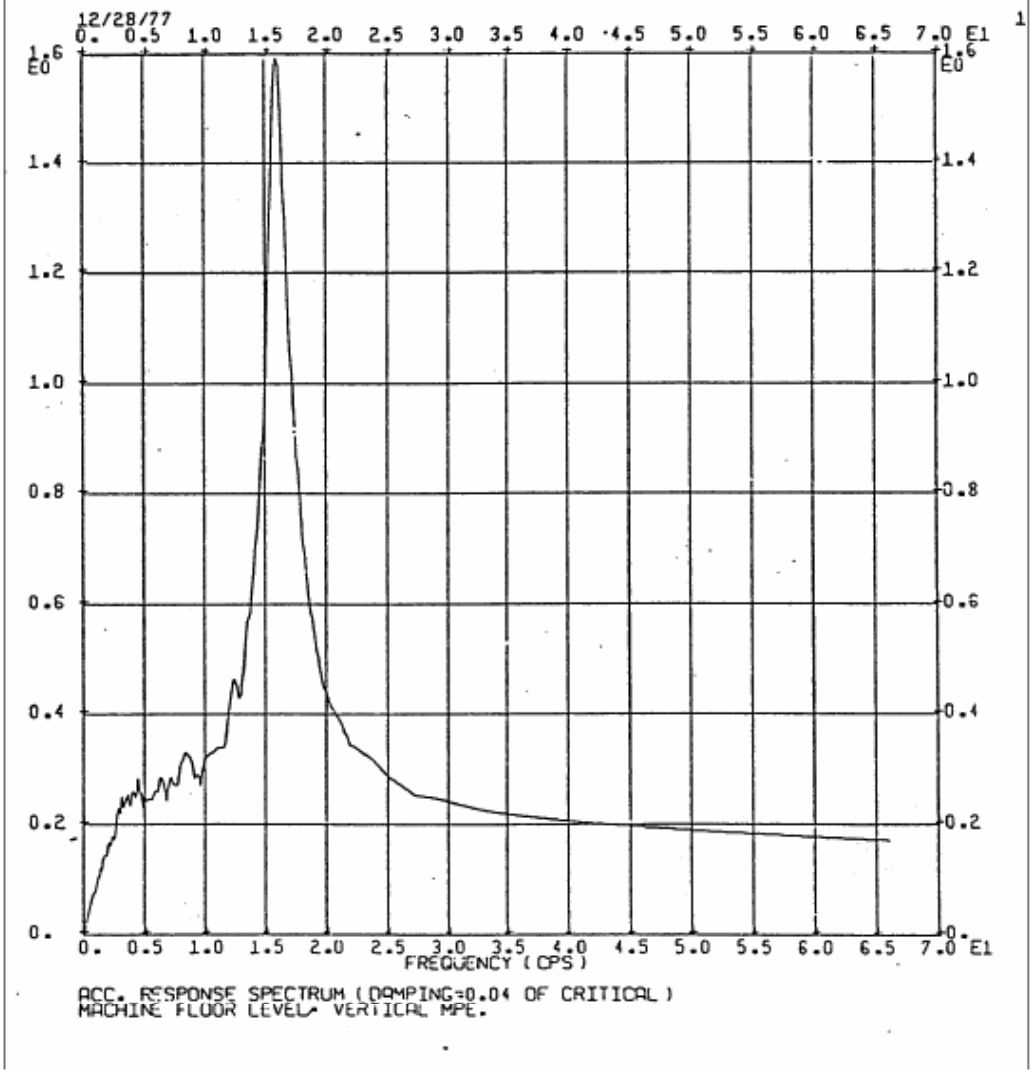

Figure 3.0-4 Vertical Response Spectrum Curve, TFTR/TPX Test Cell, ref [5]

4.0 Materials

Table 4.0-1 Tensile Properties for Magnet Structural Materials

Material	**Yield** 4 deg K (MPA)	**Ultimate** 4 deg K, (Mpa)	**Yield**, 80 deg. K (MPa)	**Ultimate** , 80 deg. K (MPa)	**Yield,** 292 deg K (MPa)	**Ultimate,** 292 deg K (MPa)
316 LN SST	992[8]	1379[8]			275.8[8]	613[8]
316 LN SST Weld	724[8]	1110[8]			324[8]	482[8]
304 SST 50% CW	1613	1896	1344	1669	1089	1241
304 Stainless Steel (Bar,annealed)	404	1721	282	1522	234	640
Aluminum 6061T6	362(20K)	496(20K)	275.8		288	310
Alum 6061 Weld	259(4K)[9]	339(4K)[9]				

Structure Room Temperature (292 K) Maximum Allowable Stresses, Sm = lesser of 1/3 ultimate or 2/3 yield, and bending allowable=1.5*Sm

Material	**Sm**	**1.5Sm**	**Seismic Allowable (K=1.2)**
316 LN SST	183Mpa (26.6 ksi)	275Mpa(40ksi)	330
316 LN SST weld	160MPa(23.2ksi)	241MPa(35ksi)	289

The general equation to compute the elastic modulus for normal concrete from ACI 318 is:

$E_c = 33\, w_c^{1.5}\, (f'_c)^{1/2}$ psi

where:

w_c = the unit weight of concrete

f'_c = the compressive strength of concrete

The general equation to compute the elastic modulus for high performance concrete from ACI 363 is:

$E_c = 40{,}000\, (f'_c)^{1/2} + 1.0 \times 10^6$ psi

For 3,000 psi < f'_c < 12,000 psi

Concrete Density, from: http://www.logicsphere.com/products/firstmix/hlp/html/mixd7zc4.htm

Range: 2100 - 2750 kg/m^3.

Concrete density from: http://hypertextbook.com/facts/1999/KatrinaJones.shtml :

1750-2400 kg/m^3

Volume generally assumed for the density of hardened concrete is 150 lb./ft^3. (2400 kg/m^3)"

5.0 Design Input

A vessel model has been provided by Fred Dahlgren in the form of a Prep7 input listing. The modular coil shell model was provided by H.M.Fan in the form pf an ANSYS *.db file. Tom brown provided a drawing of the lower support structure which also serves as a sliding assembly fixture. The local bldg. details were provided by Fred Dahlgren and Tom Brown, including the shield blocks. At present only a slab is included in the model. The edge of the slab is constrained, and is the input point for the ARS

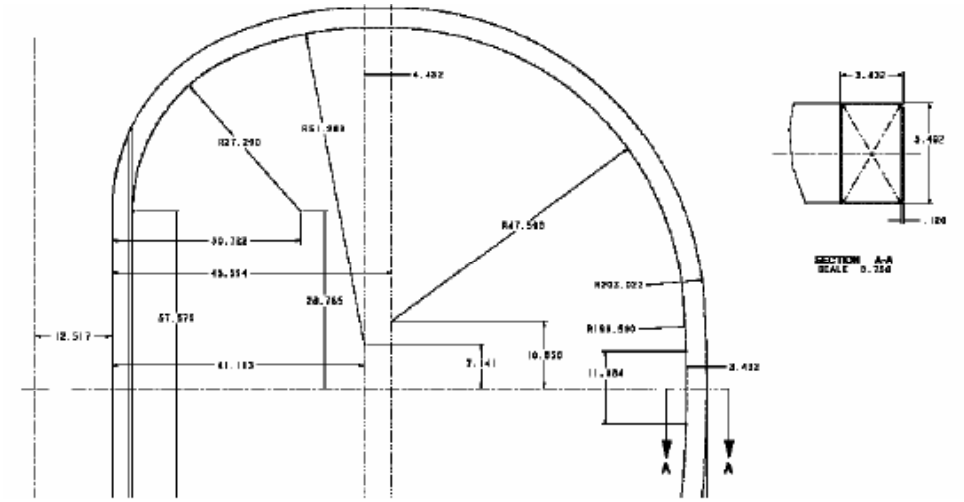

Figure 5.0-1 TF Coil Geometry – Provided by L. Myatt

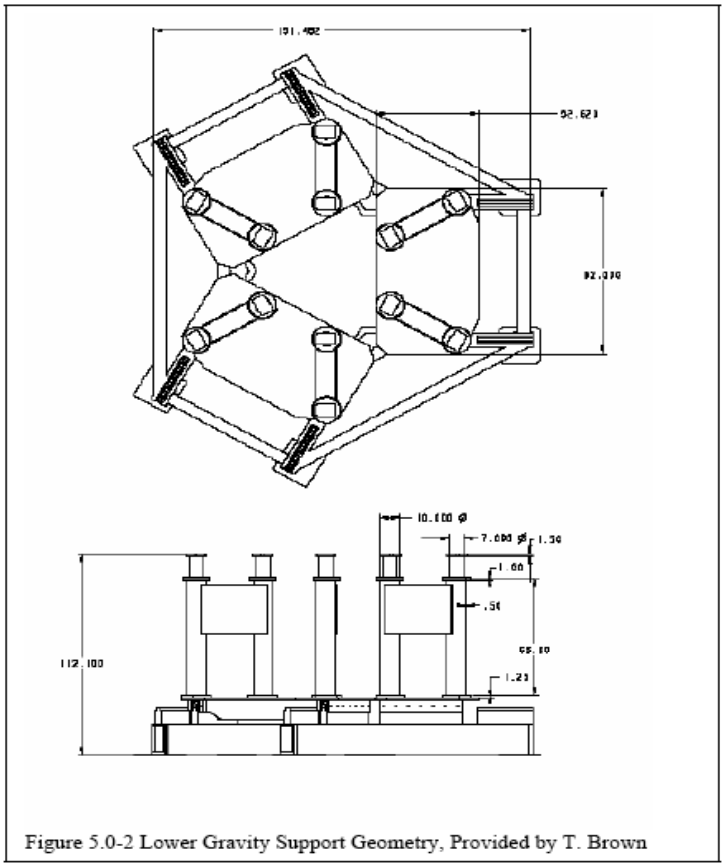

Figure 5.0-2 Lower Gravity Support Geometry, Provided by T. Brown

NCSX PF Coil Build (Provided by Len Myatt in ANSYS Parametric Language, for individual conductor modeling, converted to Coil R,Z,DR.DZ data)

R	Z	dr	dz
8.625	9.438	3.66	15.93
8.625	28.313	3.66	15.93
8.625	47.188	3.66	15.93
20.549	62.34	7.32	8.85
87.527	60.25	3.66	5.31
107.105	37.562	1.83	6.195
107.105	-37.562	1.83	6.195
87.527	-60.25	3.66	5.31
20.549	-62.34	7.32	8.85
8.625	-47.188	3.66	15.93
8.625	-28.313	3.66	15.93
8.625	-9.438	3.66	15.93

6.0 References

[1] NCSX SPECIFICATION Vacuum Vessel Systems (WBS 12) System Requirements Document (SRD) NCSX-BSPEC-120-00 18 March 2004
[2] NCSX (NATIONAL COMPACT STELLERATOR EXPERIMENT) STRUCTURAL DESIGN CRITERIA - DRAFT B - 4/30/04, I. ZATZ, EDITOR
[3] DOE-STD-1020-2002
[4] Email and attachment from Brad Nelson with the vessel support details, -excerpt from the PDR
[5] Structural Analysis of the TPX Cold-Mass Support System, Scott A. Perfect UCRL-ID-112614, TPX 16-921211-LLNL/S.P.-01, December 11 1992
[6] Seismic Dynamic Analysis of Tokamak Structures, Shaaban, AA. Ebasco Services Inc. Report # EP-D-027, February 7 1978, This is cited in [5] as the source of the ARS curves
[7] PRELIMINARY Summary and derivation of the seismic requirements for NCSX. Preliminary Rev 1 Michael Kalish 3/29/04
[8] "General Electric Design and Manufacture of a Test Coil for the LCP", 8th Symposium on Engineering Problems of Fusion Research, Vol III, Nov 1979
[9] "Handbook on Materials for Superconducting Machinery" MCIC- HB-04 Metals and Ceramics Information Center, Battelle Columbus Laboratories 505 King Avenue Columbus Ohio 43201
[10] NCSX Engineering Design Document, Design Description Vacuum Vesses (WBS12) and In-Vessel Components, NCSX Final Design Review May 19-20 2004.

7.0 Analysis and Modeling

Run#7

The modular coils are not explicitly modeled in the seismic analysis. Their mass is lumped with the support shell. In this model segments provided by H.M. Fan, the coil volume is 0.8906 m^3 and the support shell volume is 1.50228m^3. The shell density is increased by the factor (1.50228+.8906)/1.50228 to account for the coil mass. The Plasma facing components (PFC's) have not been included in the model. These are to be installed in a later phase of the project, and will be carbon composite. The PFC's are not expected to add significantly to the inertia inventory.

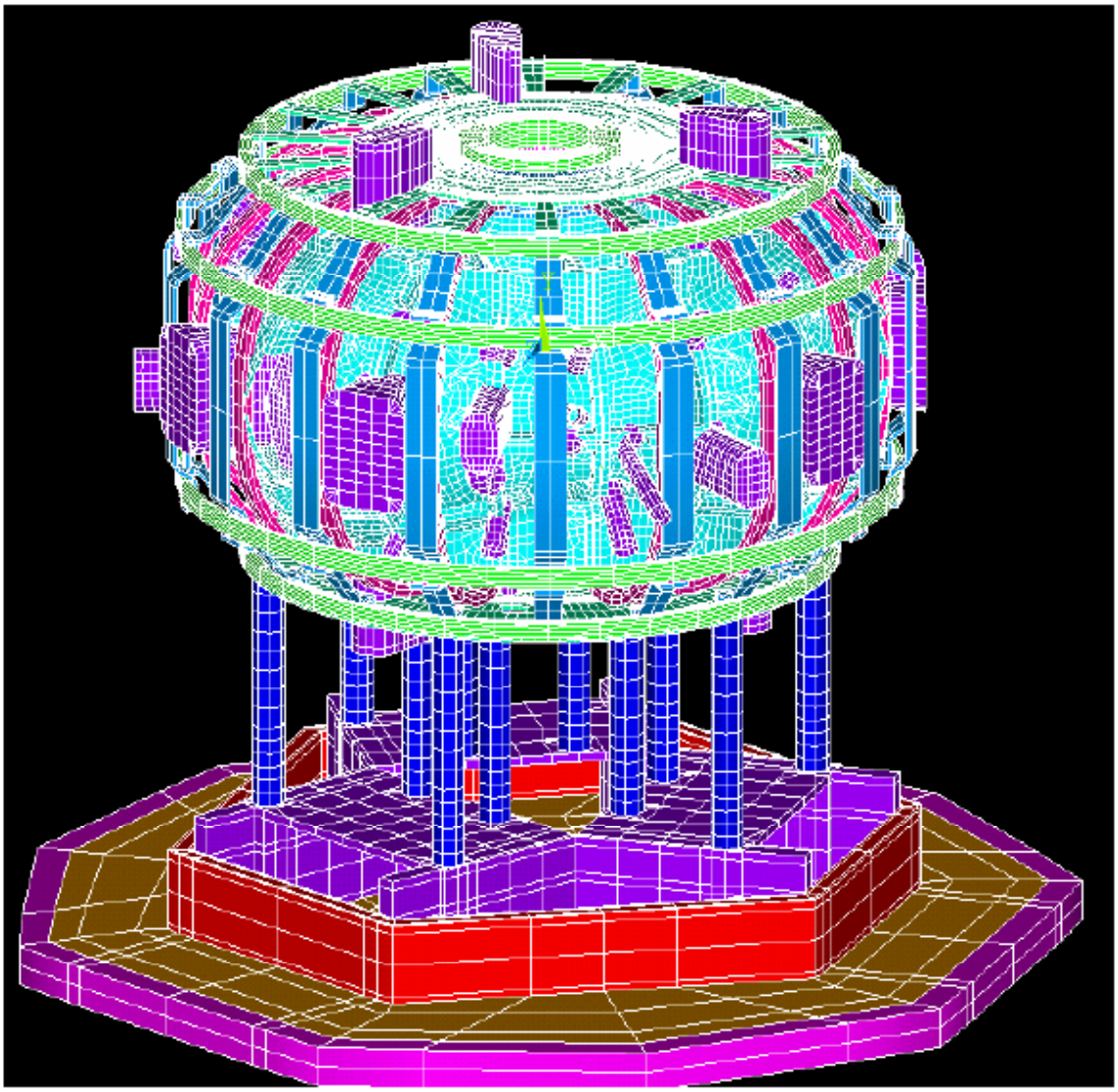

Figure 7.0-1 FEA Seismic Model

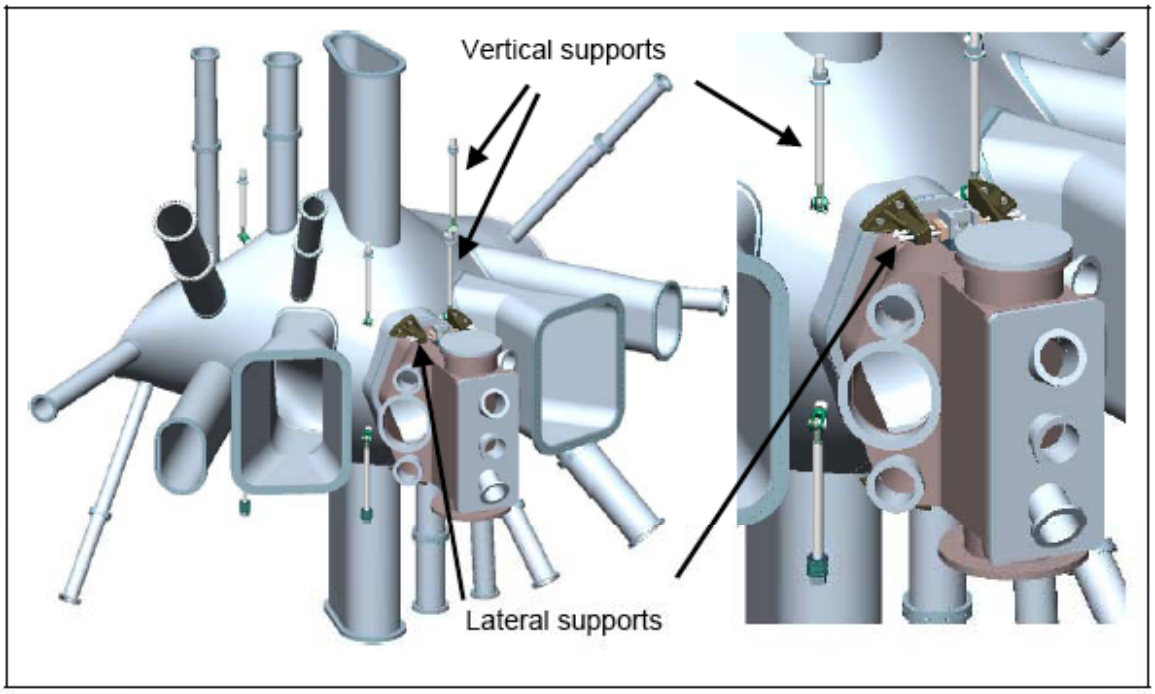

Figure 7.0-2 Vacuum Vessel Supports

From ref [4]:
The vessel will be supported from the modular coil structure via vertical support hangers and radial guide lugs(figure 6.0.2), designed for ease of adjustment and minimal heat transfer between the two structures. The vessel gravity load is taken by two hangers located on either side of the NBI ports. Two lower hangers, in each period, are used to react vertical dynamic loads. Radial supports, located at the top and bottom of each neutral beam duct, react lateral loads. The hangar geometry is illustrated in Error! Reference source not found.. Significant relative thermal growth must be accommodated when the modular coils are cooled to cryogenic temperatures or when the vacuum vessel is heated for bakeout.

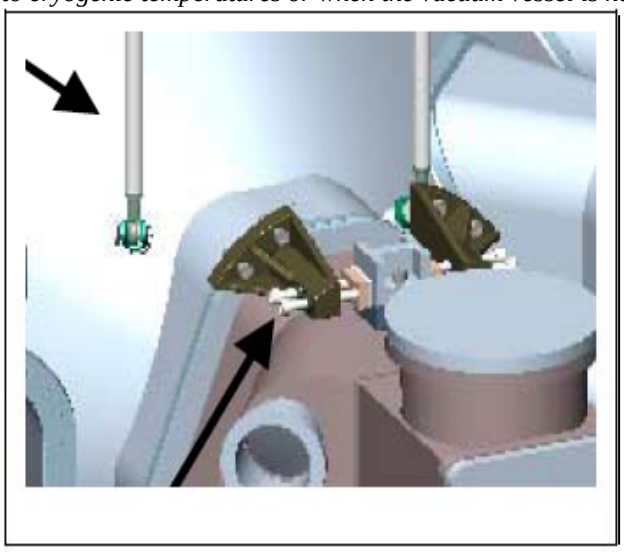

Figure 7.0-4 Upper Vessel Supports

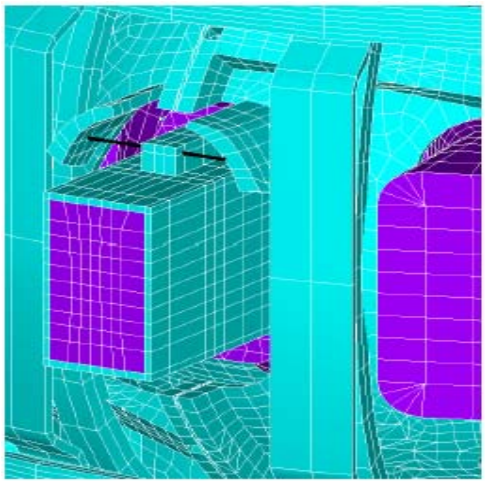

Figure 7.0-5 Vessel Support FEA Model

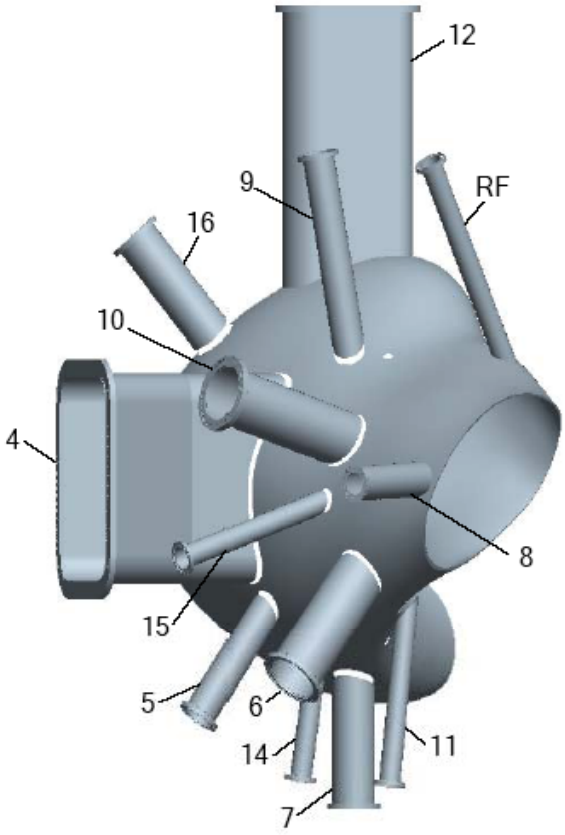

Figure 7.0-6 Vessel Port Numbering

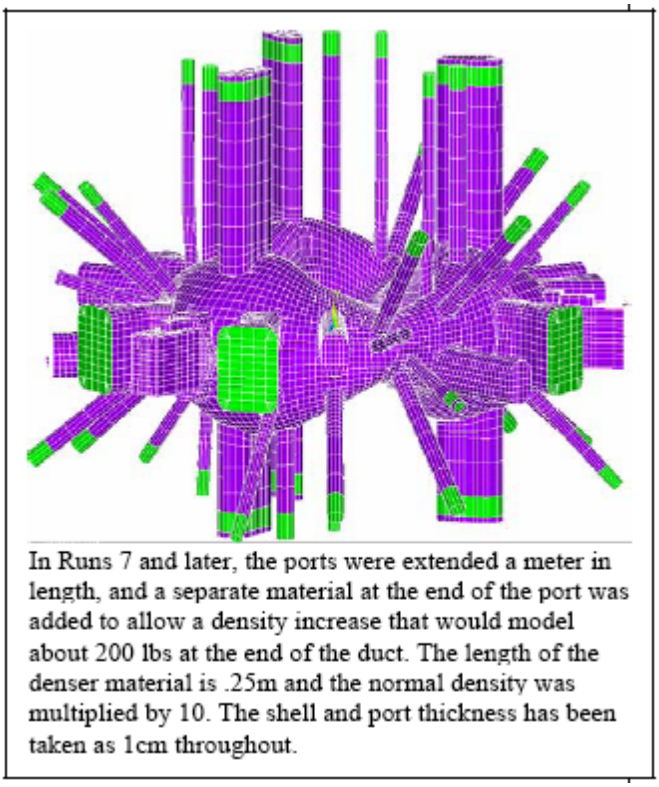

In Runs 7 and later, the ports were extended a meter in length, and a separate material at the end of the port was added to allow a density increase that would model about 200 lbs at the end of the duct. The length of the denser material is .25m and the normal density was multiplied by 10. The shell and port thickness has been taken as 1cm throughout.

Figure 7.0-7 Port Extensions (in Green)

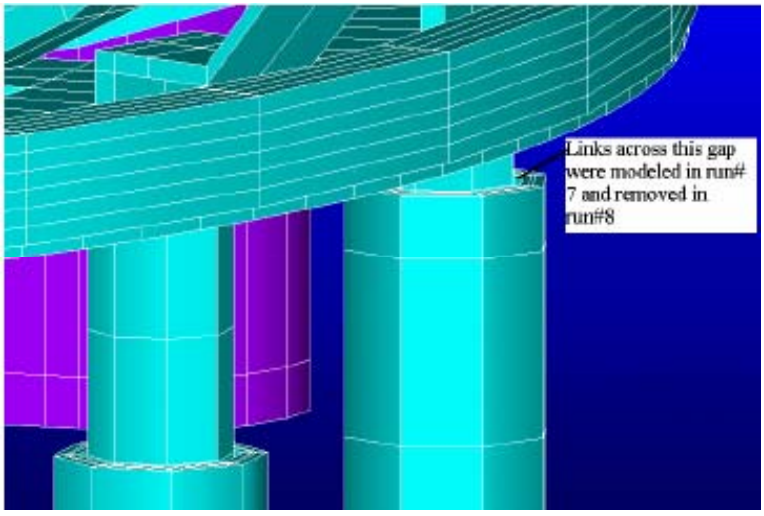

Figure 7.0-8 Mod Coil Shell Support FEA Modeling

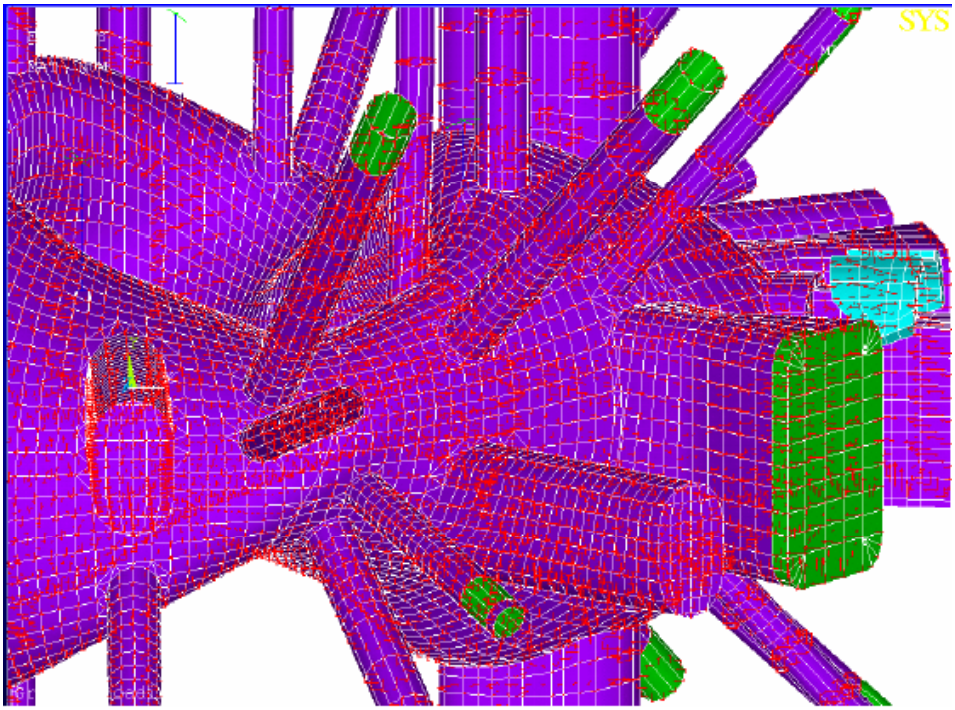

Figure 7.0-9 Vessel static analysis with vacuum nodal forces shown. This was analyzed in run#6. Cooldown behavior was also studied in this run.

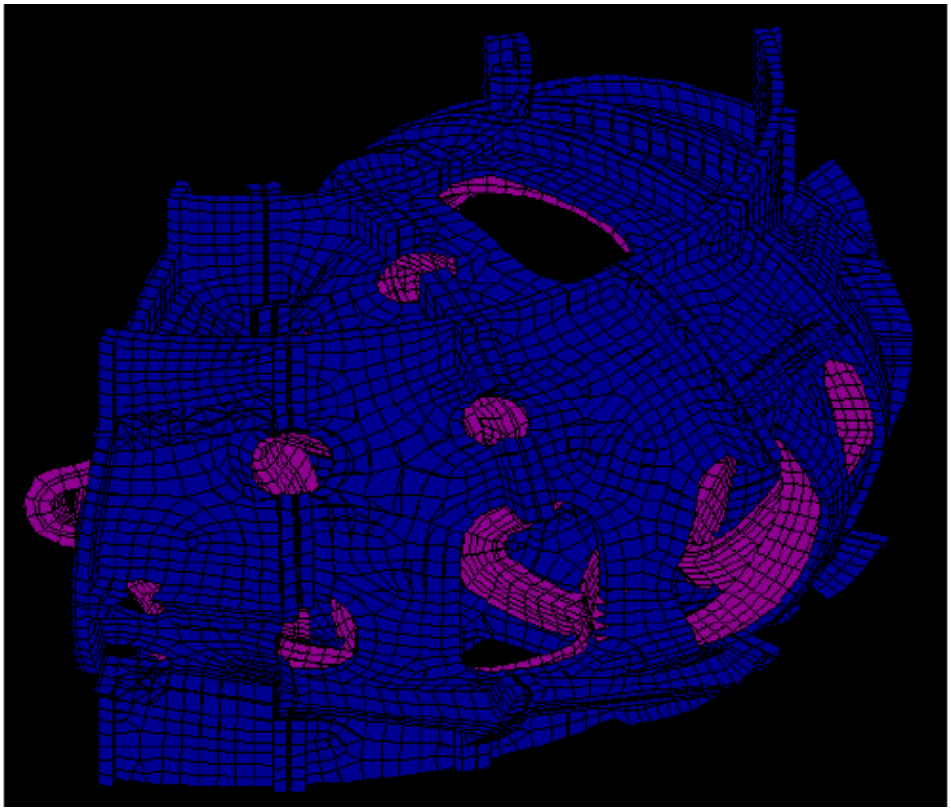

Figure 7.0-10 The modular coils are not explicitly modeled in the seismic analysis. Their mass is lumped with the support shell. In this model segments provided by H.M. Fan, the coil volume is 0.8906 m^3 and the support shell volume is 1.50228m^3. The shell density is increased by the factor (1.50228+.8906)/1.50228 to account for the coil mass.

8.0 Run Log

Table 8.0-1 Run Number and Date

Run#	Date	Analysis Type	Description
4	5-9-04	Spectrum	8 modes extracted
5	5-12-04	Static	Cooldown, Deadweight
6	5-11-04	Static	Vacuum Vessel Pressure, Deadweight and Cooldown
7	5-12-04	Spectrum	Port Extensions added, 10 Modes
8	5-12-04		12 Modes Extracted, no gaps in nested columns
9	5-14-04	Static	Cooldown, Deadweight
10	5-16-04	Spectrum	14 Modes Extracted

9.0 Displacement Results

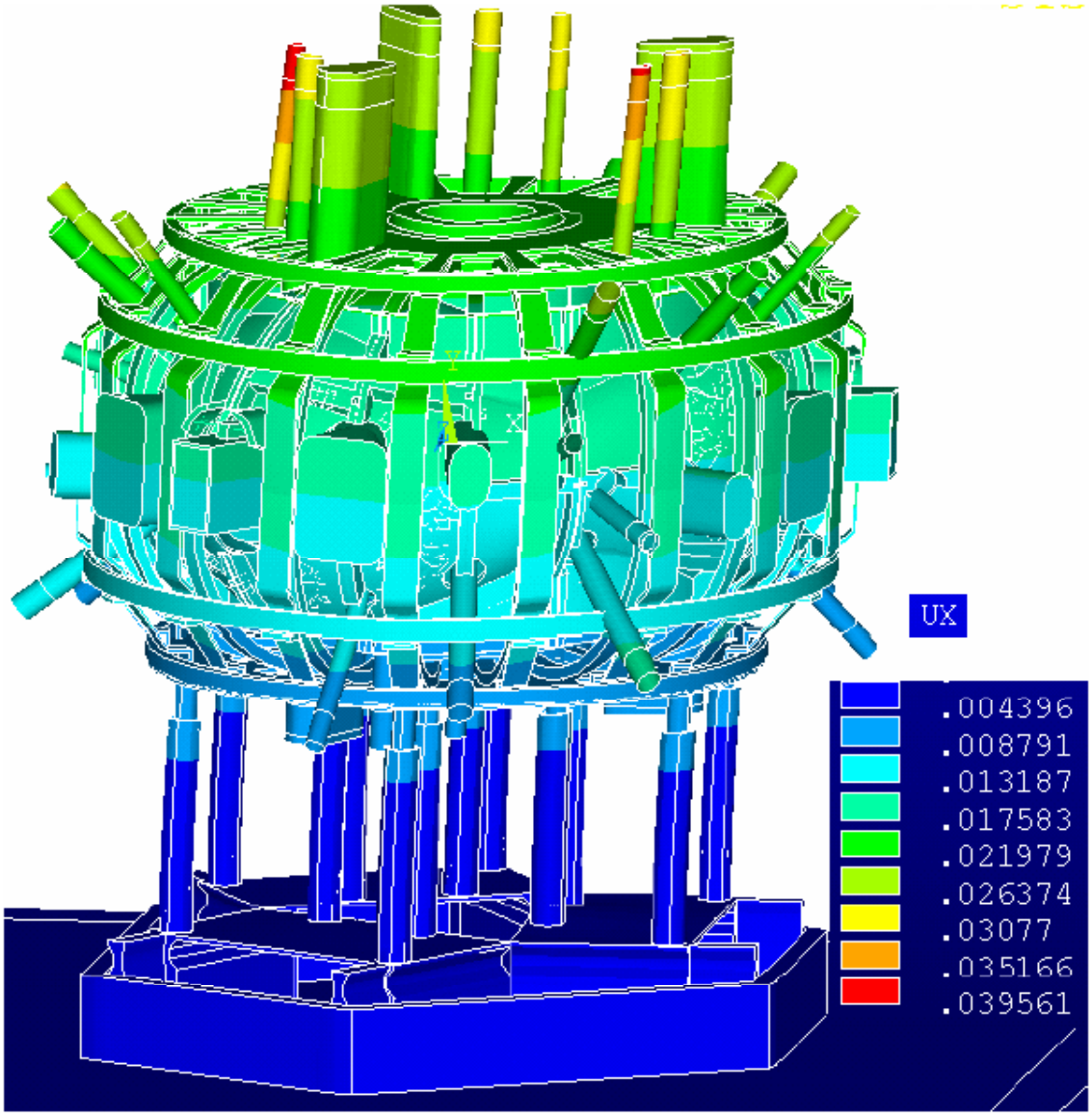

Figure 9.0-1 Spectrum Analysis Lateral Displacement Results, Run#7. This is with a single horizontal response spectrum applied. Results for run#10, in which 4 more modes contributed to the response, the peak displacement went up to 03995m

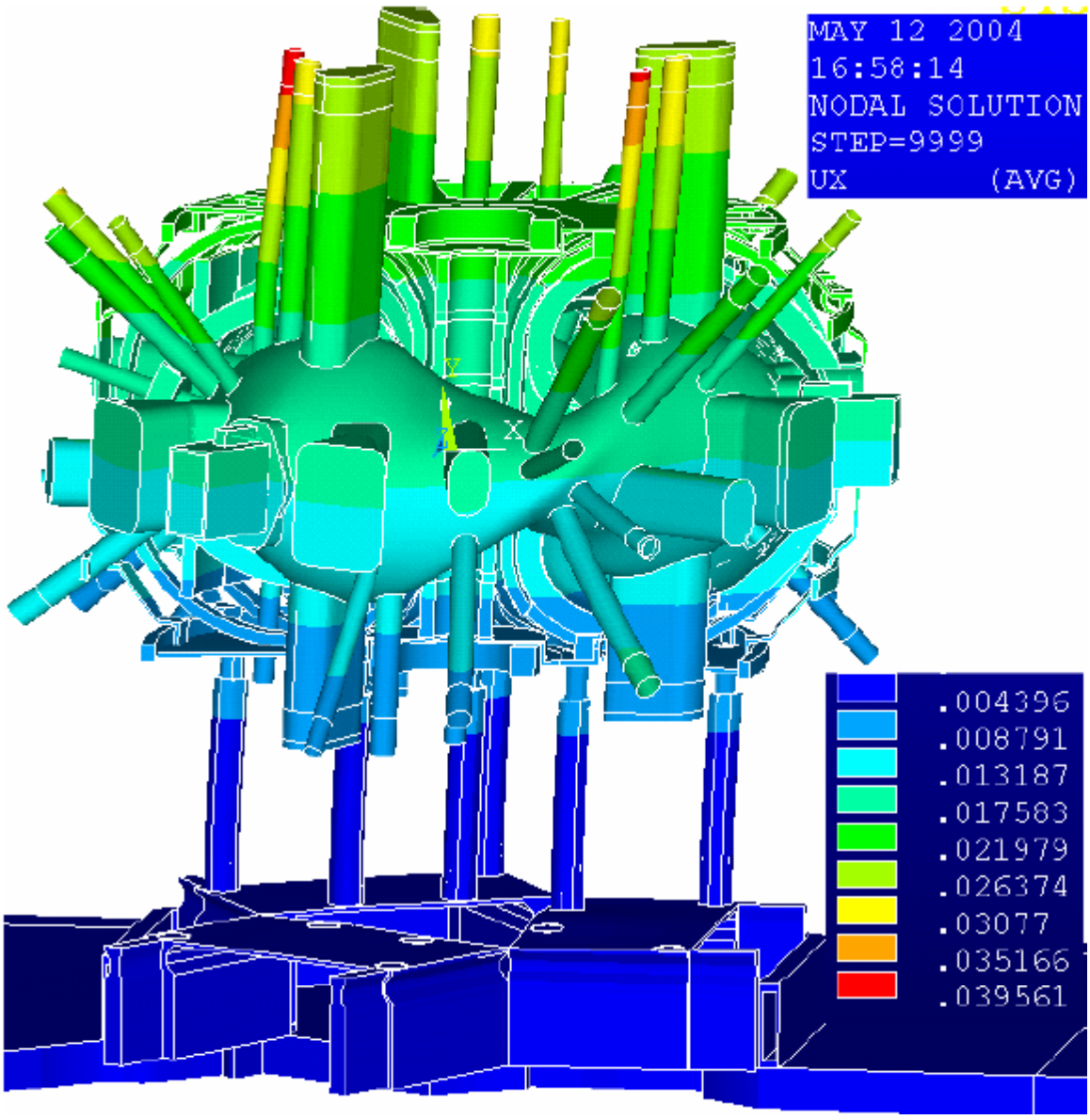

Figure 9.0-2 Spectrum Analysis Lateral Displacement Results, Run#7, With half the coil structure cut away to show vessel relative displacements. This is the SRSS combination of mode shapes. Interesting relative displacements may also be found in the modal deformations section, section 12.0 in which the individual mode displacements are presented.

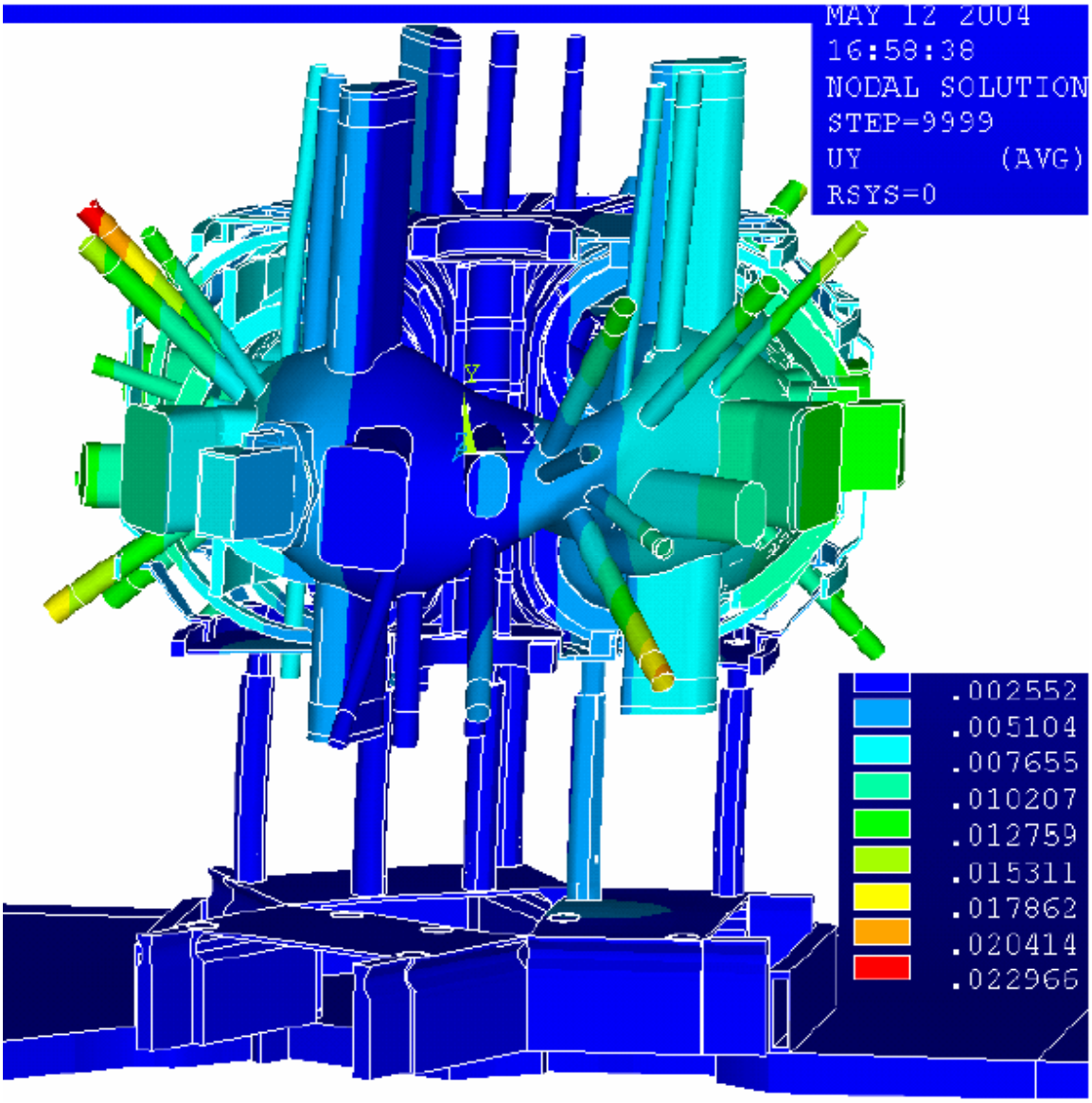

Figure 9.0-3 Spectrum Analysis Vertical Displacement Results, Run#7, With half the coil structure cut away to show vessel relative displacements. This is the SRSS combination of mode shapes. Interesting relative displacements may also be found in the modal deformations section, section 12.0 in which the individual mode displacements are presented.

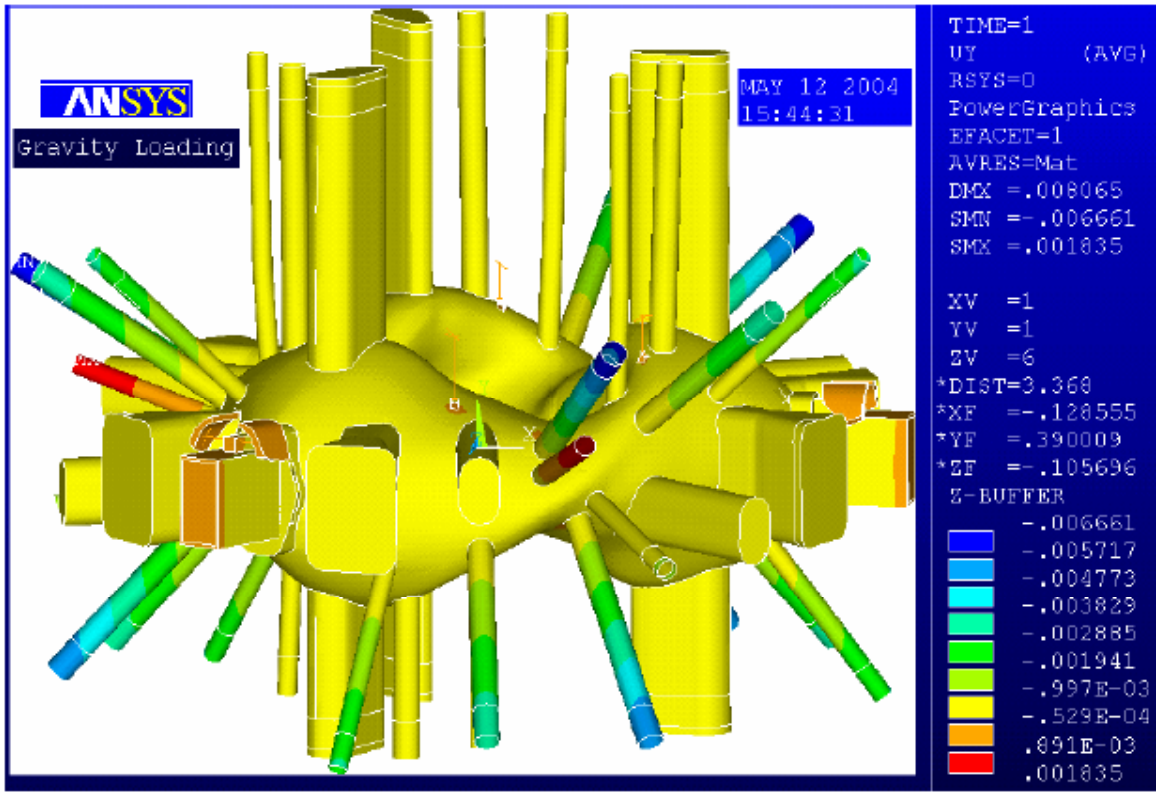

Figure 9.0-4Vessel and port displacements under deadweight only. Note the interesting behavior of the ports at the reduced region of the vessel where downward displacement of one port causes the upward motion of a neighboring port.

10.0 Stress Results
10.1 Vessel Stresses

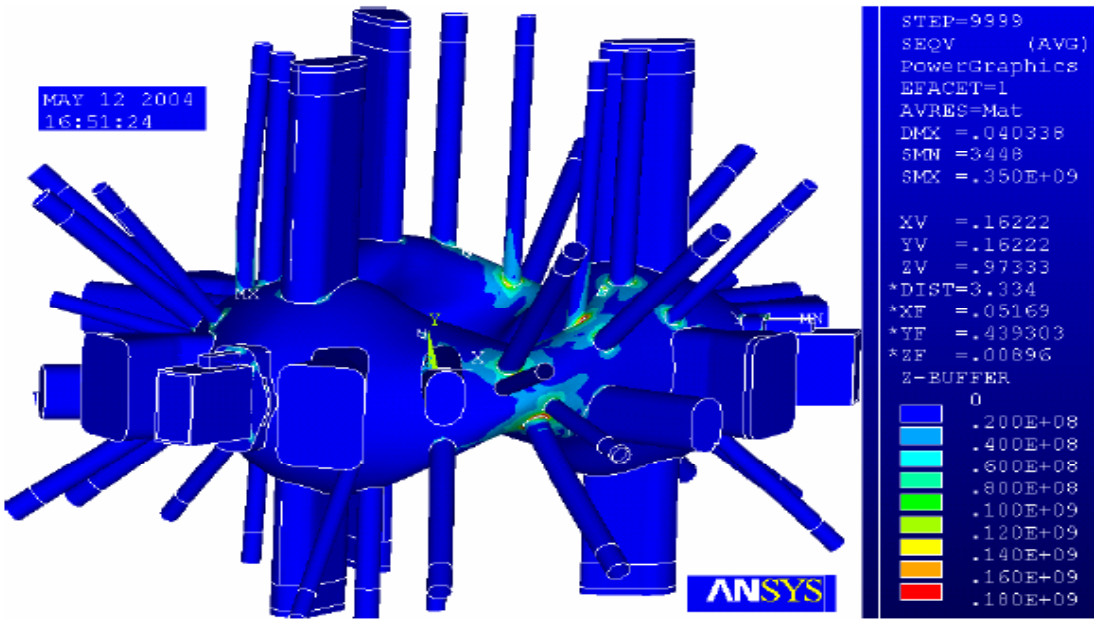

Figure 10.1-1 Spectrum Analysis Results – Single Horizontal Direction

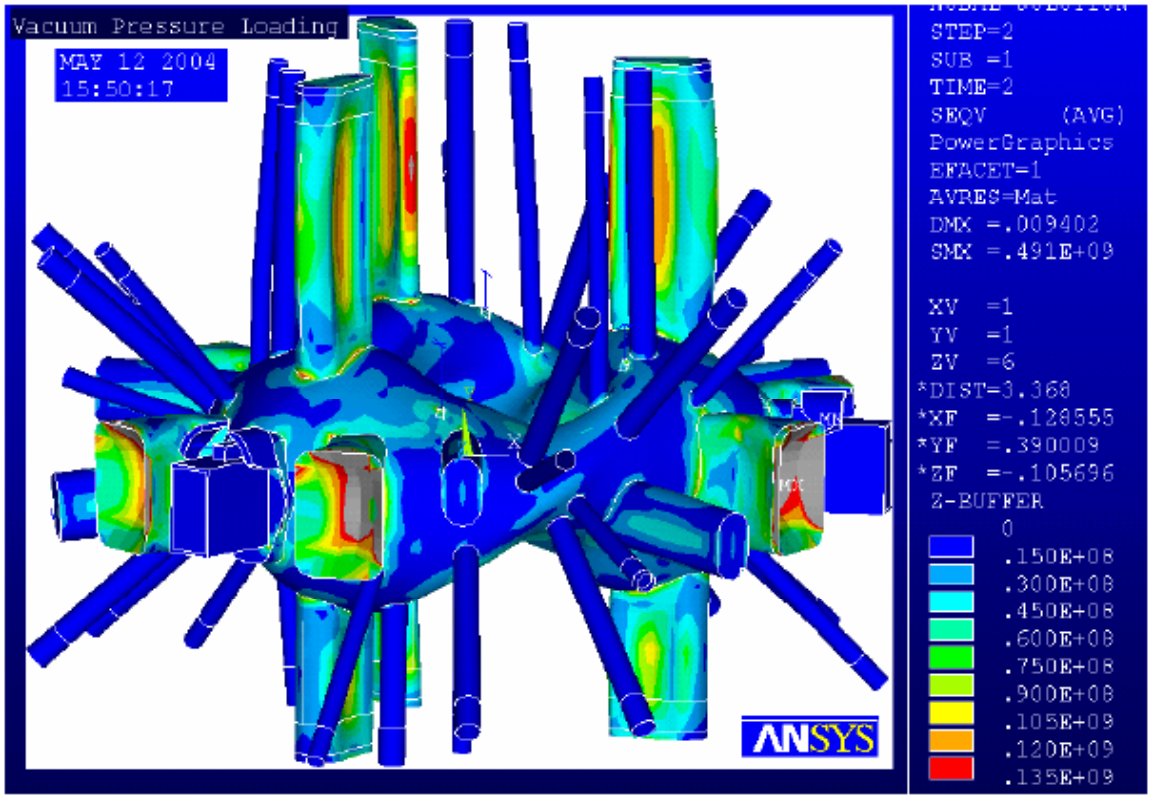

Figure 10.1-2 Vacuum Pressure Loading Stresses

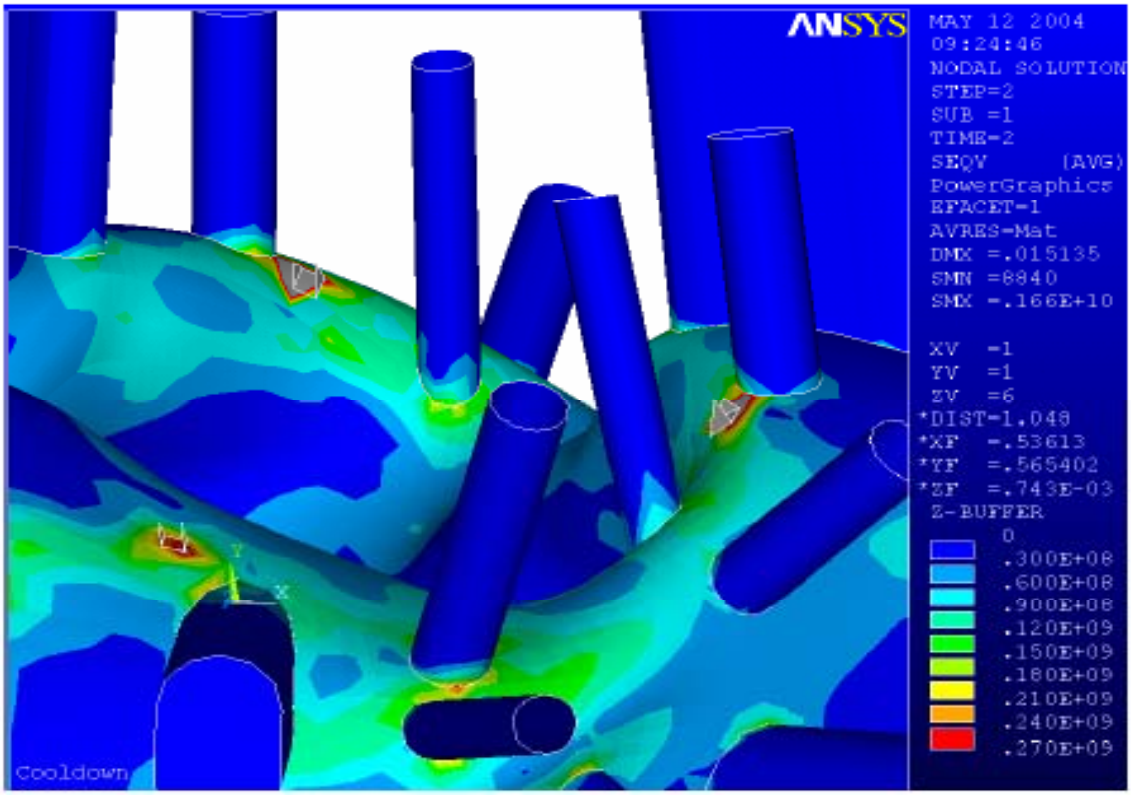

Figure 10.1-3 Stresses in the Vacuum Vessel from only cooldown. These result from different length hangers, and also include shell rotations.

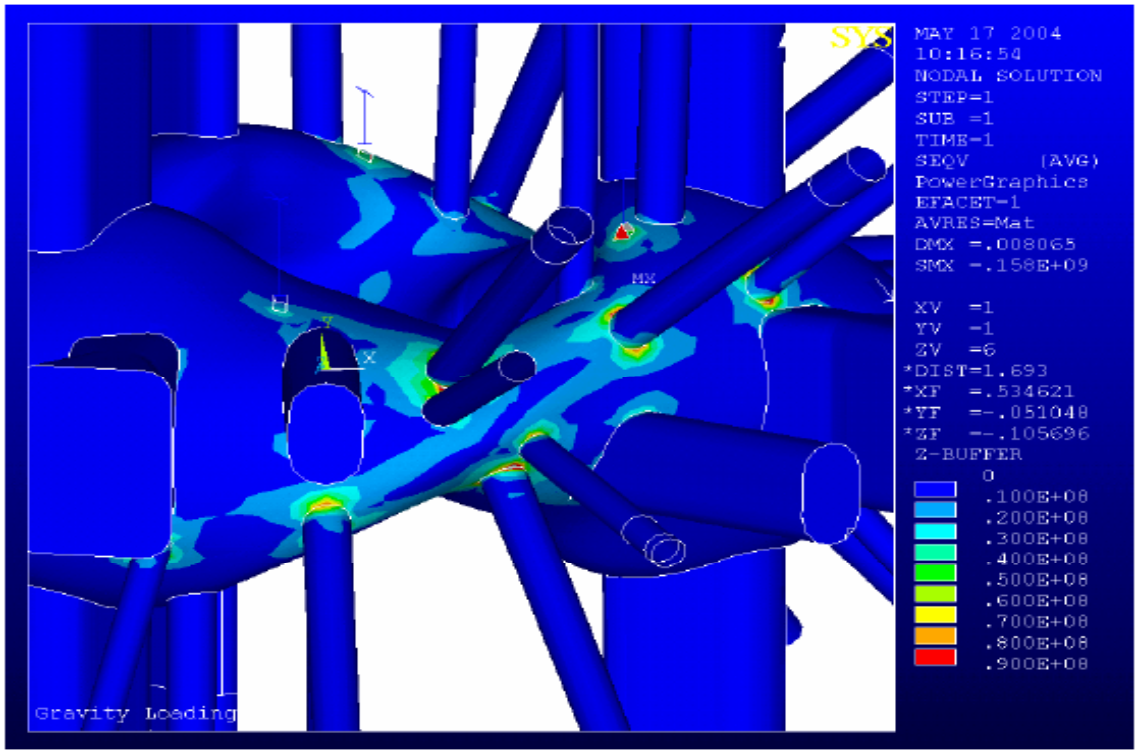

Figure 10.1-4 Deadweight Stress in the vessel

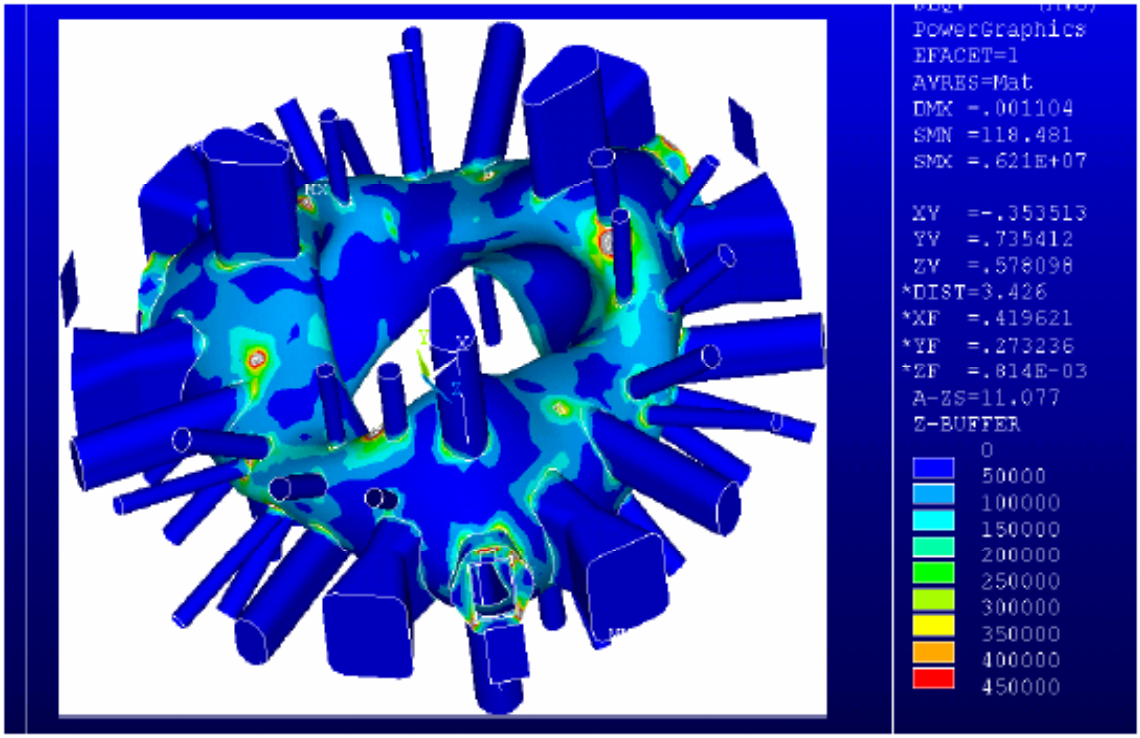

Figure 10.1-5 Spectrum Analysis Results from an earlier analysis in which the port extensions and inertias were not modeled. In this run, the seismic stresses in the vessel due to hanger dynamic loads. This run needed the ARS to be scaled up by 9.8 and 2. The peak stress would then be 8.8 MPa, compared with 18 MPa at the port/vessel interface shown in figure 10,0-1

10.2 Modular Coil Case

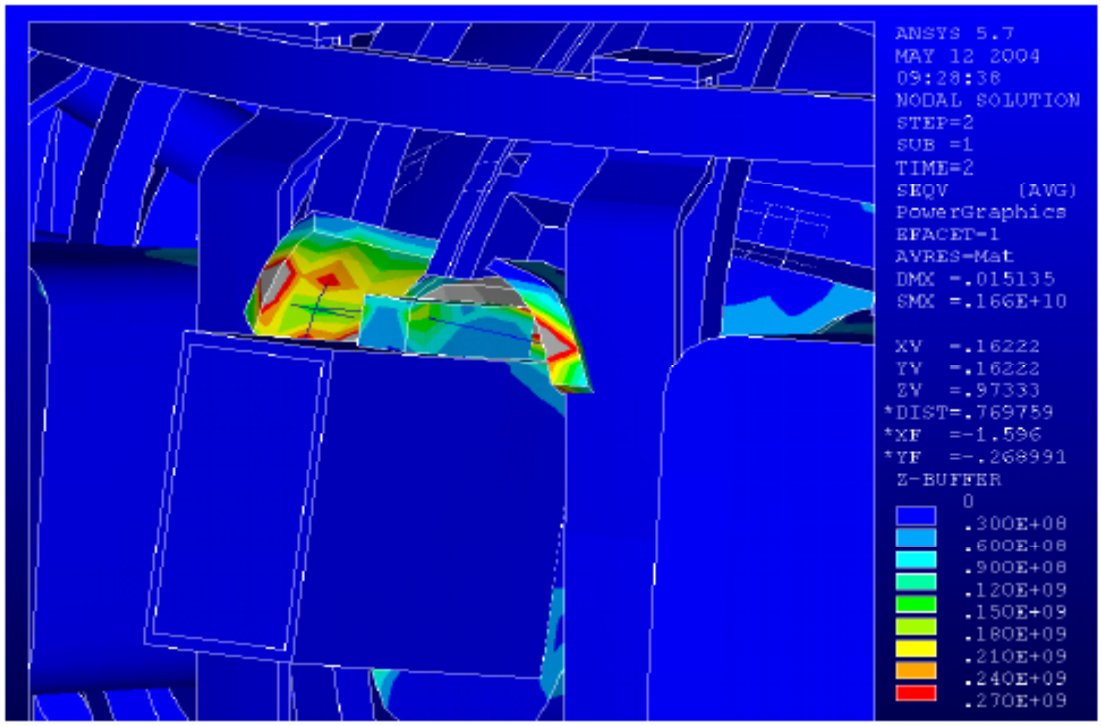

Figure 10.2-1 Stress due to cooldown – If lateral restraints are hard up against the port lug prior to cooldown. A one-sided radius rod type restraint might be wiser.

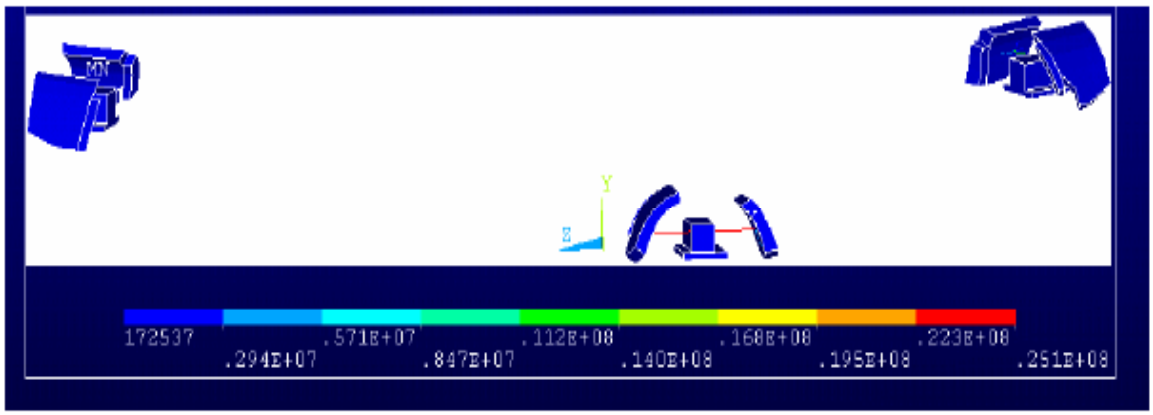

Figure 10.2-2 Restraint Link Stresses. These are modeled as having a 1 square in cross section. These are modeled as taking tension and compression, but the design appears to allow only compression. The load at each restraint is :25.1e6/6895*2* 1.0in^2= 7251.6 lbs

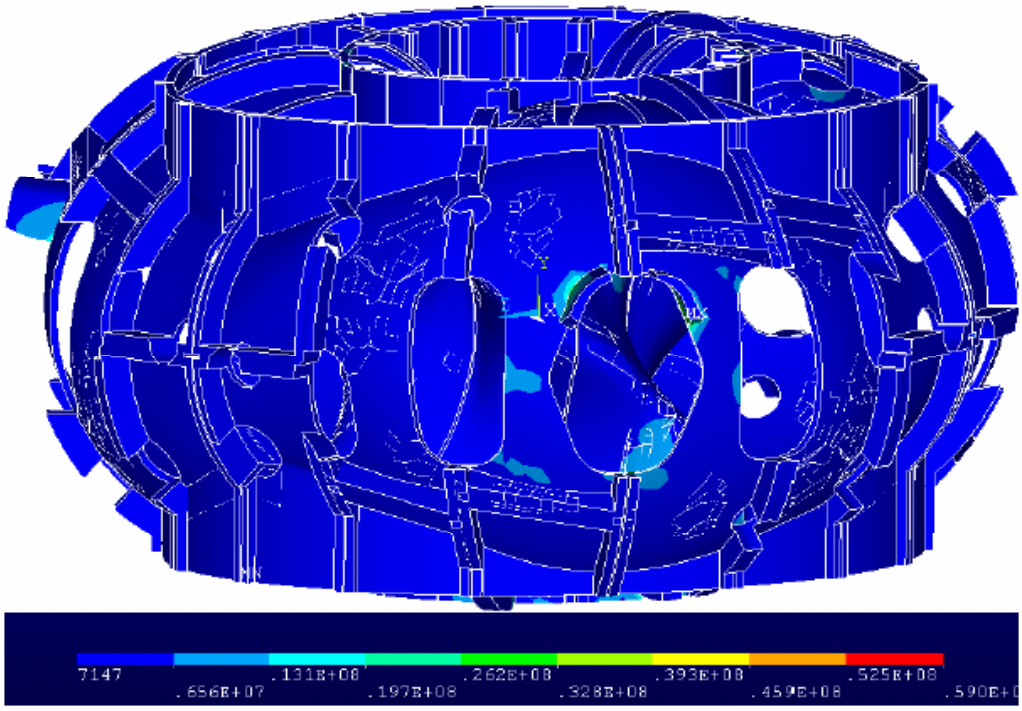

Figure 10.2-3 Modular Coil Shell Stress. The only appreciable stress is in the vessel lateral support brackets. As long as the thermal stress is improved, the bracket stresses do not appear to be a problem. The major loading of this shell are the modular coil Lorentz forces. The areas of the shell which support these stresses are essentially un effected by the seismic loading.

10.3 Support Columns

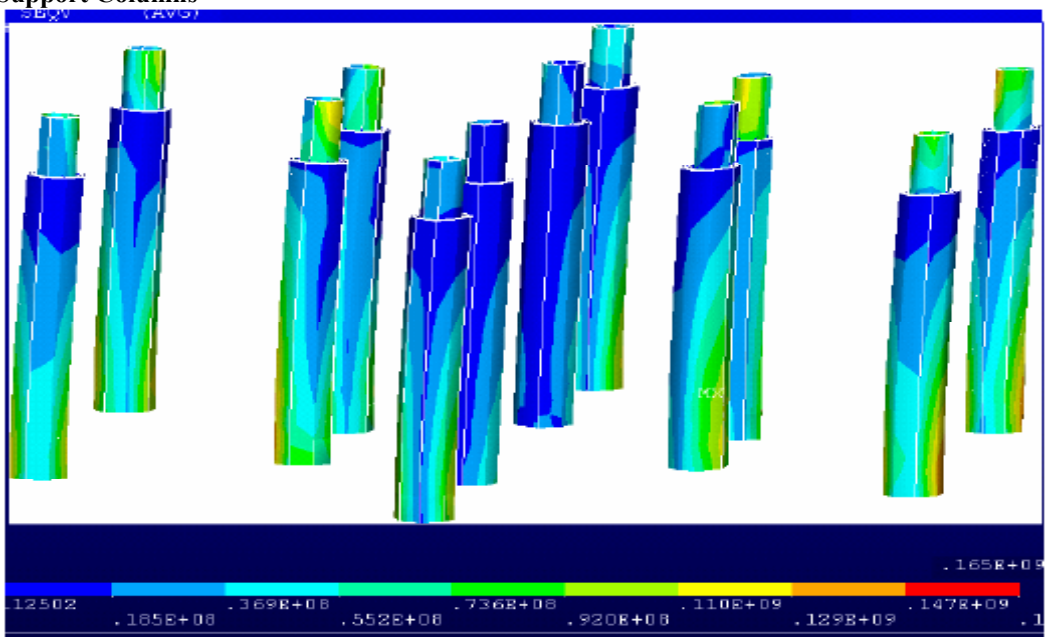

Figure 10.3-1 Spectrum Analysis Results, Single Horizontal Direction ARS, run#7. Run #7 had 10 modes extracted. This analysis was re-run with 14 modes extracted in run#10 and the peak stress went from 165 MPa to 167 MPa.

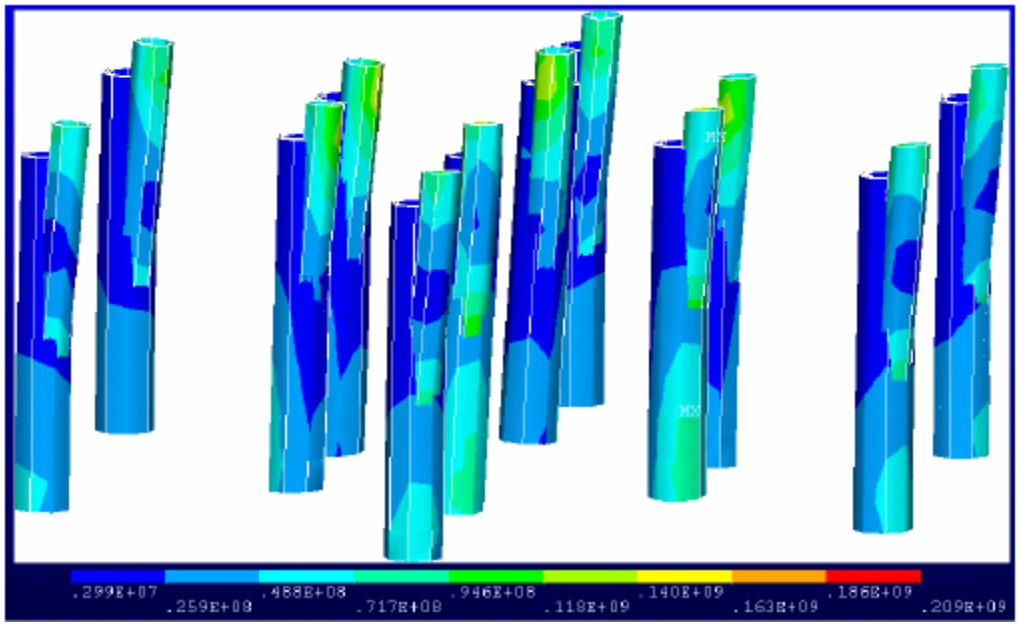

Figure 10.3-2 Spectrum Analysis Results, Single Horizontal Direction ARS, run#8. This is for the case where the gap at the top pf the column, between nested cylinders is not filled.

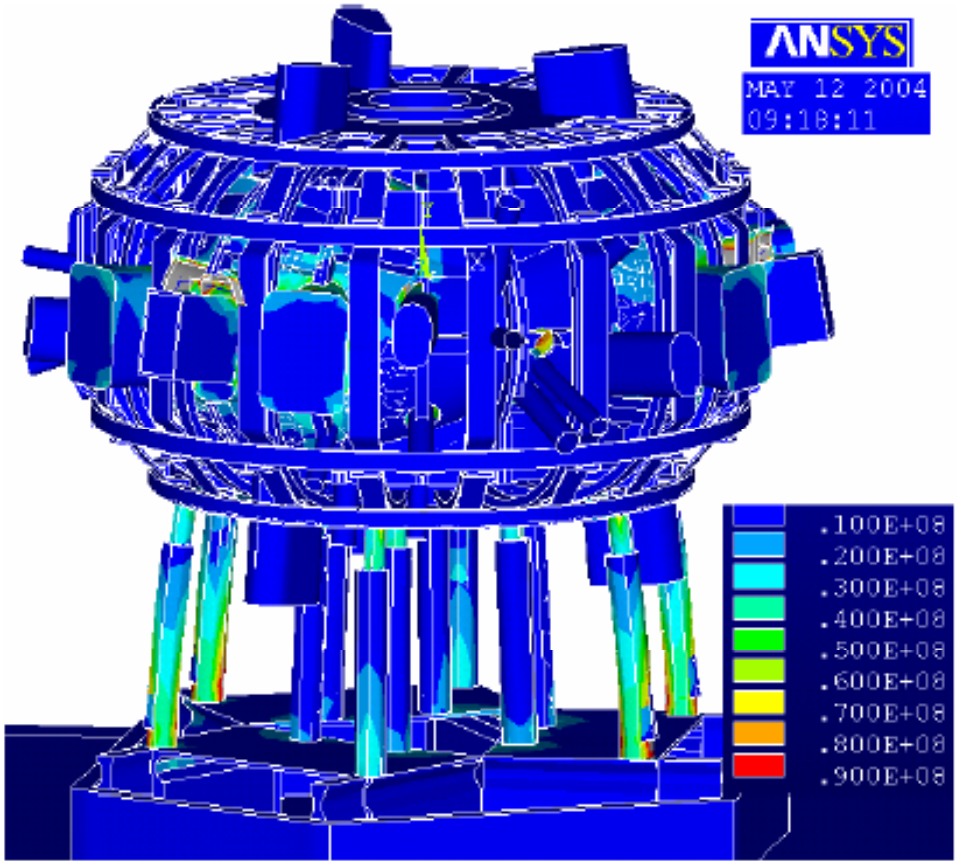

Figure 10.3-3 Run #5 Cooldown to LN2 Temperature

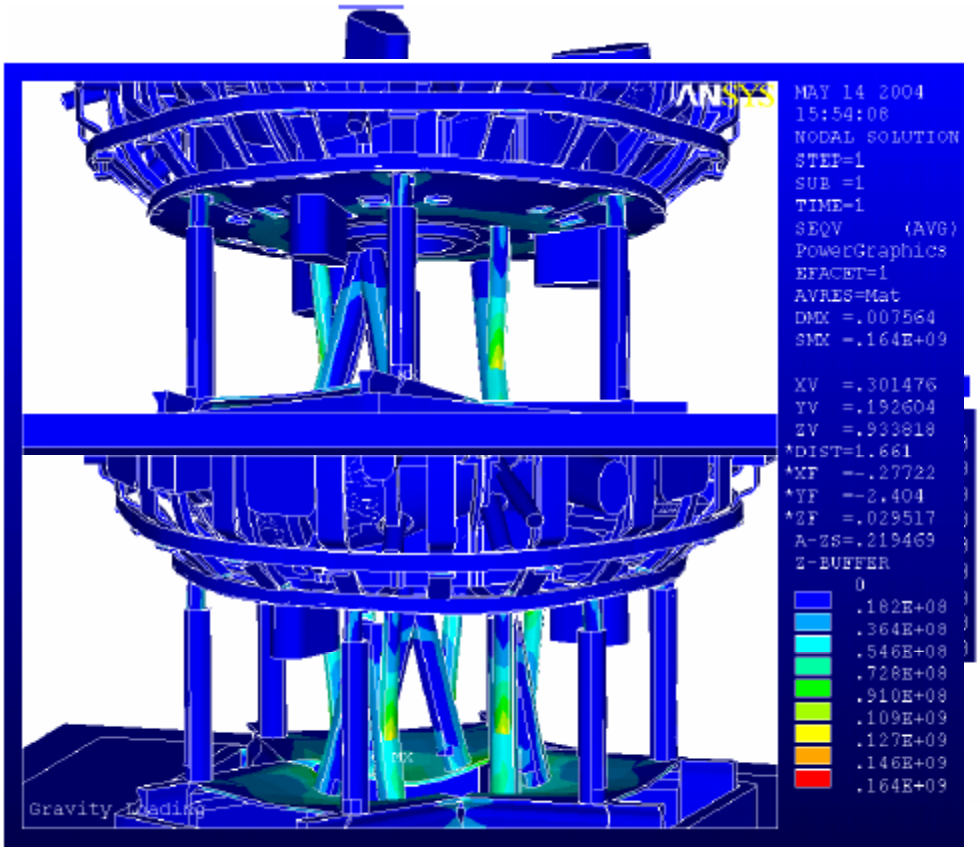

Figure 10.3-4 Run #5 Cooldown to LN2 Temperature

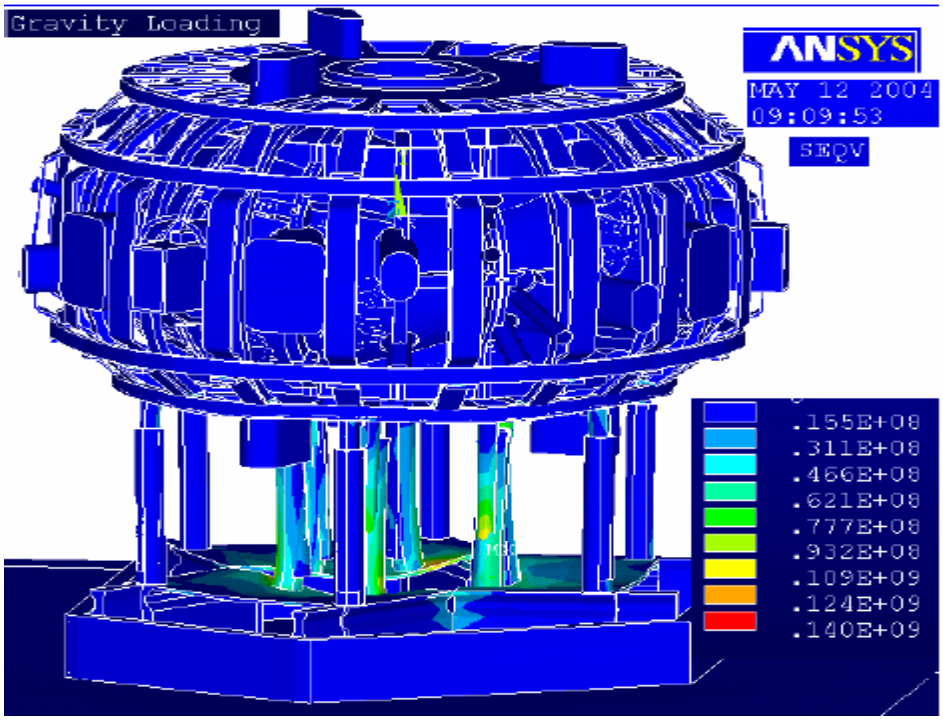

Figure 10.3-5Run #5 Deadweight from the Static Analysis

11.0 Modes and Mode Shapes

With the addition of the port extensions and the added mass at the end of the ports, mode shapes involving port motion predominated. Earlier runs show more of the mode shapes involving global motion. Figure 11.0-1 shows the vertical mode which was around 10 hz.

Table 11.0-1 Modal Run Results

Run#	Frequency cps		Description
1	7	2.105	Rocking Mode
2	7	2.618	Rocking
3	7	3.11	Global Twist about a Vertical Axis
4	7	4.692	Vessel Port Rotation
5	7	4.743	Vessel Port Rotation
6	7	4.84	Vessel Port Rotation
7	7	4.8625	Vessel Port Rotation
8	7	4.886	Vessel Port Rotation
9	7	5.021	Vessel Port Rotation
10	7	5.29	Vessel Port Rotation

***** PARTICIPATION FACTOR CALCULATION *****

Table 11.0-2 RUN#7 X (HORIZONTAL) DIRECTION CUMULATIVE

MODE	FREQUENCY	PERIOD	PARTICIPATION FACTOR	RATIO	EFFECTIVE MASS	MASS FRACTION
1	2.10470	0.47513	-0.30572	0.000954	0.0934649	0.866092E-06
2	2.61764	0.38202	320.45	1.000000	102690.	0.951575
3	3.11108	0.32143	-0.086956	0.000271	0.756134E-02	0.951575
4	4.69222	0.21312	1.9722	0.006155	3.88971	0.951611
5	4.74312	0.21083	-0.82273	0.002567	0.676892	0.951617
6	4.84035	0.20660	-45.370	0.141581	2058.42	0.970692
7	4.86256	0.20565	3.3938	0.010591	11.5181	0.970798
8	4.88580	0.20467	-56.133	0.175168	3150.91	0.999996
9	5.02102	0.19916	0.24012	0.000749	0.576581E-01	0.999997
10	5.29082	0.18901	0.57879	0.001806	0.334998	1.00000
		SUM OF EFFECTIVE		MASSES=		107916.

***** PARTICIPATION FACTOR CALCULATION *****

Table 11.0-3 Y DIRECTION (VERTICAL) CUMULATIVE RUN#7

MODE	FREQUENCY	PERIOD	PARTICIPATION FACTOR	RATIO	EFFECTIVE MASS	MASS FRACTION
1	2.10470	0.47513	-0.29200	0.009149	0.0852669	0.740569E-04
2	2.61764	0.38202	-6.6399	0.208029	44.0881	0.0383660
3	3.11108	0.32143	-0.55075	0.017255	0.303324	0.0386294
4	4.69222	0.21312	31.918	1.000000	1018.77	0.923460
5	4.74312	0.21083	-0.32076	0.010049	0.102885	0.923549
6	4.84035	0.20660	-1.6432	0.051480	2.69995	0.925894
7	4.86256	0.20565	1.2547	0.039310	1.57428	0.927261
8	4.88580	0.20467	-3.1297	0.098053	9.79475	0.935768
9	5.02102	0.19916	8.5937	0.269241	73.8511	0.999910
10	5.29082	0.18901	0.32139	0.010069	0.103291	1.00000
		SUM OF EFFECTIVE		MASSES=		1151.37

***** PARTICIPATION FACTOR CALCULATION *****

Table 11.0-4 RUN#7 Z (HORIZONTAL) DIRECTION CUMULATIVE

MODE	FREQUENCY	PERIOD	PARTIC.FACTOR	RATIO	EFFECTIVE MASS	MASS FRACTION
1	2.10470	0.47513	342.15	1.000000	117068.	0.965828
2	2.61764	0.38202	0.26121	0.000763	0.0682315	0.965828
3	3.11108	0.32143	-4.5350	0.013254	20.5662	0.965998
4	4.69222	0.21312	0.10075	0.000294	0.0101496	0.965998
5	4.74312	0.21083	-59.436	0.173713	3532.65	0.995143
6	4.84035	0.20660	1.2189	0.003562	1.48565	0.995155
7	4.86256	0.20565	-12.510	0.036564	156.508	0.996446
8	4.88580	0.20467	-1.1359	0.003320	1.29018	0.996457
9	5.02102	0.19916	-0.052562	0.000154	0.00276280	0.996457
10	5.29082	0.18901	20.723	0.060566	429.438	1.00000
		SUM OF EFFECTIVE		MASSES=		121210.

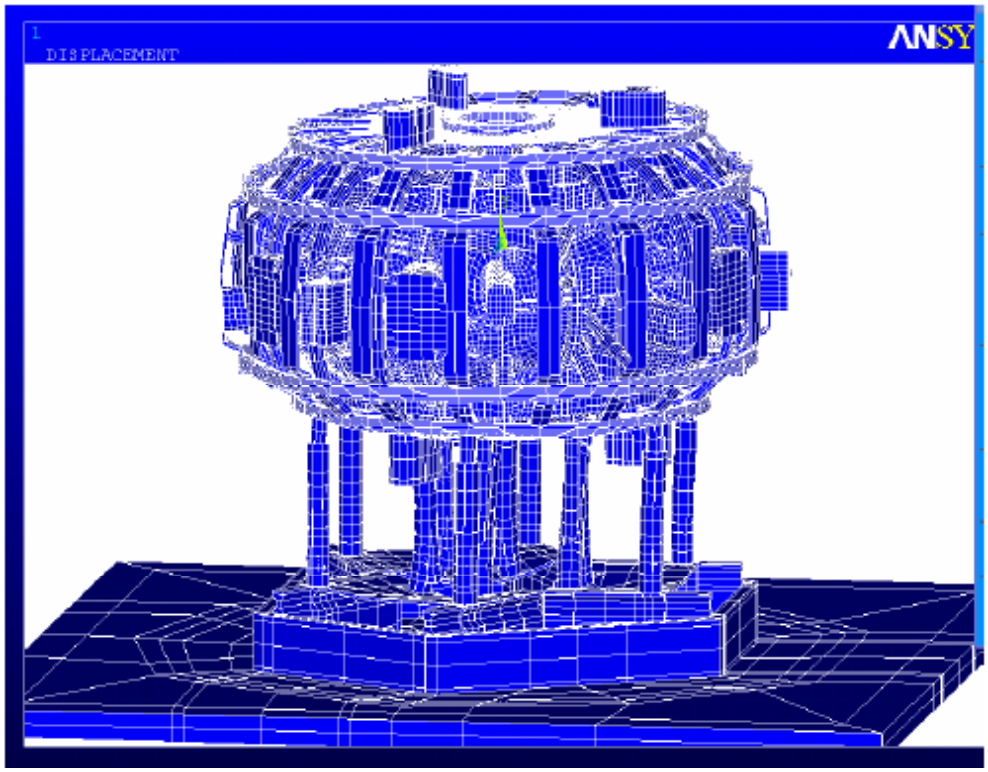

Figure 11.0-1 Mode 6 Vertical This was around 10 hz.

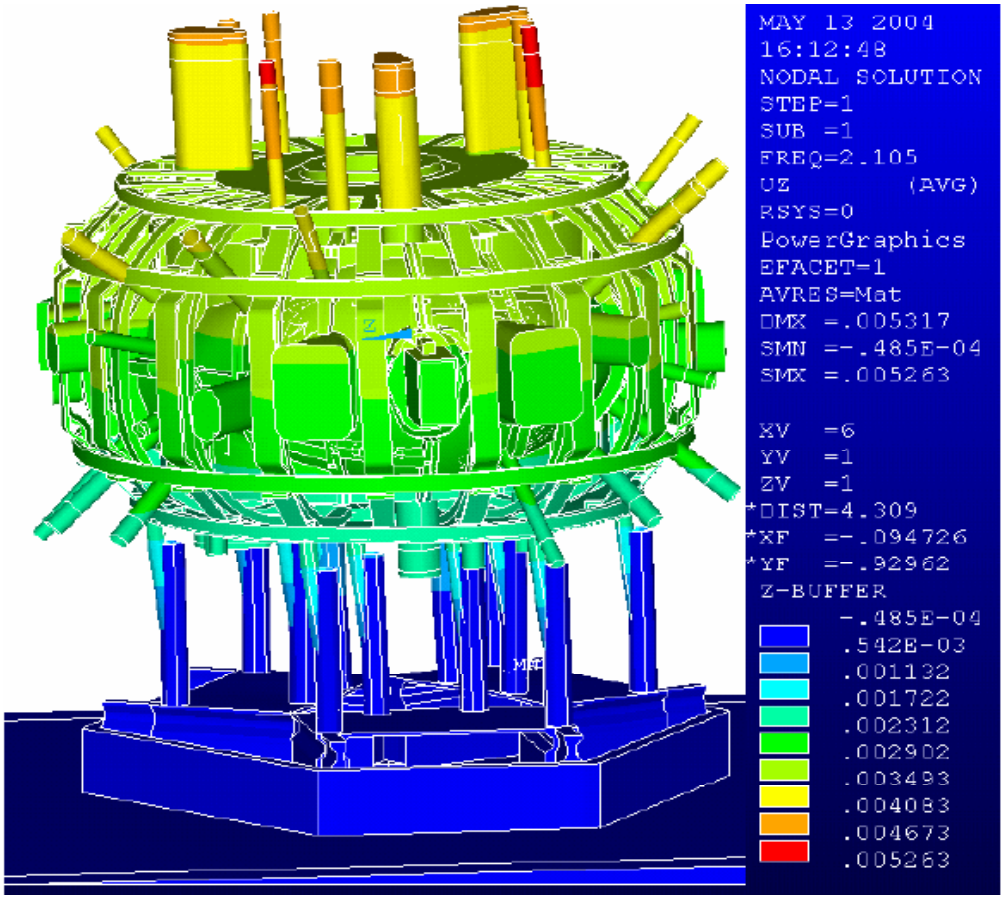

Figure 11.0-2 Run #7 First Mode, Global translation in Z. Displacements are not multiplied by the modal participation factor

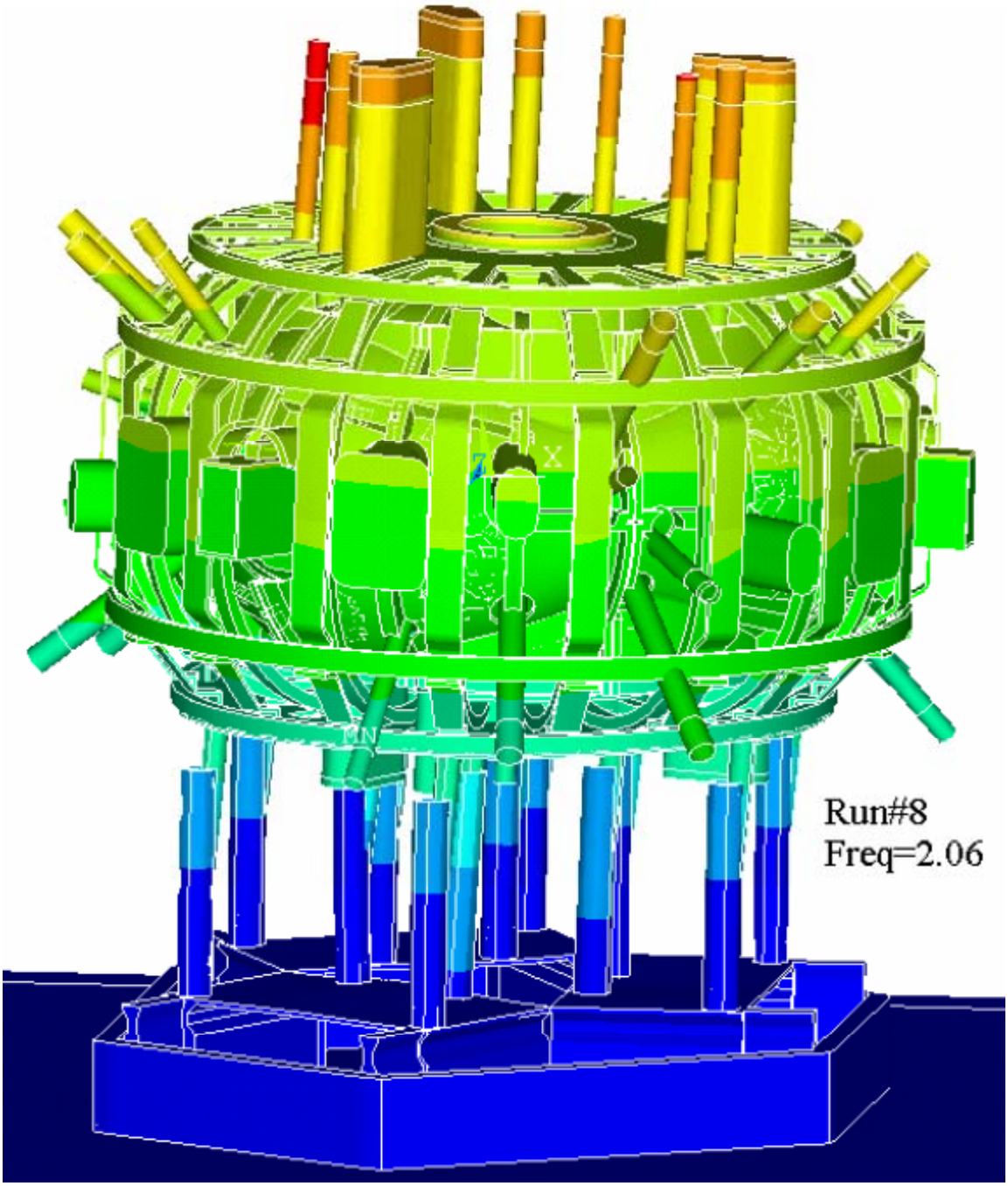

Figure 11.0-3 Run #8 First Mode, Global translation in X

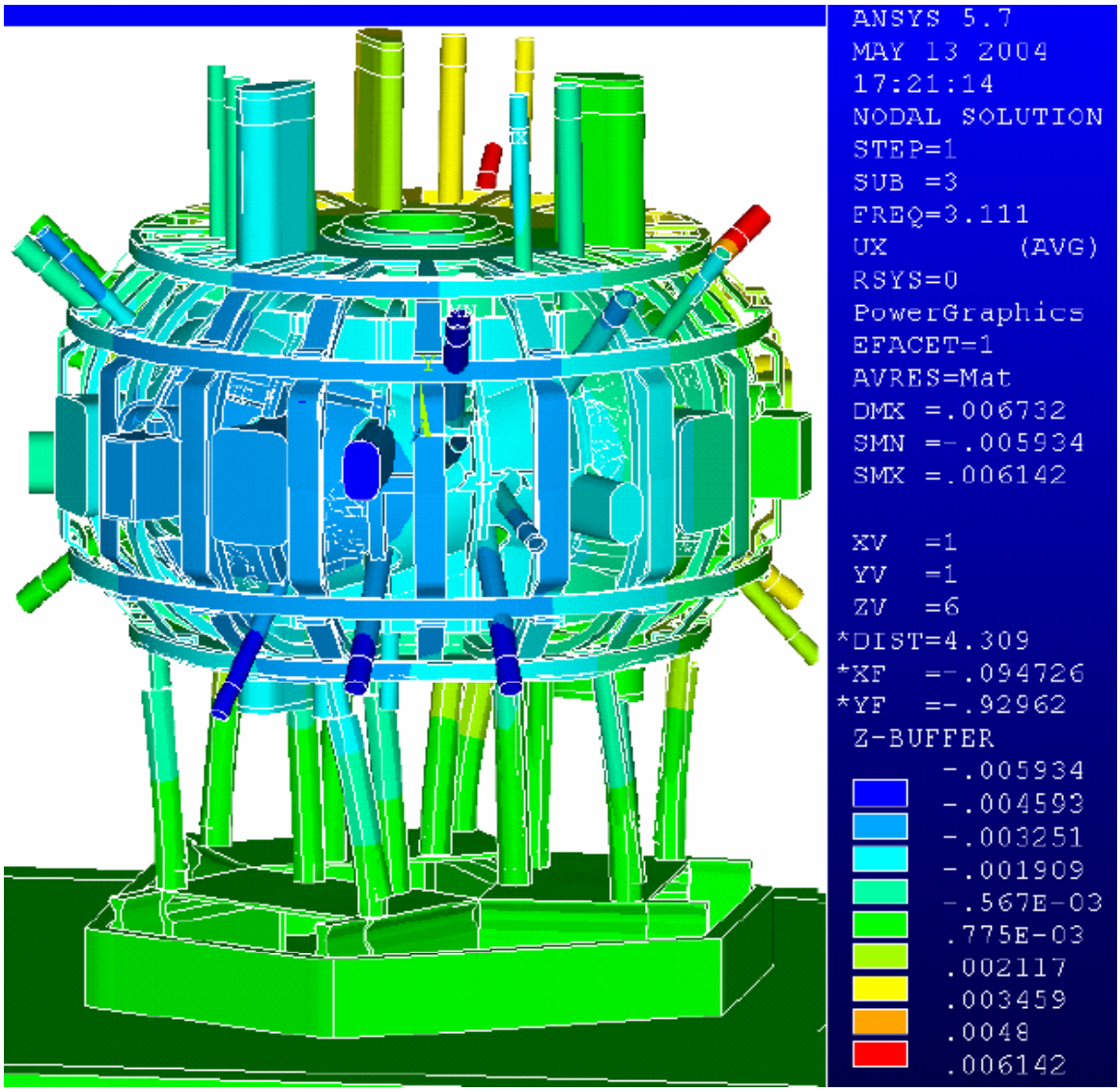

Figure 11.0-4 Mode Three – Global Twist about a Vertical Axis

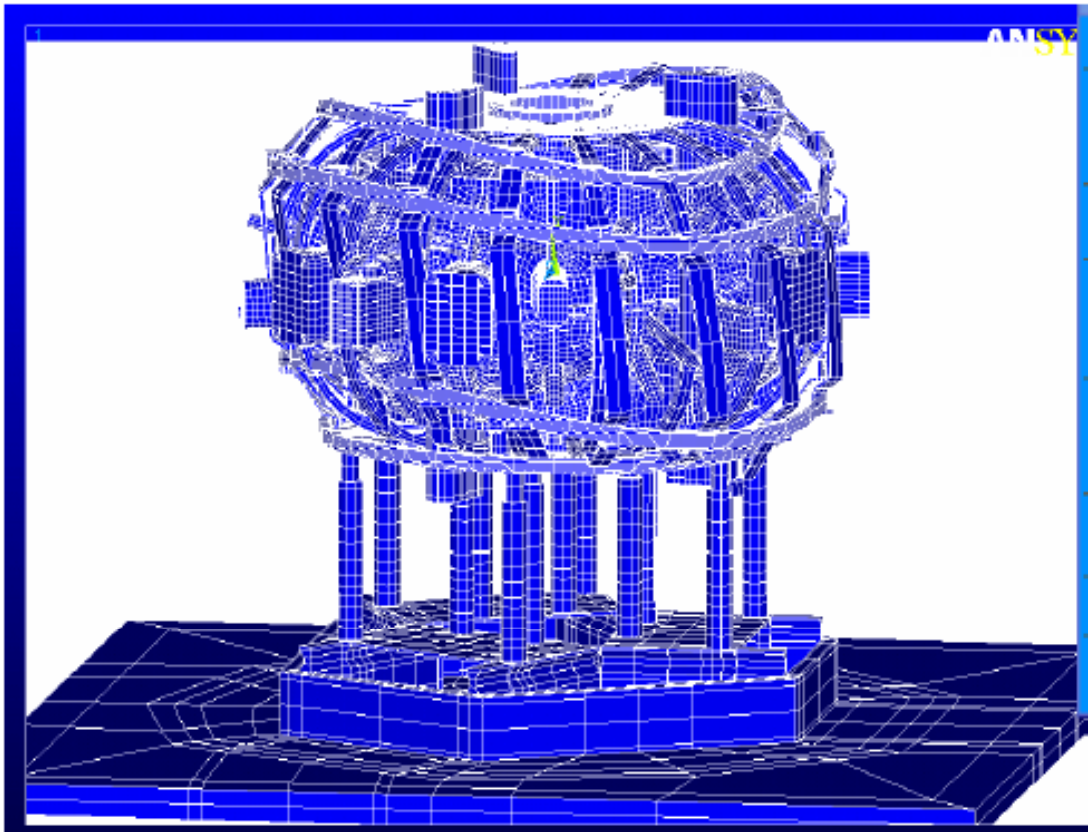

Figure 11.0-5 Mode 7 Run #4

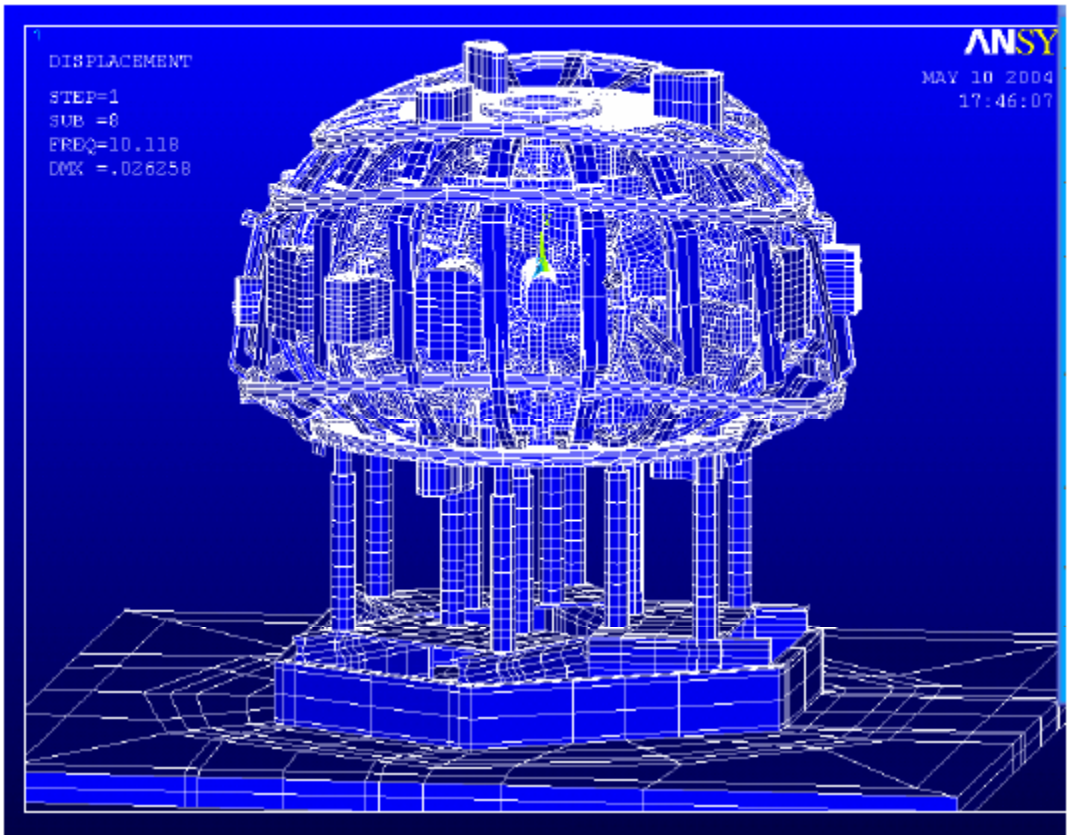

Figure 11.0-6 Mode 8, Run #4 Before Port Extensions

12.0 Modal Deformations - Animations

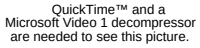

Figure.12.1 Animation of 1st Flexible Mode of the NCSX Structure – 2.1 Hz.

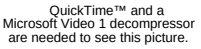

Figure.12.2 Animation of 2nd Flexible Mode of the NCSX Structure – 3.1 Hz.

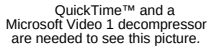

Figure.12.3 Animation of 3 rd Flexible Mode of the NCSX Structure-port-flex – 4.7 Hz.

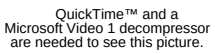

Figure.12.4 Animation of 4th Flexible Mode of the NCSX Structure – Rocking – 6.0 Hz.

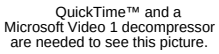

Figure.12.5 Animation of 5th Flexible Mode of the NCSX Structure – Lateral – 6.6 Hz.

Appendix B: Weld Stresses

B.1 Stresses in the Port Inconel-Stainless transition area. – K. Freudenberg

Port 4 Shear Stress plots considering ss stub and weld bead:

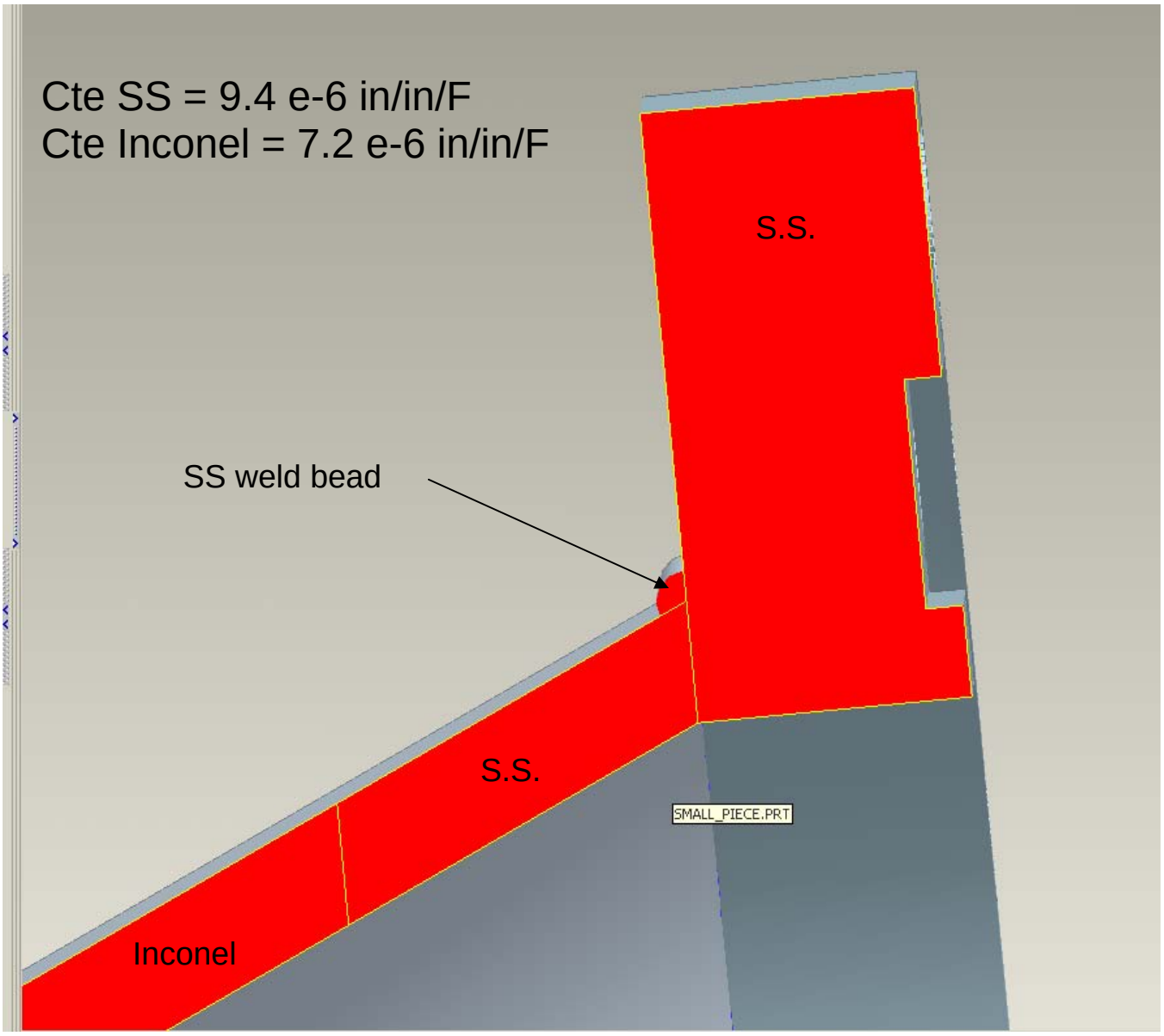

Max Shear Stress

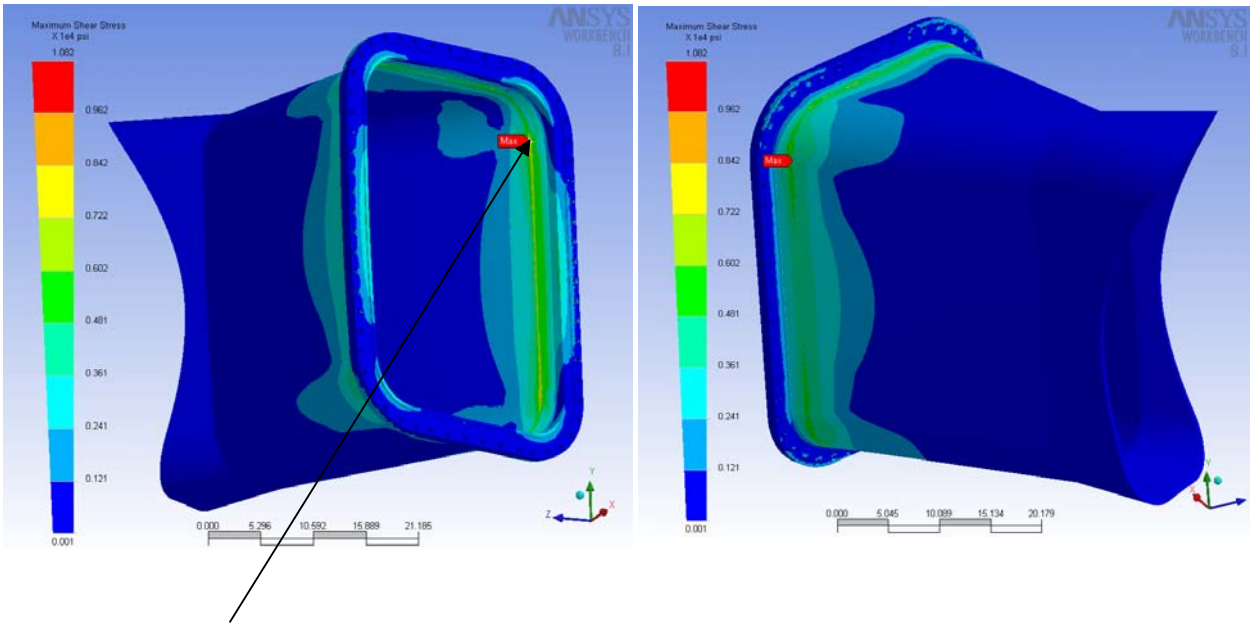

Max Shear Stress = 10 ksi (does not occur at weld but at interface between SS and Inconel)

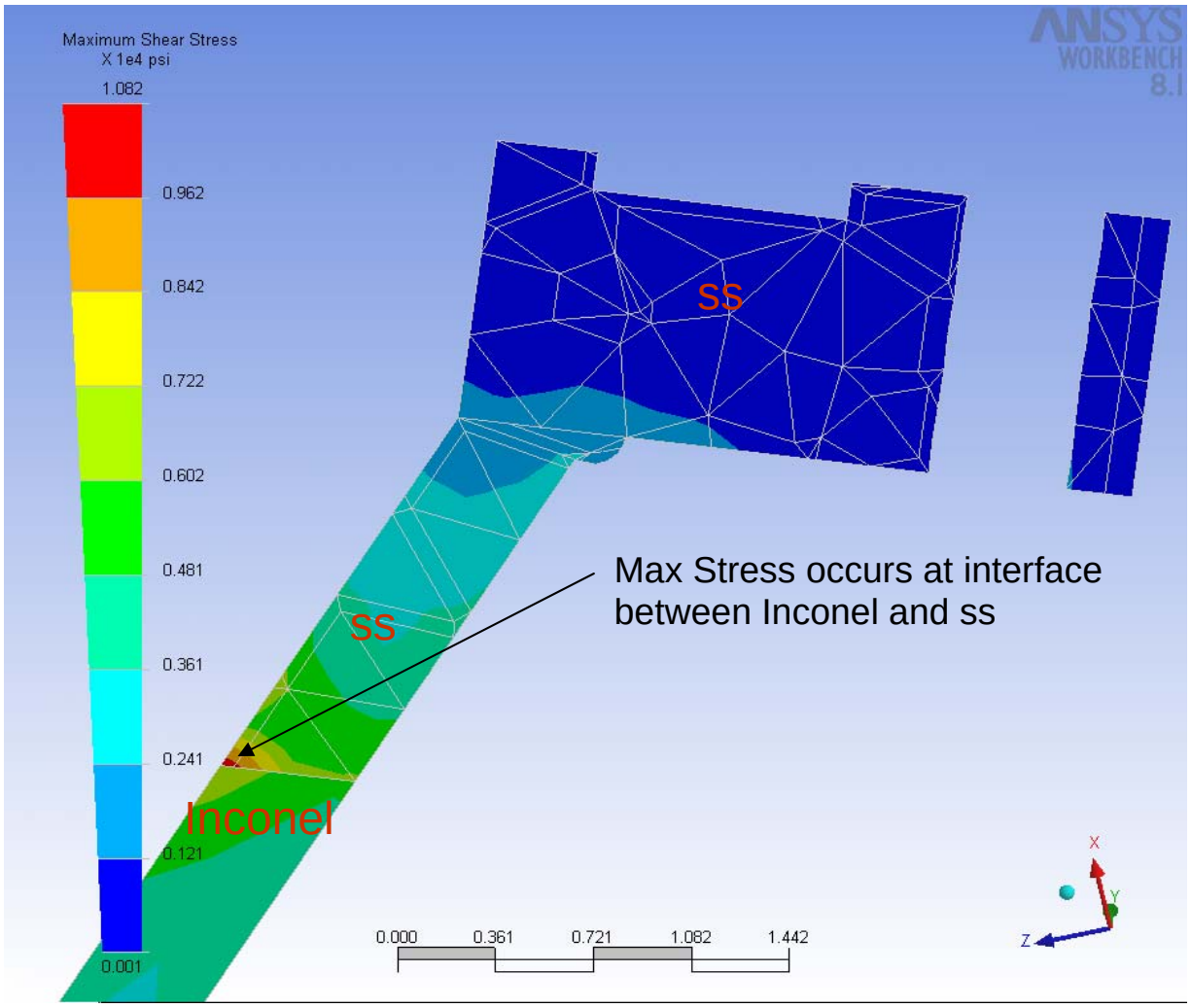

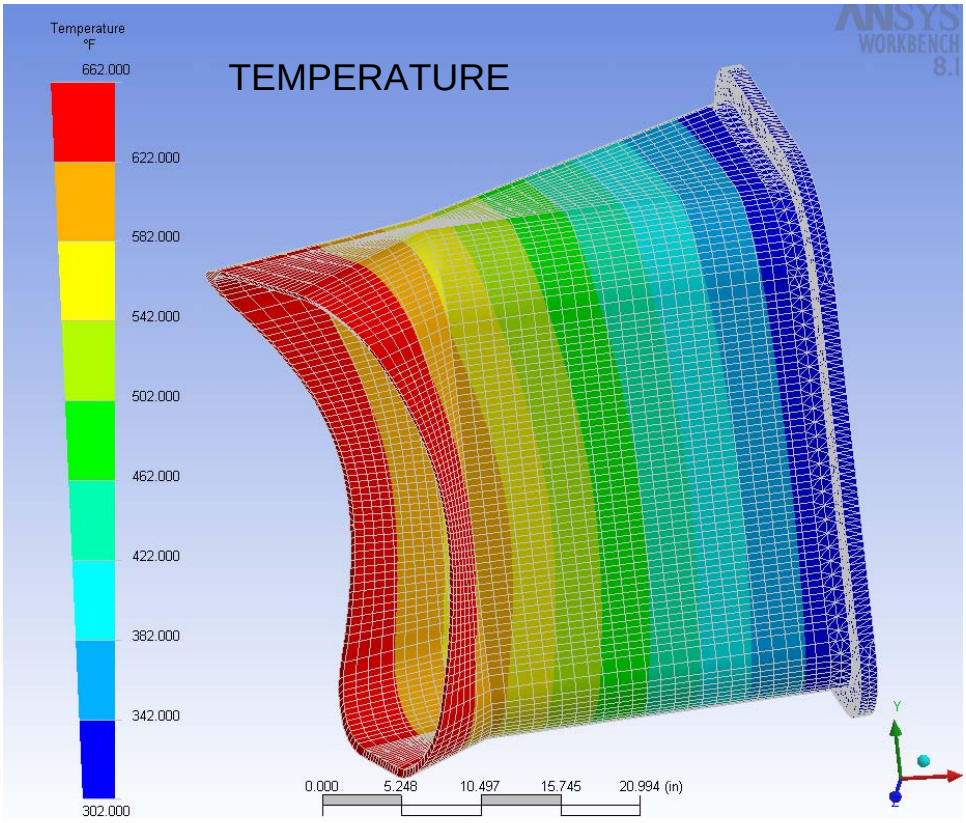
Temperature
°F
662.000
622.000
582.000
542.000
502.000
462.000
422.000
382.000
342.000
302.000
TEMPERATURE
ANSYS
WORKBENCH
8.1
0.000
5.248
10.497
15.745
20.994 (in)
Y

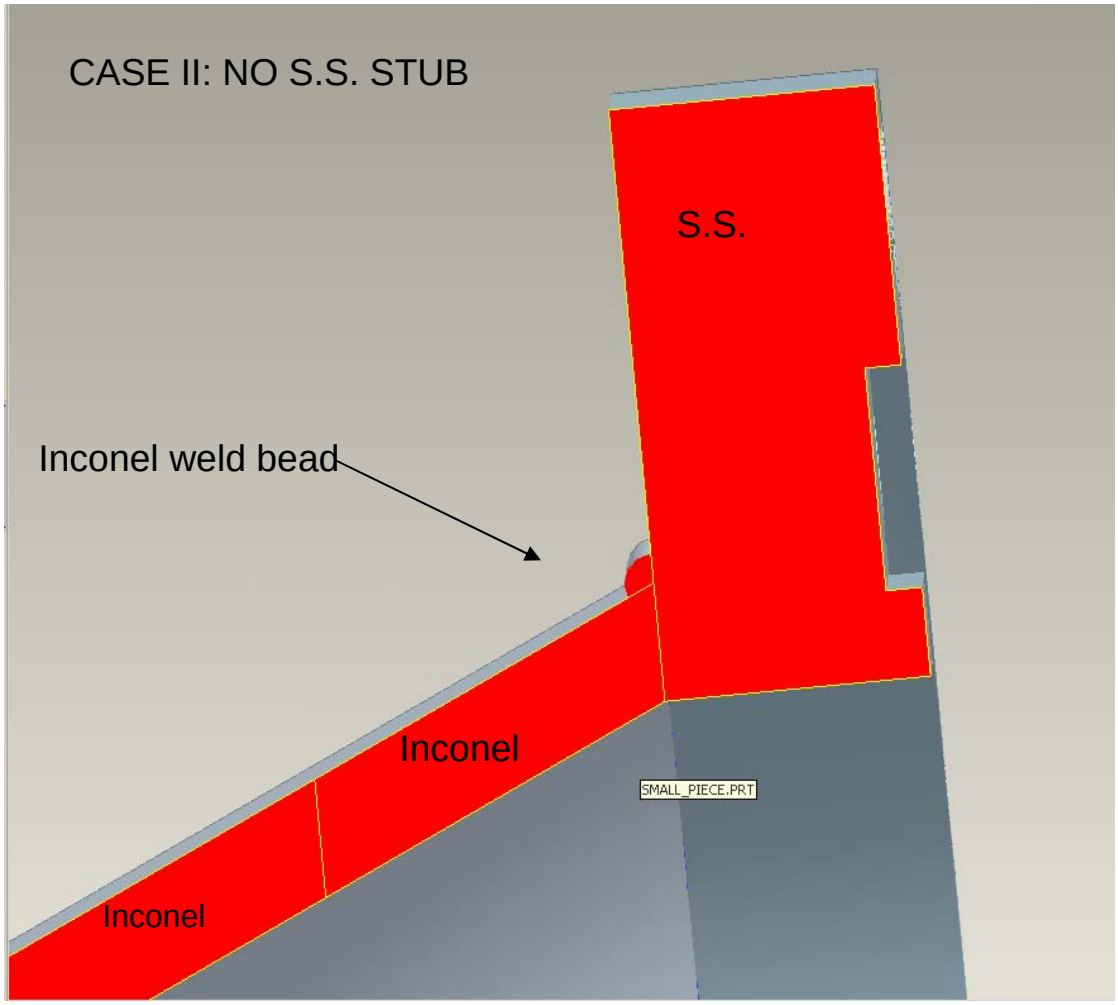
CASE II: NO S.S. STUB
S.S.
Inconel weld bead
Inconel
SMALL_PIECE.PRT
Inconel

Max Shear Stress (No SS Stub)

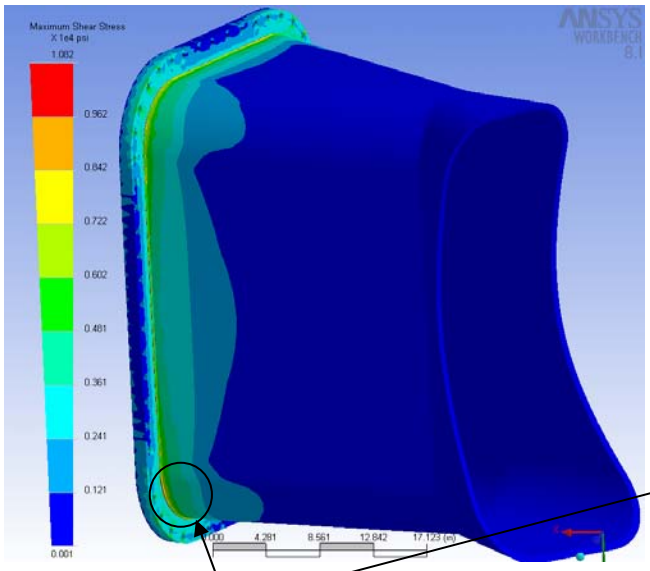

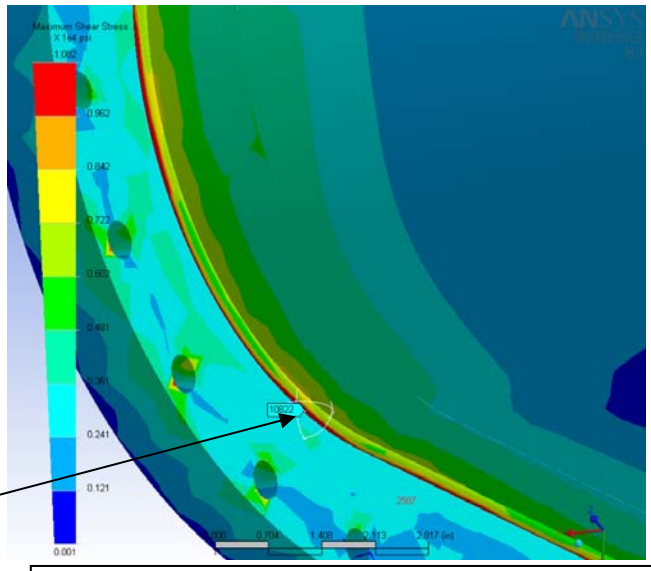

Max Shear Stress = 10.8 ksi

Close up view of max Stress area on weld

Max Shear Stress Cross Section (No SS Stub)

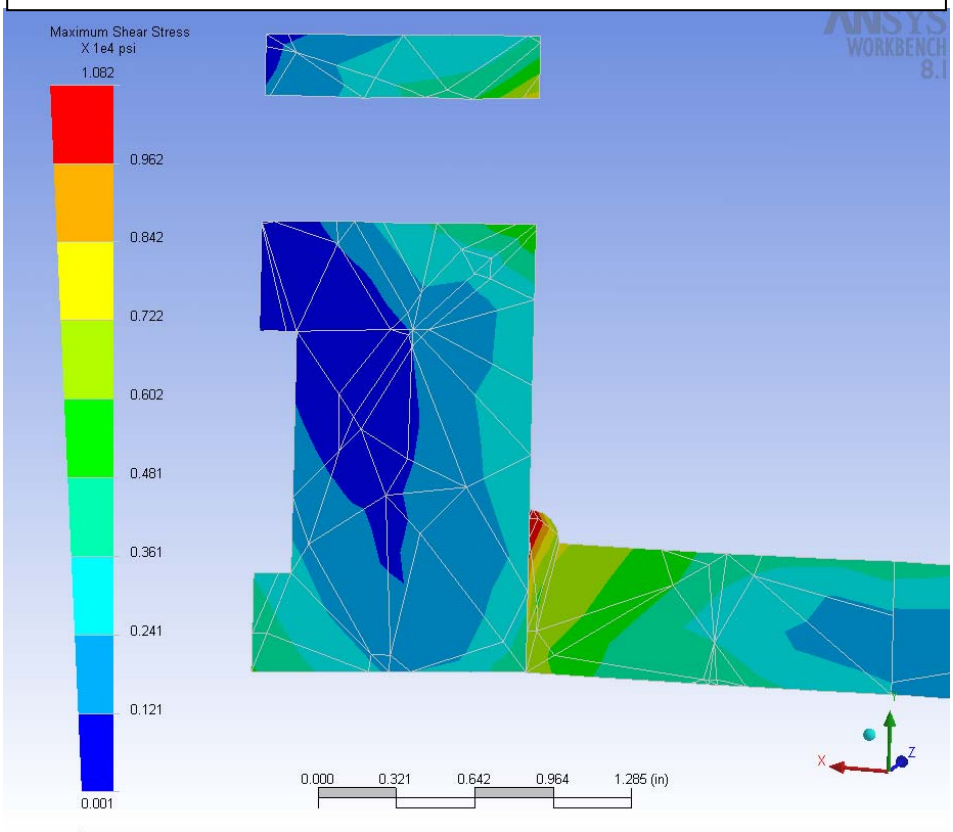

- The Magnitude of the max Shear stress appears to be independent of whether the SS stub is present or not.
- The location of the max stress is, of course, dependent on whether the stub is in place.

Appendix B.2 Supplementary V.V. Analysis – Kevin Freudenberg

Vacuum Vessel Mesh

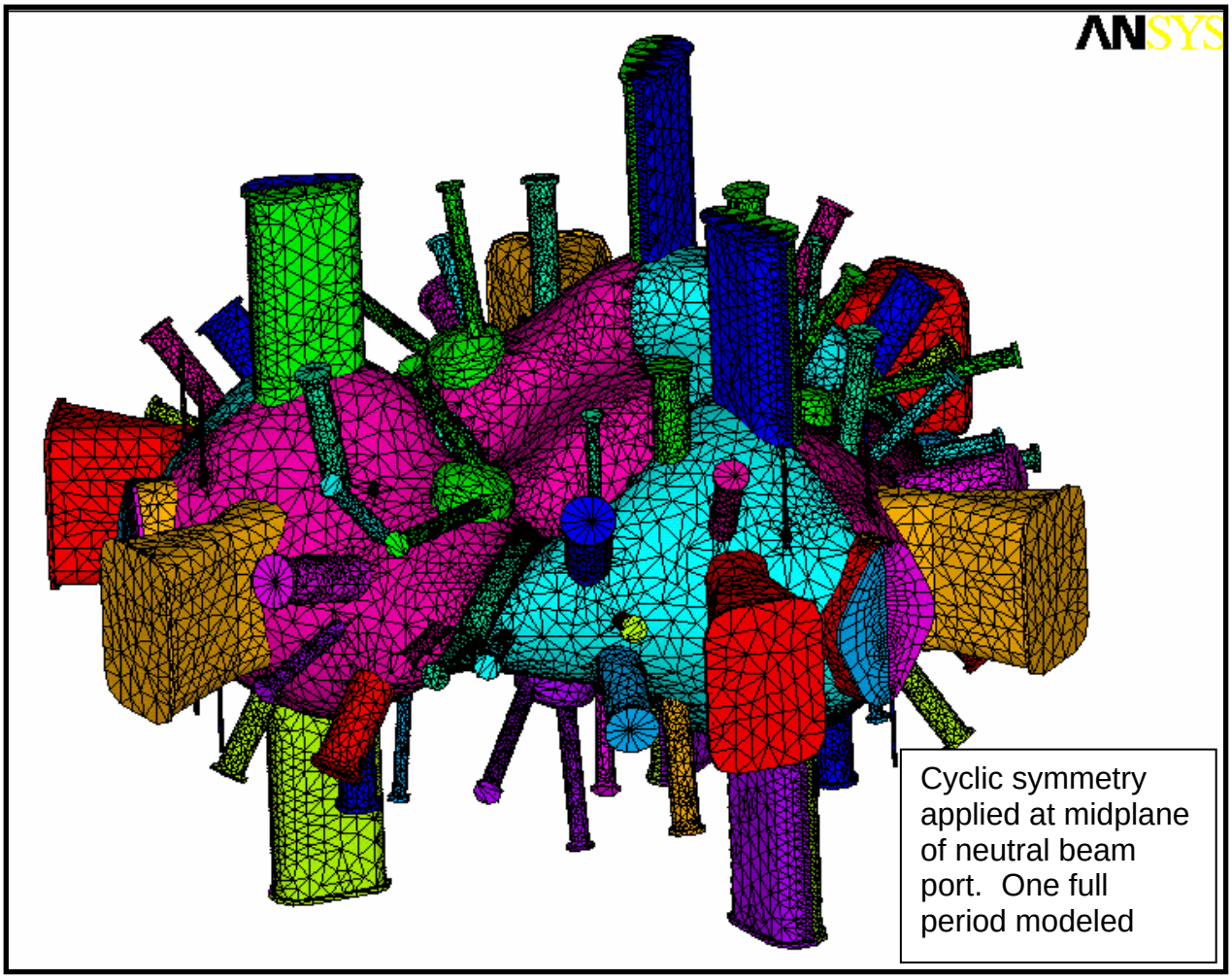

Loading and Restraints

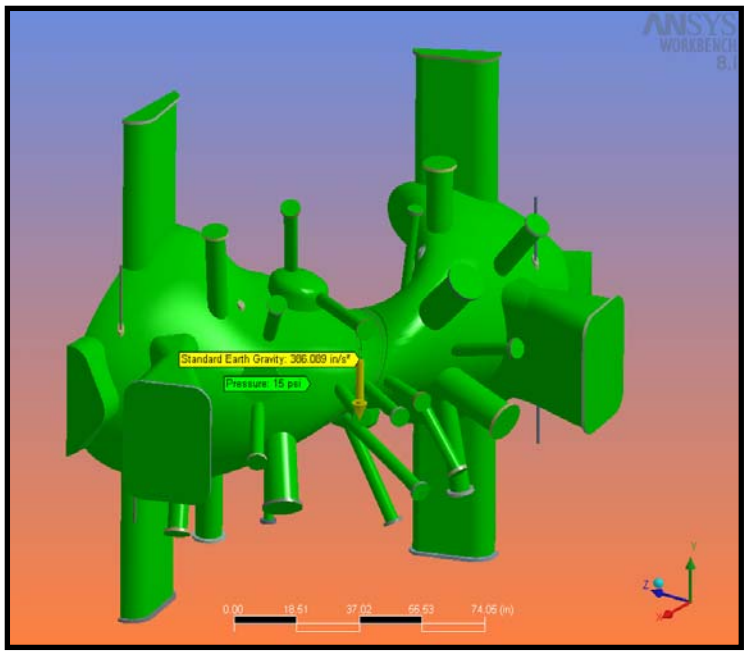

- Atmospheric pressure (15 psi) is applied to all exterior surfaces of the vessel. Pressure is shown in green in the image.
- Vessel is restrained by support pins attached to the two front clevises.
- Cyclic symmetry conditions are applied on the exterior cuts at the mid plane of the Vessel period.
- Standard Earth Gravity Applied.

Port Extension Weight compensation

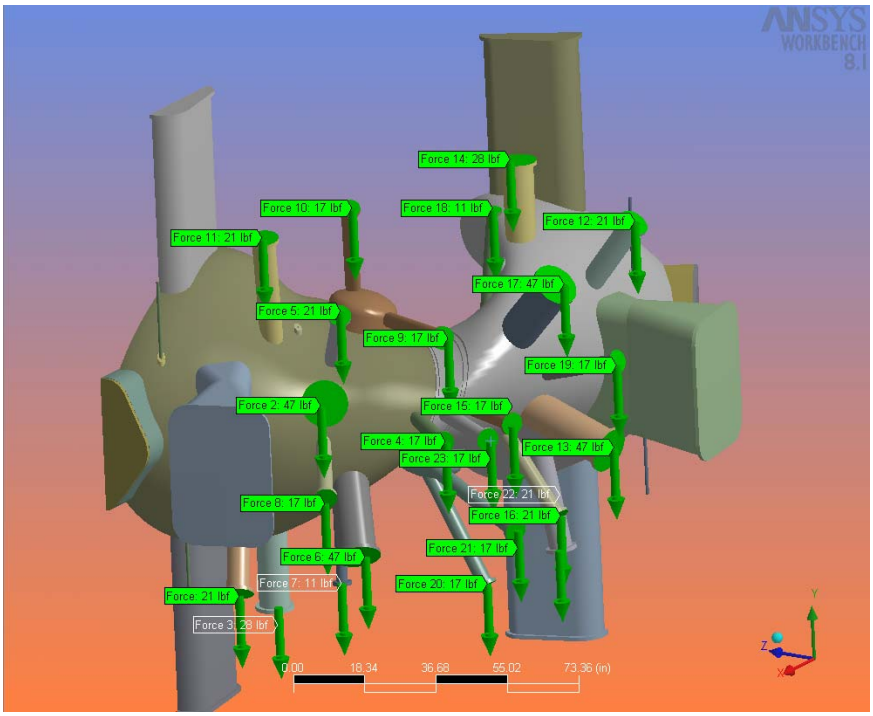

- Port Extension weights have been added

Vessel Global Displacement

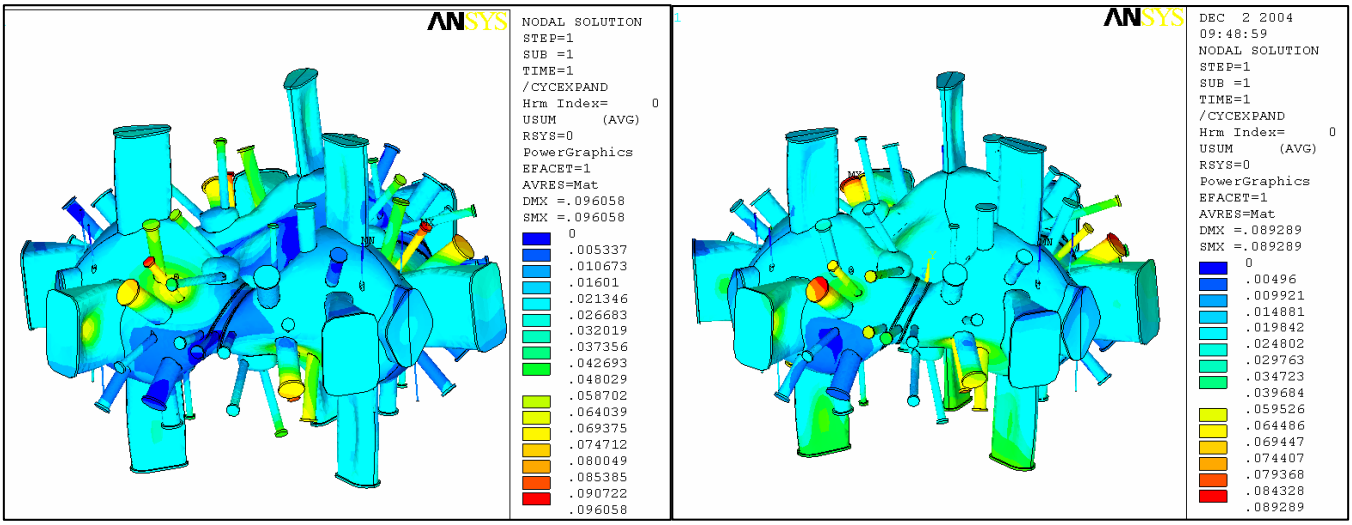

Without Gravity

With Gravity

Stress Intensity of Vacuum Vessel (Tresca Stress)

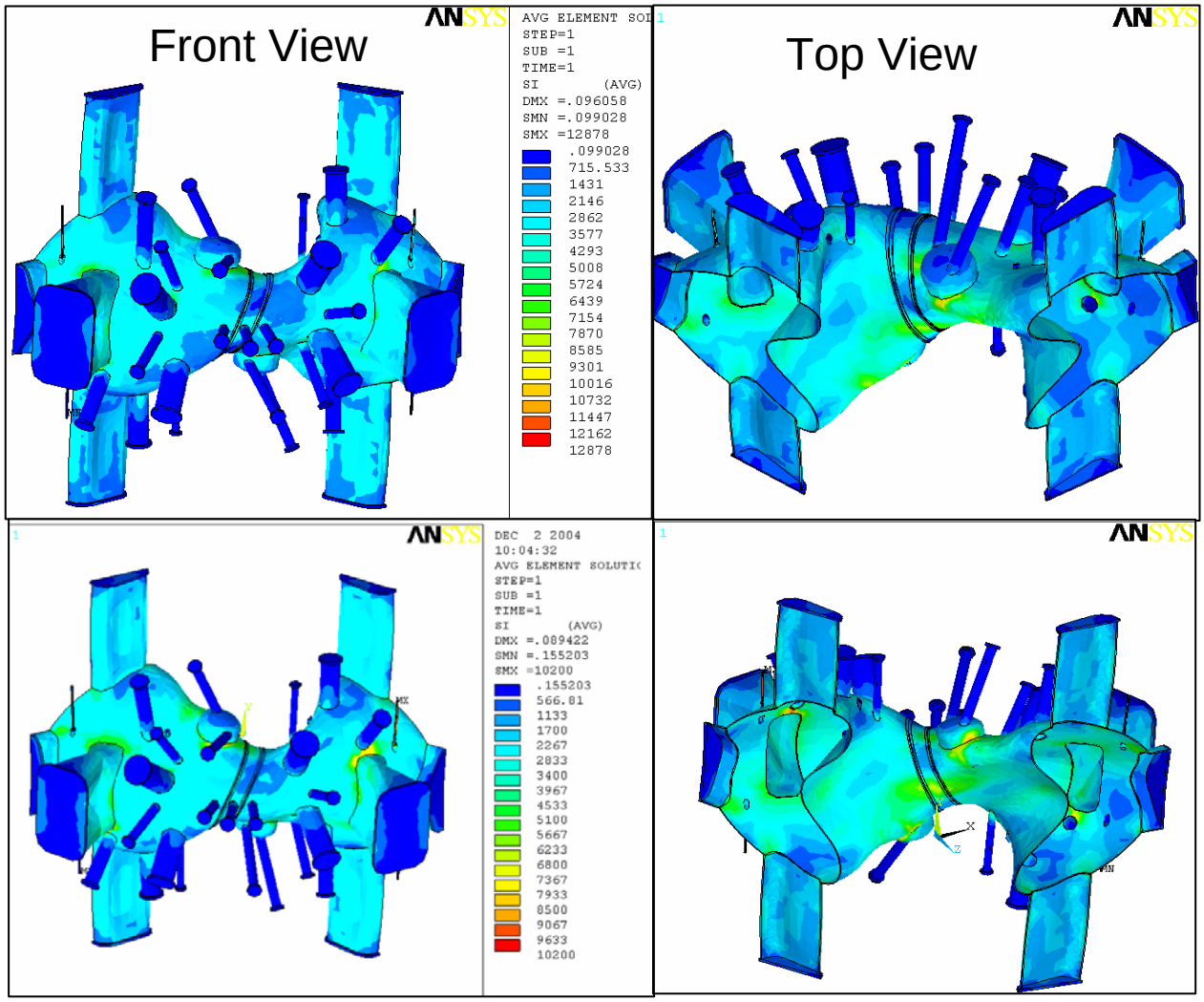

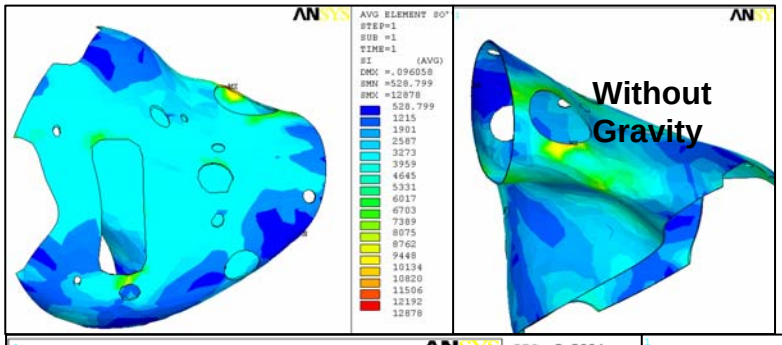

Stress Intensity on Vessel Shell (Tresca Stress)

Max Stress occurs near the turret port as shown in both images

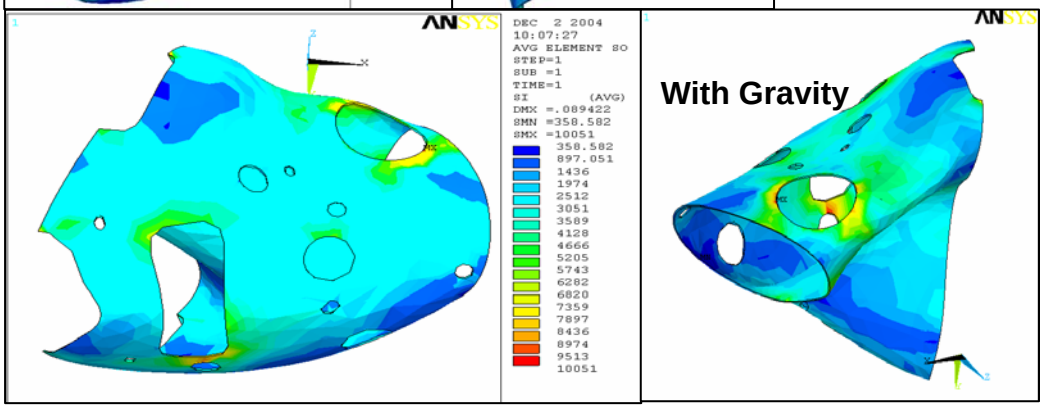

Detailed Cross Section of elements around weld

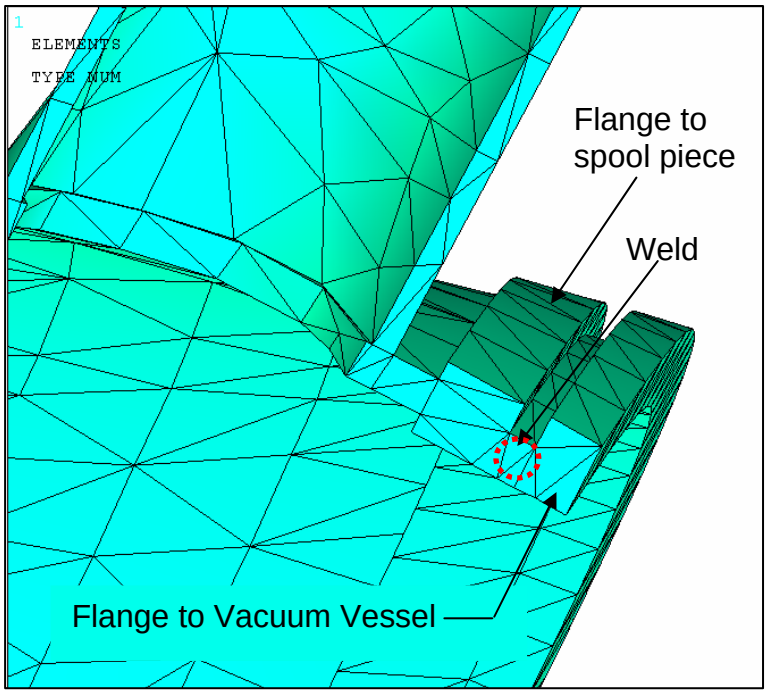

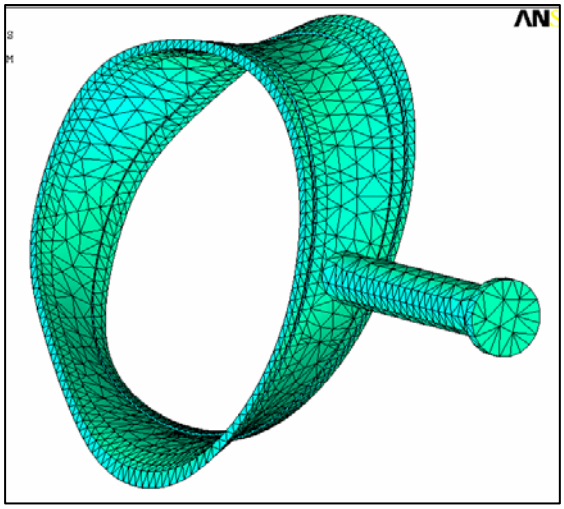

Overall mesh of spool piece

Original Stress of Spool Piece and surrounding flanges

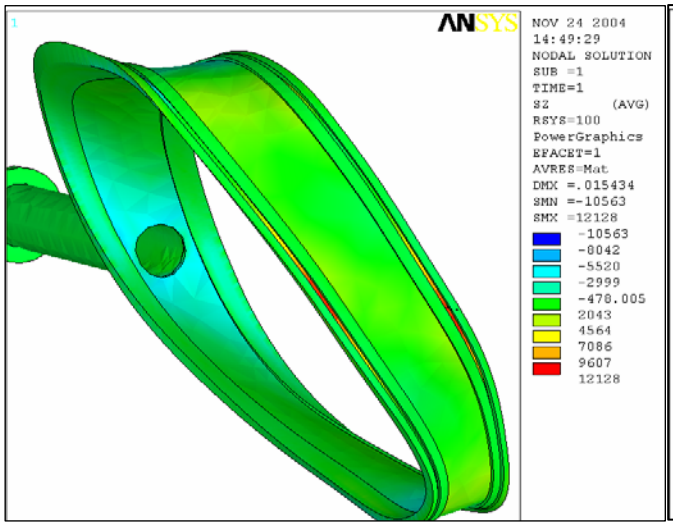

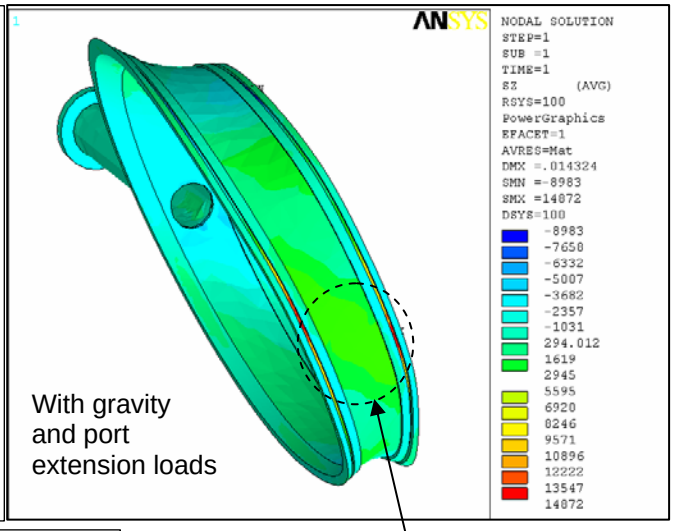

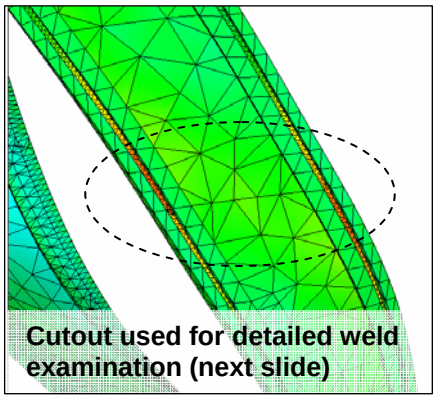

Same area of weld is still in tension (increase stress by 2.6 ksi)

Stress in Z direction (compression toward flange)

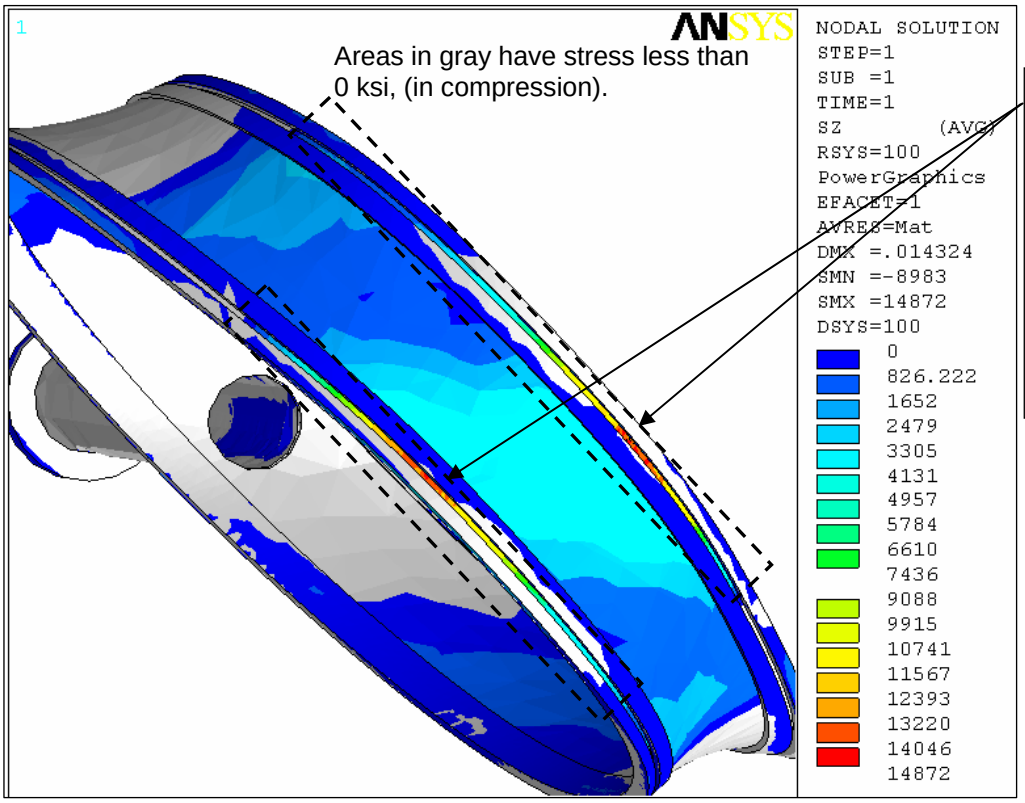

Dashed areas are the only places where the weld is placed under tension loading

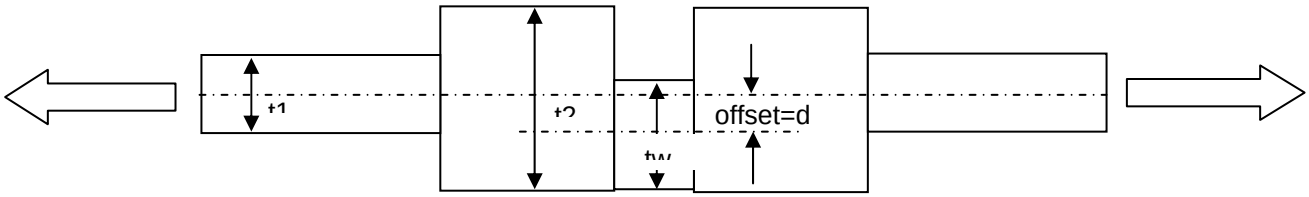

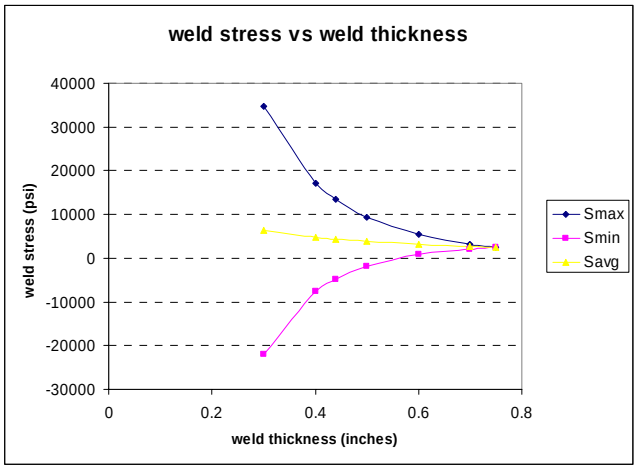

FEA Prediction:
Smax = 12 ksi
Smin = -6 ksi
Savg = 3 ksi